



The author of the PhD dissertation: Anna Selwent
Scientific discipline: chemical technology

DOCTORAL DISSERTATION

Title of PhD dissertation: **Studies on Micellar Aggregation of Nonionic Surfactants in Imidazolium Ionic Liquids**

Title of PhD dissertation (in Polish): **Badania nad agregacją micelną surfaktantów niejonowych w imidazoliowych cieczach jonowych**

Supervisor	Second supervisor
<i>signature</i>	<i>signature</i>
prof. dr hab. inż. Jan Hupka	dr inż. Justyna Łuczak

Składam serdeczne podziękowania

*Promotorowi, Panu prof. dr hab. inż. Janowi Hupce,
za umożliwienie realizacji tej pracy, opiekę naukową oraz życzliwość;*

*dr inż. Justynie Łuczak,
za wsparcie merytoryczne, cenne uwagi i sugestie;*

*Pracownikom i Doktorantom Katedry Technologii Chemicznej,
za dobre słowo, wsparcie i jedyną w swoim rodzaju atmosferę;*

*Dziękuję także - a może przede wszystkim - mojej Rodzinie i Przyjaciółom,
za spokój, wsparcie i wiarę – od początku do końca.*



Table of contents

List of abbreviations and symbols.....	5
1. Introduction.....	7
2. Literature review.....	8
2.1. Ionic liquids as new generation solvents.....	8
2.2. Structure, interactions and physicochemical parameters of imidazolium ionic liquids.....	8
2.2.1. Nanostructure organization in imidazolium ionic liquids.....	12
2.2.2. Gordon parameter.....	14
2.3. Nonionic surface active agents in ionic liquids.....	14
2.3.1. Micellar aggregation of surface active agents.....	14
2.3.2. Micellar aggregation of nonionic surface active agents in imidazolium ionic liquids.....	15
2.3.3. Micellar aggregation of nonionic surface active agents in imidazolium ionic liquids mixtures.....	18
2.4. Literature review summary.....	20
3. Aims and scope.....	21
4. Experimental.....	23
4.1. Reagents and materials.....	23
4.1.1. Ionic liquids.....	23
4.1.2. Surfactants.....	25
4.2. Apparatus, methodology and analytical methods.....	27
4.2.1. Sample preparation.....	27
4.2.2. Density determination.....	27
4.2.3. Dynamic viscosity determination.....	28
4.2.4. Surface tension determination.....	28
4.2.5. Conductivity - determination of associated cations number.....	29
4.2.6. Hydrodynamic diameters - Dynamic Light Scattering.....	31
4.2.7. Critical micelle concentration.....	31
4.2.8. Physicochemical and thermodynamic parameters.....	32
5. Results.....	34
5.1. Gordon parameter.....	34
5.2. Isotherms of nonionic surfactants in imidazolium ionic liquids.....	36
5.2.1. Cation type influence.....	36
5.2.2. Anion type influence.....	39
5.2.3. Surfactant type influence.....	41
5.3. Temperature dependence and thermodynamics.....	43



5.4.	Isotherms, temperature dependence and thermodynamics of nonionic surfactants in mixed IL solutions	56
5.5.	Critical micelle concentration	58
5.6.	Micellar diameter	62
5.7.	Conductivity.....	66
5.8.	Statistical evaluation of results	69
6.	Discussion of the results	71
7.	Conclusions.....	76
8.	Final comments.....	78
9.	Bibliography	80
	List of figures	90
	List of tables	93
	Summary	94
	Streszczenie	95

List of abbreviations and symbols

IL(s)	– ionic liquid(s)	
RTIL(s)	– room temperature ionic liquid(s)	
CMC(s)	– critical micelle concentration(s)	
[BF ₄] ⁻	– tetrafluoroborate anion	
[PF ₆] ⁻	– hexafluorophosphate anion	
[OTf] ⁻	– trifluoromethanesulfonate anion	
[NTf ₂] ⁻	– bis(trifluoromethylsulfonyl)imide anion	
[EMIM] ⁺	– 1-ethyl-3-methylimidazolium cation	
[PrMIM] ⁺	– 1-propyl-3-methylimidazolium cation	
[BMIM] ⁺	– 1-butyl-3-methylimidazolium cation	
[PMIM] ⁺	– 1-pentyl-3-methylimidazolium cation	
[HMIM] ⁺	– 1-hexyl-3-methylimidazolium cation	
[OMIM] ⁺	– 1-octyl-3-methylimidazolium cation	
TX-100	– Triton X-100, polyoxyethylene octyl phenyl ether, 9.5 oxyethylene groups	
TX-114	– Triton X-114, polyoxyethylene octyl phenyl ether, 7.5 oxyethylene groups	
TX-45	– Triton X-45, polyoxyethylene octyl phenyl ether, 4.5 oxyethylene groups	
TX-15	– Triton X-15, polyoxyethylene octyl phenyl ether, 1.5 oxyethylene groups	
OE	– oxyethylene	
n _{ac}	– number of associated cations per surfactant molecule	
m	– number of carbon atoms in ionic liquid cations alkyl chain	
DLS	– Dynamic Light Scattering	
ρ	– density coefficient	[g/cm ³]
η	– dynamic viscosity coefficient	[mPa·s]
M	– molar mass	[g/mol]
G	– Gordon value	[J/m ³]
V _m	– molar volume	[nm ³]
γ	– surface tension	[mN/m]
γ ₀	– surface tension of pure substance	[mN/m]
γ _{CMC}	– surface tension at CMC	[mN/m]
κ	– conductivity	[mS]
ΔG _m	– free energy of micellization	[kJ/mol]
ΔG _{ad}	– free energy of adsorption	[kJ/mol]
ΔH _m	– enthalpy	[kJ/mol]
ΔS _m	– entropy	[kJ/mol]

Γ_{\max} – surface excess	[mol/m ²]
A_{\min} – minimum area occupied by one molecule	[nm ²]
Π_{cmc} – surface pressure	[mN/m]
D_h – hydrodynamic diameter	[nm]

1. Introduction

Ionic liquids (ILs) are salts composed entirely from ions, a spacious organic cation, and a less or more complex anion of organic or inorganic nature. ILs are characterized by liquid state over wide range of temperatures, especially at room temperatures (RTILs – room-temperature ILs) [1-4], or more generally - below 100°C. Within the family of ILs one may distinguish protic and aprotic species, where the aprotic ones, being the subject of this investigation, are unable to be proton donors, and on the contrary, the protic ones - donate protons. ILs are often described as “green solvents”. Due to their negligible volatility, nonflammability, chemical and thermal stability, their migration to the atmosphere is vestigial. Amongst other useful properties such as tunability or electrical conductivity, ILs were also proven to support aggregation of amphiphilic compounds [5-8]. The number of solvents capable of supporting micellization of amphiphiles is still limited [9], therefore surface chemistry of ionic liquids has been widely investigated.

The subject of amphiphiles self-aggregation in various media covers especially systems containing water and volatile organic compounds (VOCs) as solvents, which, from ecological reasons, are inadvisable nowadays [10, 11]. The presence of water, which is a perfect aggregation-supporting medium, is not always a desired reaction environment. Nevertheless, despite the fact that many ILs were proven to support self-aggregation of amphiphiles, much more studies describe their application in micellar systems in the role of amphiphiles or additives, rather than solvents. Thus, the main goal of the dissertation presents the application of ILs as perfect solvents to support aggregation of nonionic surfactants.

The current state of knowledge about the mechanism of micelle formation of surface active agents in ionic liquids is meager, whereas literature descriptions concern mainly specific examples. Therefore, to better understand the phenomenon, complex characteristic, including the role of ILs anions and cations, is needed. Broad analysis of parameters affecting micellar aggregation, such as the structure of ILs, surfactants, temperature and other, will help in the future design of IL solvents for certain purposes and processes conditions. Obtained results and drawn conclusions are expected to contribute to the field of the surface chemistry.



2. Literature review

2.1. Ionic liquids as new generation solvents

Since ionic liquids gained major attention in the last 20-30 years, their applicability as solvents became massive [9, 12, 13]. Their unique solvents properties endeared a big, and still growing, group of enthusiasts in various science areas. The branches of their application are catalysis and bio catalysis [14-17], separation processes [18-21], carbon dioxide capture [22, 23], organic and inorganic synthesis [24-26], biodiesel production [16, 27, 28], pharmaceuticals [29-31], cellulose processing [32-34], metal processing [35, 36], just to name a few.

Applicability of ILs as solvents may take place due to their intrinsic character, so called segregated solvent liquid structure, composed of polar and nonpolar domains [9, 37]. The presence of domain nanostructure gives an information whether the IL may be a solvent for amphiphilic compounds, or not. Accordingly, the structure of the IL, this is the type of anions and cations side chains and their lengths, determine whether a surface active agent will solubilize or aggregate [7, 38]. The mechanism responsible for ILs ability to support self-organization of surfactants is the solvophobic effect, which is the analogue of hydrophobic effect in aqueous solutions [9, 39, 40].

2.2. Structure, interactions and physicochemical parameters of imidazolium ionic liquids

Imidazolium ionic liquids are aprotic salts composed of simple (Cl^- , Br^-), more complex (PF_6^- , BF_4^-), or very complex (NTf_2^- , ammonium) anionic moiety, and cationic part with imidazolium ring with alkyl chain(s) attached. Figure 1 depicts ILs cation with numbered carbon atoms, present in all ionic liquids employed in this study.

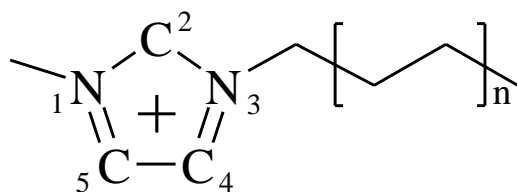


Figure 1. Structure of 1-methyl-3-alkylimidazolium cation.

The unusual character of ionic liquids is a consequence of all the inter- and intramolecular interactions, present in a single molecule, amongst a group of molecules, and between ILs and other species. There is much work being done to understand them, and a number of methods are being employed, however, studying ILs cation – anion interactions is still a challenge [41-43].

Tools and methods for analyzing ILs bonds and interactions are divided into instrumental and theoretical ones (see table 1). In most cases the studies require both types of methods, due to very complex character of the issue, and a huge diversity amongst ionic liquid species. Fundamentals of understanding ILs structures were established by Jastorff et al. by means of T-SAR approach, which is thinking in structure-activity relationship [44]. Given approach depends on a systematic analysis of a chemical species based on the structural formulas, therefore, is a theoretical method.

Table 1. Instrumental and theoretical methods for studying ILs bonds and interactions

Instrumental
- FT (fourier transform) [37]
- FT – Raman [45]
- FT IR/ATR (Fourier transform infrared/attenuated total reflection) [46]
- ¹ H NMR (nuclear magnetic resonance spectroscopy) [47]
- TGA (thermogravimetry) [48]
- SFVS (sum-frequency vibrational spectroscopy) [49]
- SAXS (small angle x-ray spectroscopy)
- RIKES (Raman-induced Kerr-effect spectroscopy) [50]
- THz-TDS (terahertz time domain spectroscopy) [51]
- NOESY (nuclear Overhauser effect spectroscopy) [52]
Theoretical
- Molecular dynamics (MD) [53]
- Car-Parrinello MD [54]
- Monte Carlo (MC) simulations [55]
- Density functional theory (DFT) [56]
- Ab initio – quantum chemistry based computational methods [57]
- Quantum theory of atoms in molecules (QTAM) [58]
- Qualitative molecular orbital theory (QMOT) [58]
- Natural bond orbital (NBO) analysis [58]

Within ionic liquids structures we may determine covalent and non-covalent interactions (see figures 2 and 3). The covalent ones are bonds between carbon and other atoms, whereas the non-covalent interactions are all the remaining forces, which mostly constitute the unique character of ILs, and include hydrogen bonds, ionic (anion-anion, cation-cation, and anion-cation), coulombic and dispersion/van der Waals forces. Despite the fact that covalent bonds are much stronger than the non-covalent interactions, the accumulation and cooperation of the weak interactions leads to a strong effect. Ionic (electrostatic) interactions are said to constitute even up to 70% of all the forces within ILs molecules, however, H-bonds, which are characterized by a bond lifetime on only nanoseconds, take the greatest contribution [58-60].

The strengths of the interactions are not fixed values, but ranges of possible energies and distances, and depend on the number of factors. In imidazolium ionic liquids the typical H-bonds are said to contribute with ionic, dispersive and covalent bonds, however, mid-range H-bonds are more dominant than the ionic ones. On the contrary, the weakest H-bonds are dominated by van der Waals interactions.

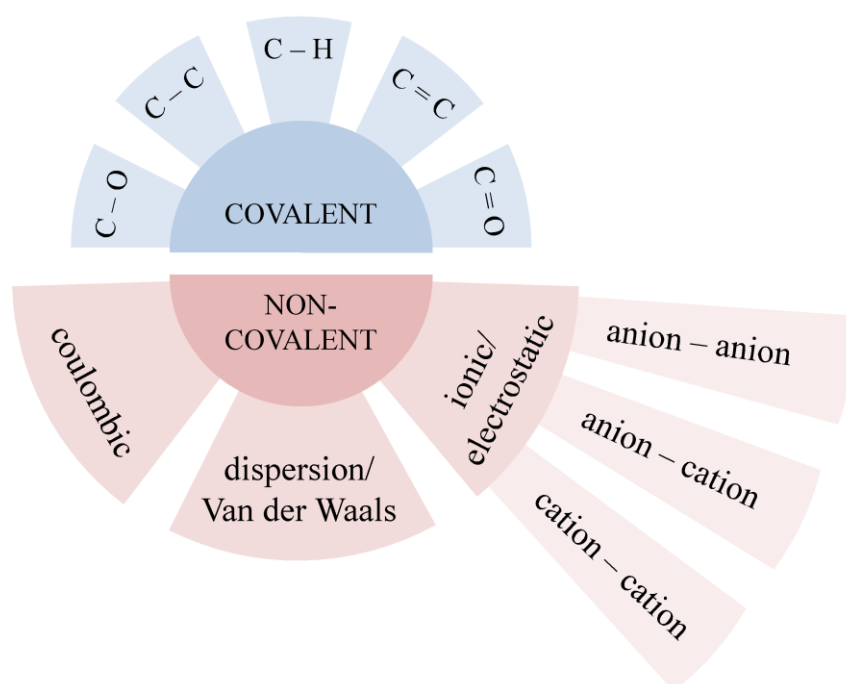


Figure 2. Types of interactions within ILs structures

Amongst H-bonds we may distinguish many specific ones, such as ionic, resonance, inverse, charge assisted and others, however, in ILs the neutral, ionic, and mostly doubly-ionic H-bonds are dominant and determine their properties [61-63]. Relatively strong

hydrogen bonds are provided by the presence of fluorine atom, (e.g. tetrafluoroborate and hexafluorophosphate anions), however, not as strong as it could be expected, which is due to constant rotational motion of the molecule. The strength of hydrogen bonds was proven to increase (parallelly with van der Waals forces) with elongation of cations alkyl chains, which results in greater viscosity of the salts. Another factor enhancing the strength of H-bonds is the decrease of anions size, and presents the following order: $[\text{Cl}]^- > [\text{OTf}]^- \approx [\text{BF}_4]^- > [\text{NTf}_2]^- > [\text{PF}_6]^-$ [58]. The anions size decrease results also in decreased strength of van der Waals interactions, and as a consequence – strengthening of the electrostatic ones.

Hydrogen bonds are also responsible for formation of aggregates and the mesoscopic structures in the bulk ILs. High density of H-bonds facilitates networking of ILs structure, while perfect matching of hydrogen donor-acceptor sites provides network rigidity [63]. ILs surface tension is said to depend on the anion cation interactions - as the increase of ILs molecular size leads to enhanced interactions between ILs ion pairs, but results in decreased surface tension values [64]. Anion cation interactions, and especially the anion moiety, together with molecular packing, are said to strongly influence the density of ILs in the following order: $[\text{PF}_6]^- > [\text{BF}_4]^-$. It is visible, that more dense molecular packing, and, therefore, higher density, results from the presence of bulkier anions, such as the hexafluorophosphate one [65].

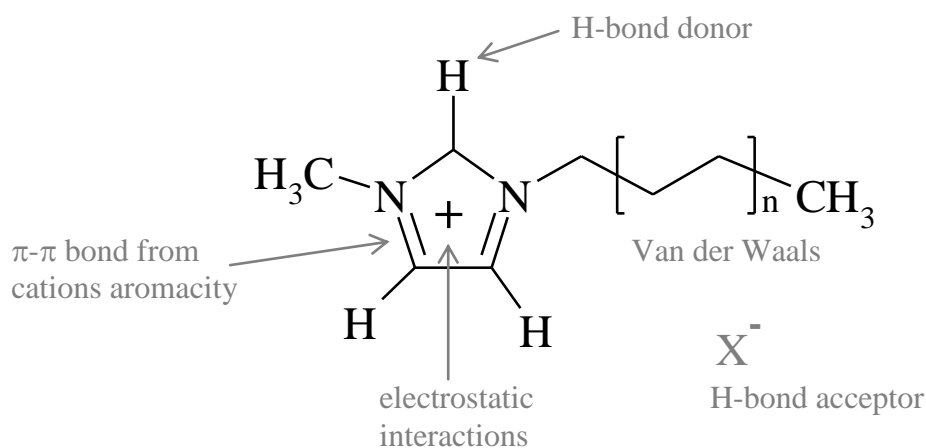


Figure 3. Interactions of n-alkyl-3-methylimidazolium ionic liquids

2.2.1. Nanostructure organization in imidazolium ionic liquids

There were many attempts to describe the organization of nanostructures within bulk imidazolium ILs, at first by means of theoretical molecular dynamics methods [37, 66], and afterwards confirmed experimentally [67, 68]. The alkyl chains segregate themselves into non-polar, nano-sized domains, whereas the imidazolium rings together with the anions form polar domains, also called an ionic network. Such mechanism was observed for ILs with alkyl chains longer than 4-6 carbon atoms, with an increase of the polar regions when the chains were elongated [37, 69]. Within bulk ILs the cations organize themselves parallel to each other, into sandwich-like arrangements, with or without a shift of imidazolium rings in the vertical plane, or perpendicularly to each other, in a T-shape arrangement (figure 4). Further overlying of the planes cations provokes formation of channels between the ions (figure 5).

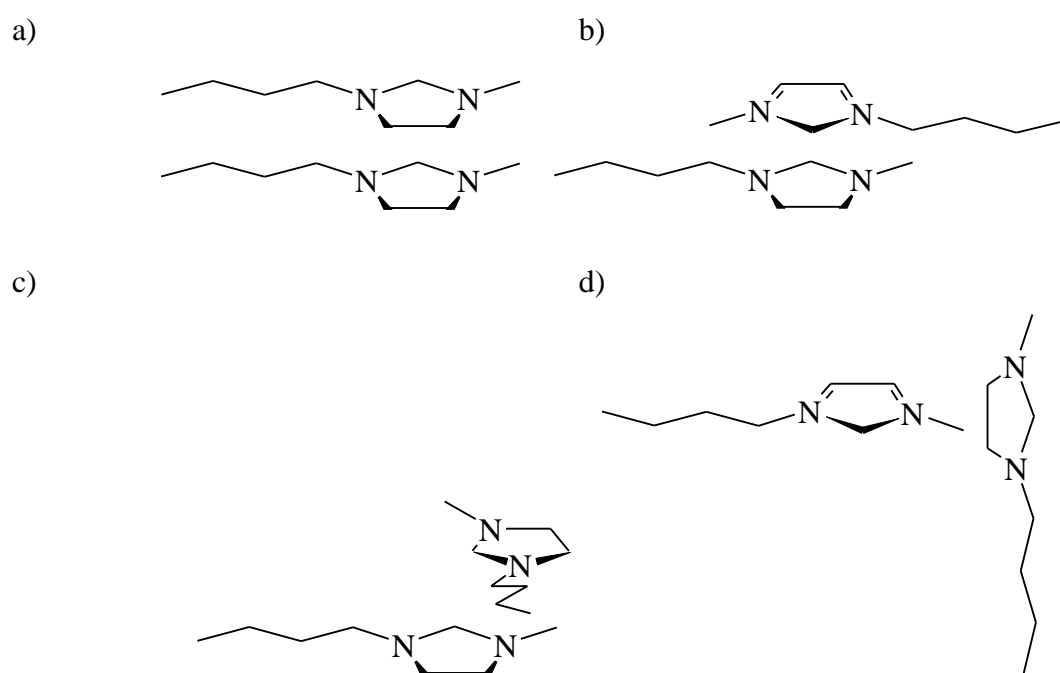


Figure 4. Spatial organization of ILs cations, a) sandwich (parallel), b) sandwich (anti-parallel) c) shifted sandwich (rotated), d) T-shape, d) sandwich

Considering ILs anions and cations as a one plane structure, due to the presence of multiple H-bonds, the ions organize themselves into a mesh-like structure (figure 6). The complexity of the mesh depends on the anion type, and the number of H-bond acceptor sites. Figure 6 depicts possible spatial arrangement of [EMIM][BF₄]. In fact, the nanostructure is three-dimensional, so the mesh structure is more complex and intricate [70]. Molecular simulation studies also provided information that their stability depends on the number of H-

bond donor-acceptor sites, which, when uneven, result in the presence of network defects and poorer mesh stability [58]. In general each cation is surrounded by anions, and each anion is surrounded by cations, but some of the conformations are more stable than others. It was computed that the most stable positions for both tetrafluoroborate and hexafluorophosphate anions together with the range of n-alkyl-3-methylimidazolium cations, was beneath the C2-H region (for the numbering of ILs atoms see figure 1 and 3), which is an acidic, positively charged area of the imidazolium ring [43].

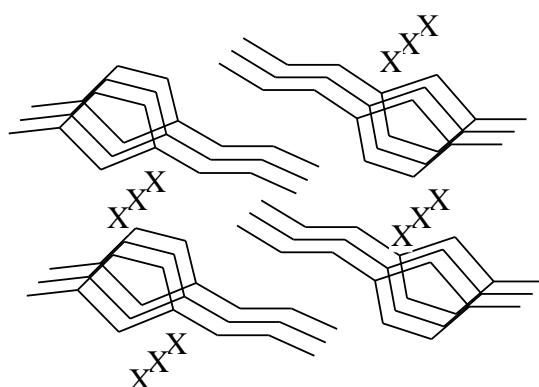


Figure 5. Schematic depiction of channels between imidazolium cations, where X denotes anions

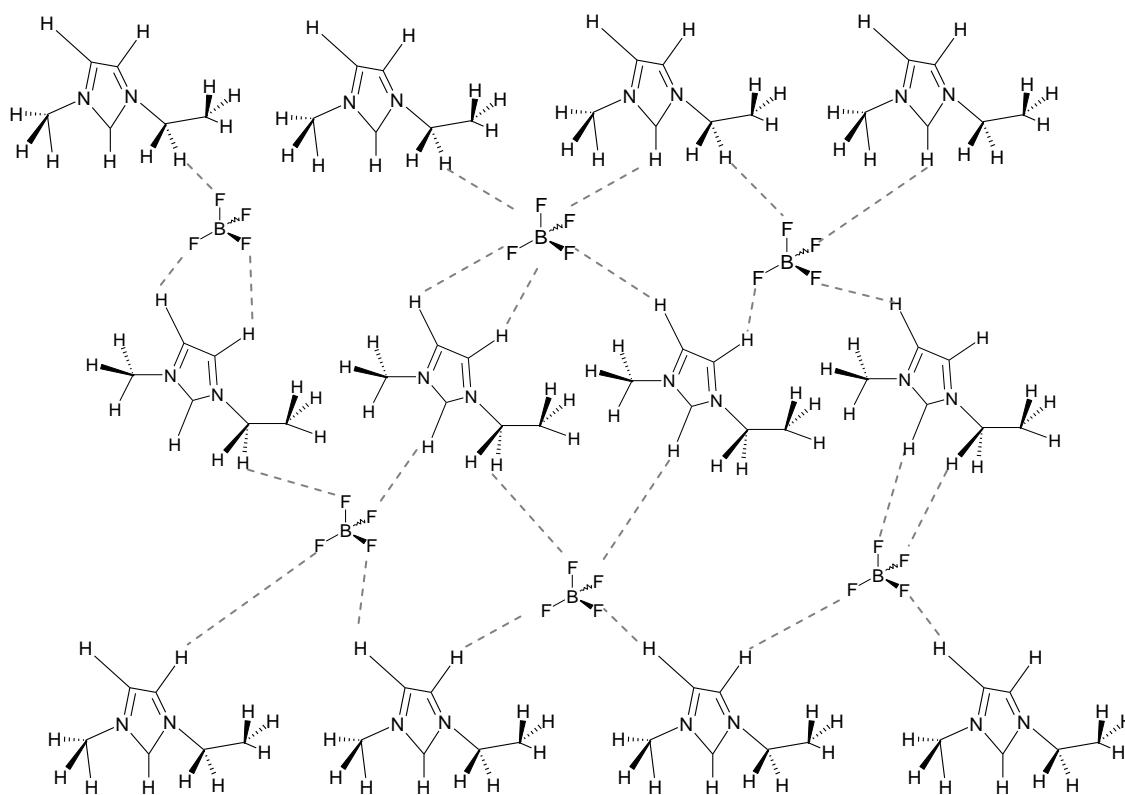


Figure 6. Mesh-like organization of [EMIM][BF₄] ions [43], [58]

2.2.2. Gordon parameter

Gordon parameter (G) is a measure of cohesive energy density of a solvent, and was described for the first time in year 1975 [71]. This parameter is often used as a measure of solvents ability (including ionic liquids [10, 72]) to provide self-ordering of amphiphiles, this may be employed as a predictive factor of this feature, and is calculated from surface tension value divided by molar volume, which is the molar mass divided by density (equation 19). The higher is the Gordon value of a solvent, the higher is its solvophobic effect, therefore the better are its self-assembly promoting properties [10, 73]. For better presentation of the micellization, Gordon parameter G is usually plotted against Gibbs free energy ΔG_m .

Due to the literature, in order to support aggregation, the Gordon value of a solvent must exceed 1.2 J m^{-3} [74], however, it was already reported that in many cases, e.g. for *N*-tert-butylformaldehyde, much lower value ($G = 0.53 \text{ J m}^{-3}$), still enables aggregation [9]. In contrary, e.g. 3-methylsyndone, has very high Gordon value ($G = 15 \text{ J m}^{-3}$), but shows no evidences for supporting amphiphilic self-ordering, what is explained with a lack of three-dimensional hydrogen-bond structure [75]. The highest known Gordon values for solvents supporting self-assembly of surfactants, were reported for water ($G = 2.74 \text{ J m}^{-3}$) and hydrazine ($G = 2.12 \text{ J m}^{-3}$) [76].

2.3. Nonionic surface active agents in ionic liquids

2.3.1. Micellar aggregation of surface active agents

The phenomenon of self-aggregation of surface active agents is not a new topic, thus self-ordering in ionic liquids was reported for the first time by Evans in 1983 [77], for cationic tetradecyl pyridinium bromide and hexadecyl pyridinium bromide in a simple IL, ethylammonium nitrate (EAN). His research involved determination of the micelles, their sizes and aggregation numbers. Since then both ionic and nonionic surfactants were examined for micellization in many protic and aprotic ionic liquids of more or less complex structures.

Micellar aggregation phenomenon of amphiphilic compounds is an entropy-driven, spontaneous process, in which surfactant monomers arrange themselves into spheres, in order to minimize their contact with the surrounding solvent [78]. Micellar aggregation is best

understood and characterized in aqueous systems, nevertheless numerous researches were dedicated to characterize this process in a variety of non-aqueous solvents, such as glycols, amides, some acids and other organic compounds, as reported by Greaves [9].

Micelle formation phenomenon of surface active agents in water takes place by means of hydrophobic effect, which leads to organization of the amphiphilic structures with their hydrophilic heads towards surrounding water molecules, and hydrophobic tails towards micelle core (figure 7). Micellization in ionic liquids is said to be driven by the solvophobic effect, which is also elucidated by the aggregation of alkyl groups in a solvent [9, 72]. There are claims, that the solvophobic effect causes change of Gibbs energy of micellization, and is connected with cohesive energy density, and thereby with the Gordon value [79]. Nevertheless, when talking about the solvophobic effect, the issue of its quantification is rarely mentioned. Therefore, the depiction of its magnitude is given by Gibbs energies and enthalpies of solvation, which enable to understand it both qualitatively and quantitatively [80, 81].

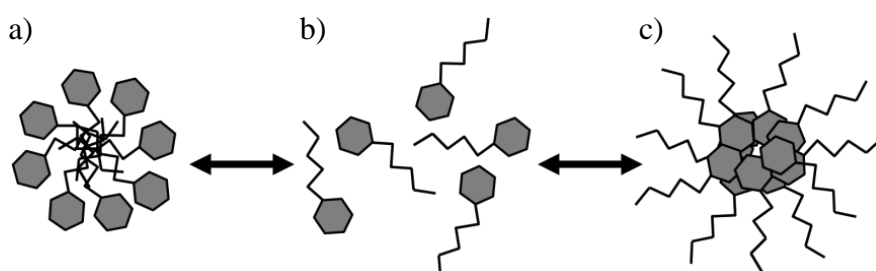


Figure 7. Formation of a) normal and c) reverse micelles from b) surfactant monomers

2.3.2. Micellar aggregation of nonionic surface active agents in imidazolium ionic liquids

Development of micellar systems consisting of amphiphiles in ionic liquids was firstly based on ionic surface active agents. The first publication on ionic surfactant micelles in ILs was released in year 1983 [77], the research on nonionic surfactant micelles in ILs was published until 20 years later, in year 2003, by Anderson and Pino [82]. They analyzed aggregation behavior of polyoxyethylene-type (POE-type) surfactants, Brij-35 and Brij-700, in two ionic liquids, 1-butyl-3-methylimidazolium chloride and more complex 1-butyl-3-

methylimidazolium hexafluorophosphate. It was observed that analogously to aqueous solutions, the surface tension plot in the function of surfactant concentration undergoes firstly sudden decrease and then stabilization. They called the observed mechanism a solvophobic effect, as it proceeded similarly to the hydrophobic effect in aqueous solutions. However, obtained values of critical micelle concentrations (CMCs) were significantly higher than in water. It was concluded, that surfactants organize themselves in normal micelles and deplete surface tension of the ionic liquids, just in other solvents.

Fletcher and Pandey [8] performed a research on the aggregation of a number of surfactants, including nonionic Tween-20, Triton X-100, Brij-35, Brij-700, in 1-ethyl-3-methylimidazolium bis(trifluoromethylsulfonyl)imide. The measurements included solvatochromic probes response, as an alternative to commonly used methods. According to the authors, all of the analyzed nonionic surfactants were proven to self-aggregate within [EMIM][NTf₂] ionic liquid. However, presented results were focused on the interactions of systems' components with the dye, rather than solvent-solute relations.

Formation of micelles in Brij 76/[BMIM][BF₄] system was confirmed by Tang and group [83]. The measurements were performed under elevated temperatures employing FT-IR, DSC, NMR methods and polarized optical microscopy to confirm formation of surfactant aggregates.

Tran and Yu [84] presented a different method for CMC determination, which was near-infrared spectroscopic technique used for analysis of nonionic Triton X-100, Brij-35, Brij-700, in [BMIM][PF₆] and [EMIM][NTf₂] ionic liquids. CMC values obtained by the authors agreed with literature CMC determined with other methods.

In the study on solvent dynamics and rotational relaxation of Coumarin 153, Chakrabarty and coworkers [85] examined micellar system of nonionic Brij-35 surfactant in [BMIM][PF₆]. The analysis involved observation of the dynamics in pure IL and in the presence of micelles, at which, due to increased viscosity, the dynamics was slower, and so was the rotational relaxation.

Patrascu and coauthors [86] reported aggregation behavior of a series of PEG surfactants, C_nE_m, with varying structures (C₁₆E₈, C₁₄E₈, C₁₂E₈, C₁₂E₆, C₁₂E₄), in 1-butyl-3-methylimidazolium ILs with three different counterions, tetrafluoroborate [BF₄],

hexafluorophosphate, $[\text{PF}_6]$ and bis(trifluoromethylsulfonyl)amide $[\text{NTf}_2]$. The measurements involved tensometric technique (surface tension) and DLS, to confirm the presence and provide the hydrodynamic diameters of the micelles. Due to the authors, obtained aggregates had similar size to the ones found in formamide, and smaller than in water, whereas the CMCs were higher comparing to aqueous solutions.

Seth and group [87] continued the study on the solvation time in micellar systems of C_{14}E_8 and C_{12}E_8 in $[\text{BMIM}][\text{BF}_4]$. The measurements revealed, that in comparison to neat IL the solvation time in micellar systems is increased, however, in much smaller manner than in water-based systems. Determined micellar diameters of C_{12}E_8 were smaller than of C_{14}E_8 , what is explained by the alkyl chain length.

Wu and group [6] performed surface tension measurements of binary solutions of oleyoxyethylene (20) sorbitan monolaurate (Tween 20) in $[\text{BMIM}][\text{BF}_4]$ and $[\text{BMIM}][\text{PF}_6]$ ionic liquids. Critical micelle concentrations in different temperatures enabled calculation of thermodynamic parameters. Obtained CMC values showed, that lower surfactant concentration was required to form micelles in tetrafluoroborate ionic liquid than in hexafluorophosphate one. Moreover, the freeze-fracture transmission electron microscopy provided size and shape of formed surfactant aggregates. Obtained results together with ^1H NMR analysis confirmed that Tween 20 aggregates are indeed micelles similar to the ones found in aqueous solutions.

Gao et al [88] performed a study on another PEG surfactant, commercially known as Triton X-100, in two 1-butyl-3-methylimidazolium ILs with $[\text{BF}_4]$ and $[\text{PF}_6]$ counterions. Again the tensometric technique was used to determine the formation of micelles from the surface tension plots, obtaining CMCs higher than in water. Additionally the ^1H NMR analysis showed that ILs ion pair became separated due to presence of surfactant molecules

Misono and Inoue [89] presented a research on clouding of POE-type surfactants ($\text{C}_{12}\text{E}_5, \text{C}_{12}\text{E}_6, \text{C}_{12}\text{E}_7, \text{C}_{10}\text{E}_6$, and C_{14}E_6) in $[\text{BMIM}][\text{BF}_4]$, regarded as a model ionic liquid. They observed that the same as in aqueous systems, the hydrodynamic diameters of micelles increase with increasing temperature. Performed analysis provided useful data on the character of the systems, giving good background for aggregation studies.

Later on the same researchers [90] performed an analysis of $C_{12}E_5$ clouding behavior in [BMIM][PF₆], revealing that hydrodynamic diameters of the micelles grow with the temperature increase. It was concluded, that solvophobicity of used IL is weaker than of the previously used [BMIM] [BF₄], therefore micelle formation promoting properties are weaker, resulting in higher CMC values.

Inoue group [39] analyzed aggregation behavior of a series of PEG-type surfactants with varying chain length ($C_{10}E_6$, $C_{12}E_6$, $C_{14}E_6$, $C_{12}E_5$) in 1-butyl-3-methylimidazolium tetrafluoroborate ([BMIM][BF₄]). The values of CMCs were determined by ¹H NMR analysis. The measurements were performed in different temperatures, to determine the thermodynamic parameters of micellization, and afterwards it was stated that in room temperatures micellization is entropy-driven. Further on the same group [91] extended the research with [BMIM][PF₆] ionic liquid, what enabled to determine the influence of ILs counterion on the CMC values. It was observed, that given surfactants aggregate in lower concentrations in ILs with hexafluorophosphate rather than with tetrafluoroborate anions.

Li and coworkers [92] conducted a research on the interactions of 1-decyl-3-methylimidazolium bromide and 1-decyl-3-methylimidazolium tetrafluoroborate with added POE surfactant, C_8E_4 . They stated that the surfactant is more miscible with IL containing [Br] anion due to higher attracting interactions, whereas [BF₄] anion forms more bonds with ILs cation rather than with the oxyethylene chain of the surfactant. The final conclusion was that besides size and polar nature of ILs anion, also the interactions are to be included when considering interactions with surfactants.

2.3.3. Micellar aggregation of nonionic surface active agents in imidazolium ionic liquids mixtures

Application of mixtures of ILs as self-ordering supporting media for surface active agents was already confirmed to broaden their aggregation-supporting properties, enable modification of both critical micelle concentration values and sizes of micellar aggregates.

Inoue et al [93] performed a broad study on PEG surfactants ($C_{10}E_5$, $C_{12}E_5$, $C_{14}E_5$, $C_{14}E_6$, and $C_{14}E_8$) clouding and aggregation in 1-ethyl-3-methylimidazolium tetrafluoroborate and 1-hexyl-3-methylimidazolium tetrafluoroborate, and in their mixtures with varying

weight fractions, in a broad range of temperatures. The ^1H NMR analysis enabled to observe, that in the mixture of used ILs, [HMIM][BF₄] was predominant to interact with the surfactants. The group concluded that self-assembly supporting properties of ILs (which have different affinities towards given surfactants) can be tuned by mixing two of them. The same group [94] analyzed the ability of some other PEG surfactants (C₁₀E₆, C₁₂E₆, C₁₄E₆, C₁₂E₅) to aggregate in [EMIM][BF₄] and [HMIM][BF₄], and in their mixtures. As a result, surfactants initially unable to dissolve in [EMIM][BF₄] and to form micelles in [HMIM][BF₄], aggregated in the 1:1 weight mixture of both ILs in 30°C. The results were confirmed with ^1H NMR and DLS analysis. What is more, an increase of [EMIM][BF₄] weight ratio in the solution caused decrease of CMCs and increase of micellar hydrodynamic diameters.

Rao and coworkers [95] characterized micellization of Triton X-100 in the mixtures of EAN and [BMIM][PF₆], considering two cases in which one or another IL constituted the dominant mass fraction. Prepared system were analyzed by means of ^1H NMR, pulsed-field gradient spin-echo NMR (PFGSE NMR), and methyl orange (MO) and coumarin 153 (C-153) as absorption and emission probes, respectively. The group observed micellar aggregation of TX-100 and penetration of the added ILs into the surfactant micelles. The group observed an increase of solvation dynamics when adding EAN to TX-100/[BMIM][PF₆], whereas change was reported when adding [BMIM][PF₆] to TX-100/EAN.

Thomaier and Kunz [96] performed a study on two surfactant-like ILs aggregation in EAN, another ionic liquid. CMC values were determined from surface tension isotherms, whereas micellar diameters were provided with DLS method. Temperature analysis was performed using NMR and DSC techniques. The study confirmed that the mixture of two ILs forms colloidal systems in the manner surfactants form in aqueous solutions. It was underlined, that presented systems were stable up to 250°C, what may broaden the application of such aggregates in high temperature nanoscale applications.

2.4. Literature review summary

Numbers of methods have been proposed in the literature throughout the years to study the ability of imidazolium ionic liquids to support micellar aggregation of nonionic surface active agents. Those methods represent the simplest physicochemical measurements (surface tension, density, viscosity) but also indirect experiments such as solvatochromic probes, DLS or FF-TEM, often complemented with theoretical approaches like molecular dynamics. Withdrawn conclusions provide new insight into the phenomenon of self-ordering of surfactants in imidazolium ILs, and show the variety of methods to examine such systems from different perspectives.

Although known data provide a lot of information on selected surfactant/IL micellar systems, a dependence of ILs and surfactants structures on micellization and micellar parameters has not been yet determined. What is more, a comprehensive characteristic of micellar systems of nonionic surfactants in imidazolium ionic liquids is missing.

3. Aims and scope

The scientific aim of this work is to elucidate and characterize micellar aggregation of nonionic surface active agents in imidazolium ionic liquids with selected anions and cations. The relationship between the structures of the constituents of surfactant/IL systems was considered including the structure of nonionic surface active agents, the number of chains, their branching and length (the number of oxyethylene units), and the structure of ILs, i.e. the anion type, and length of cations alkyl chain. Ionic liquids, which are organic salts, may be referred to typical solvents – water and ethylene glycol.

The main hypothesis is: nonionic surface active agents undergo self-ordering in ionic liquids. However, the knowledge on this behavior is scarce and requires better understanding, further research and systematization, as listed below

- imidazolium ionic liquids support self-organization (micellization) of nonionic surface active agents,
- mixtures of imidazolium ionic liquids support self-organization (micellization) of nonionic surface active agents,
- self-organization of nonionic surface active agents in imidazolium ionic liquids takes place in a manner similar to aqueous and ethylene glycol solutions
- micelle formation depends on the structures of both ILs and surfactants
- critical micelle concentration (CMC) values may be controlled by the type of ILs ions, type of surfactant and temperature
- Gordon parameter allows prediction of the ability of ionic liquids to support micellar aggregation of nonionic surfactants
- determination of aggregation numbers of nonionic surfactants in imidazolium ionic liquids micellar systems may be based on conductometric measurements

The scope of the work includes examination of surfactant/IL systems for the presence of micellar aggregates, characteristics of the systems, determination of the CMC values from surface tension and additionally from apparent molar volume plots, surface and thermodynamic parameters, and elucidation of the interfacial interactions.

The investigation based mainly on experimental surface tension determination, and presentation of obtained data in the form of surface tension isotherms for different surfactant concentrations.



Determined parameters included:

- critical micelle concentration (CMC)
- surface excess value (Γ_{\max})
- minimum area occupied by surfactant molecule (A_{\min})
- surface tension value at CMC (γ_{CMC})

The presence of micellar aggregates was investigated by means of DLS analysis and conductometric measurements, while characteristics of analyzed systems included determination of micelle size distribution, water content, density and viscosity data.

Thermodynamic measurements were carried out at 15.0, 25.0, 35.0 and 45.0°C, and Gibbs free energy of micellization (ΔG_m), Gibbs free energy of adsorption (ΔG_{ad}), surface pressure (Π_{CMC}), enthalpy (ΔH_m), entropy (ΔS_m) were calculated.

Series of IL mixtures with different volumetric proportions were analyzed at 25.0°C as media capable of supporting micelle formation of nonionic surfactants.

For better description and characteristics, obtained results for nonionic surfactants in imidazolium ionic liquids were compared with corresponding water and ethylene glycol-based systems.

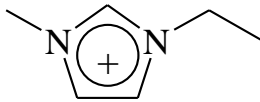
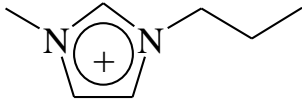
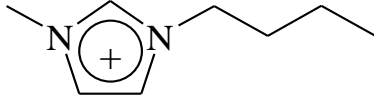
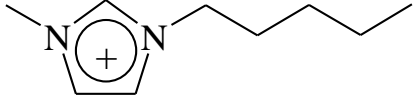
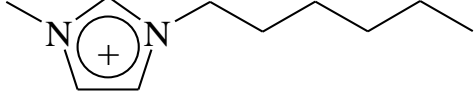
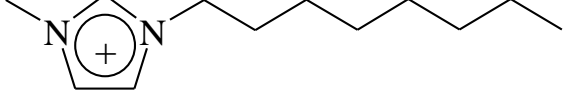
4. Experimental

4.1. Reagents and materials

4.1.1. Ionic liquids

Alkyl-3-methylimidazolium ionic liquids containing 2, 3, 4, 5, 6 and 8 carbon atoms in the cation alkyl chain (table 2), and four types of anions, namely tetrafluoroborate, $[\text{BF}_4]$, hexafluorophosphate, $[\text{PF}_6]$, bis(trifluoromethylsulfonyl)imide, $[\text{NTf}_2]$ and trifluoromethanesulfonate, $[\text{OTf}]$ (table 3) were used in the research. 1-butyl-3-methylimidazolium hexafluorophosphate IL was obtained from Merck, Germany. The remaining ILs were obtained from IoLiTec, Germany.

Table 2. Structures of ILs cations

Cations	Structures
1-ethyl-3-methylimidazolium, [EMIM]	
1-propyl-3-methylimidazolium, [PrMIM]	
1-butyl-3-methylimidazolium, [BMIM]	
1-pentyl-3-methylimidazolium, [PMIM]	
1-hexyl-3-methylimidazolium, [HMIM]	
1-octyl-3-methylimidazolium, [OMIM]	

The purity of solvents, declared by producers, exceeds 99 percent. The water content determined by means of Karl-Fisher coulometric titration, remained as above, in table 4. Before use ILs were maintained in 70.0°C in vacuum for 24h, to remove any volatile impurities. All the ionic liquids used in the study remained liquid at 15.0 – 45.0°C.

Table 3. Structures of ILs anions

Anions	Structures
tetrafluoroborate, [BF ₄]	$\begin{array}{c} \text{F} \\ \\ \text{F}-\text{B}-\text{F} \\ \\ \text{F} \end{array}$
hexafluorophosphate, [PF ₆]	$\begin{array}{c} \text{F} \\ \\ \text{F}-\text{P}-\text{F} \\ \quad \\ \text{F} \quad \text{F} \\ \\ \text{F} \end{array}$
trifluoromethanesulfonate, [OTf]	$\begin{array}{c} \text{O} \\ \\ \text{O}-\text{S}-\text{CF}_3 \\ \\ \text{O} \end{array}$
bis(trifluoromethylsulfonyl)imide, [NTf ₂]	$\begin{array}{c} \text{O} \quad \quad \text{O} \\ \quad \quad \\ \text{FC}_3-\text{S}-\text{N}-\text{S}-\text{CF}_3 \\ \quad \quad \\ \text{O} \quad \quad \text{O} \end{array}$

Table 4. Water content in ionic liquids used in the study

Ionic liquids		Water content [ppm]
1-ethyl-3-methylimidazolium tetrafluoroborate	[EMIM][BF ₄]	511
3-methyl-1-propylimidazolium tetrafluoroborate	[PrMIM][BF ₄]	690
1-butyl-3-methylimidazolium tetrafluoroborate	[BMIM][BF ₄]	320
3-methyl-1-pentylimidazolium tetrafluoroborate	[PMIM][BF ₄]	185
1-hexyl-3-methylimidazolium tetrafluoroborate	[HMIM][BF ₄]	199
1-octyl-3-methylimidazolium tetrafluoroborate	[OMIM][BF ₄]	290
1-butyl-3-methylimidazolium hexafluorophosphate	[BMIM][PF ₆]	256
3-methyl-1-pentylimidazolium hexafluorophosphate	[PMIM][PF ₆]	254
1-hexyl-3-methylimidazolium hexafluorophosphate	[HMIM][PF ₆]	245
1-octyl-3-methylimidazolium hexafluorophosphate	[OMIM][PF ₆]	190
1-ethyl-3-methylimidazolium trimethylsulfonate	[EMIM][OTf]	220
1-butyl-3-methylimidazolium trimethylsulfonate	[BMIM][OTf]	270
1-hexyl-3-methylimidazolium trimethylsulfonate	[HMIM][OTf]	119
1-octyl-3-methylimidazolium trimethylsulfonate	[OMIM][OTf]	230
1-ethyl-3-methylimidazolium bis(trifluoromethanesulfonyl)imide	[EMIM][NTf ₂]	191
1-butyl-3-methylimidazolium bis(trifluoromethanesulfonyl)imide	[BMIM][NTf ₂]	110
1-hexyl-3-methylimidazolium bis(trifluoromethanesulfonyl)imide	[HMIM][NTf ₂]	173
1-octyl-3-methylimidazolium bis(trifluoromethanesulfonyl)imide	[OMIM][NTf ₂]	162

Analogue analyses were done for surfactants in deionized water and ethylene glycol. Water was demineralized using HLP 5 by Hydrolap, and used without further preparation. Ethylene glycol was obtained from Sigma Aldrich, with purity grade over 99.9 percent, provided by the producer, and used as received.

4.1.2. Surfactants

The surface active compounds were commercial Triton X and Tween nonionic surfactants. Triton X is a polyoxyethylene octyl phenyl ether surfactant with polyoxyethylene groups within the structure (a hydrophobic part), and an aromatic hydrocarbon (hydrophobic) group. In the investigation four Triton X types were used, which were Triton X-100, Triton X-114, Triton X-45 and Triton X-15, having 9.5, 7.5, 4.5 and 1.5 oxyethylene groups (n), respectively (figure 8). Tween compounds are polysorbate-type nonionic surfactants, obtained from sorbitol derivatives and fatty acids estrification.

The research involved application of Tween 20 (polyoxyethylene (20) sorbitan monolaurate), Tween 40 (polyoxyethylene (20) sorbitan monopalmitate), Tween 60 (polyoxyethylene (20) sorbitan monostearate), and Tween 80 (polyoxyethylene (20) sorbitan monooleate) (figure 9). Both Triton X and Tween types of surfactants are mixtures of species of varying numbers of oxyethylene groups, therefore, the given numbers are the mean values of OE units. Triton X-100 surfactant was obtained from Roth, Germany, Triton X-114, Triton X-45 and Triton X-15 from Sigma Aldrich, Germany. Tween surfactants were obtained from Croda, Poland. All the surfactants were used without additional preparation.

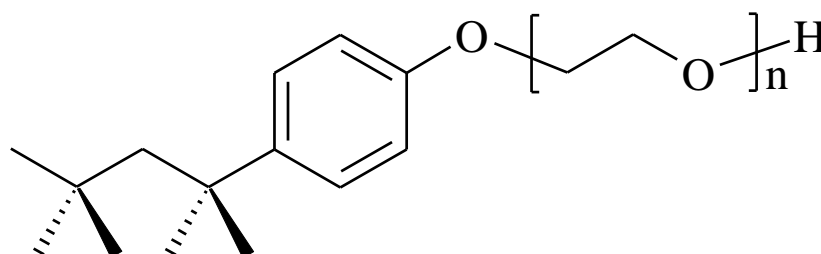


Figure 8. Structure of Triton X surfactants, where $n = 9.5, 7.5, 4.5$ and 1.5 for TX-100, TX-114, TX-45 and TX-15, respectively

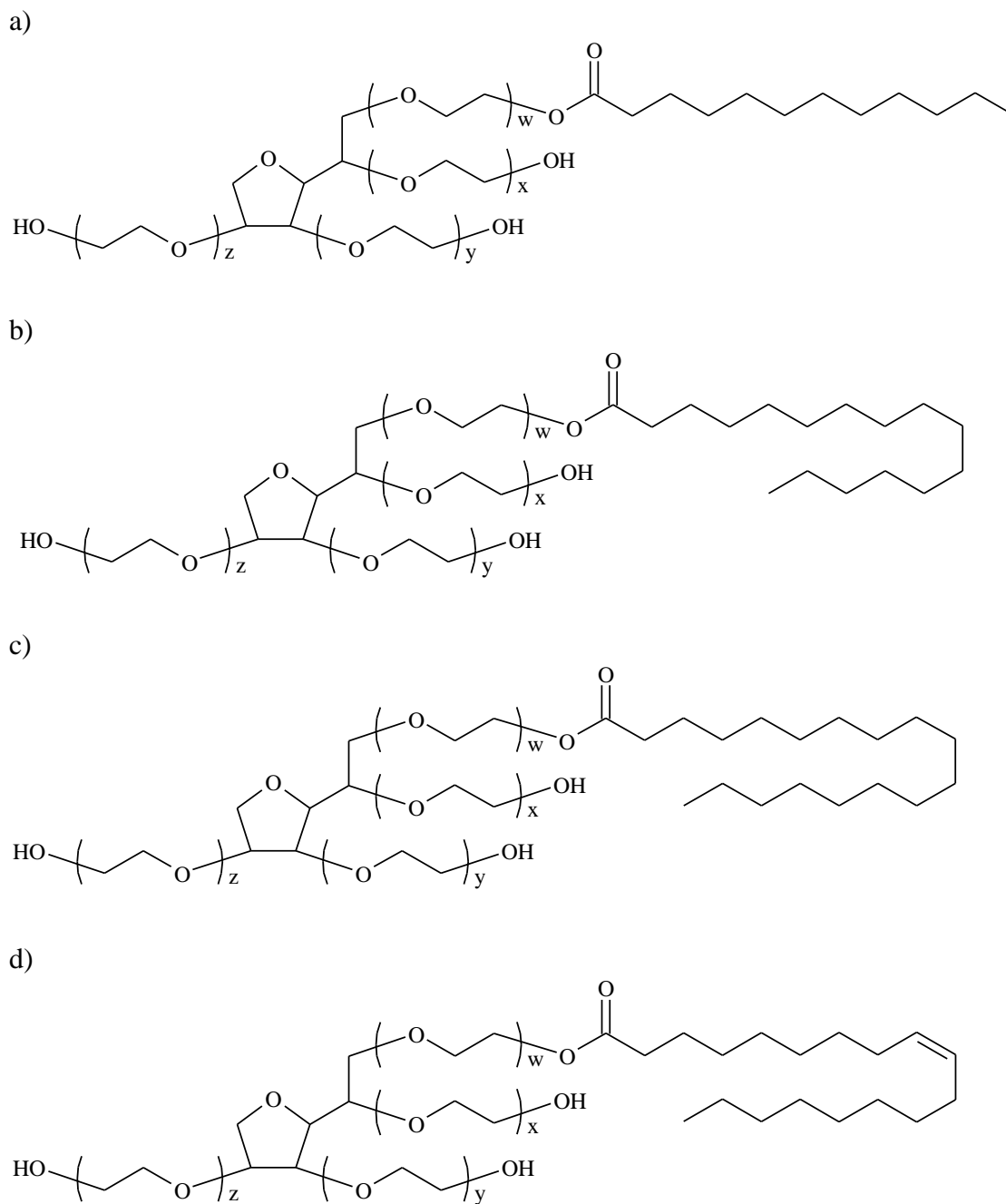


Figure 9. Structures of Tween surfactants: a) Tween 20, b) Tween 40, c) Tween 60, c) Tween 80

4.2. Apparatus, methodology and analytical methods

4.2.1. Sample preparation

The samples of nonionic surfactants in preconditioned ILs and in model solvents were prepared in 5 to 25 cm³ volumetric flasks. Before use, the glassware was rinsed with acetone and distilled water and dried. Surfactants were weighted using laboratory analytical balance at 25.0°C. For each system a series of 10-20 surfactant concentrations was prepared and left for 24h at 25.0°C to reach equilibrium. Afterwards the samples were subjected to the series of analyses, described below.

4.2.2. Density determination

The density was measurement using digital density meter with oscillating U-tube, model DM40, Mettler Toledo, USA. The principle of the device bases on the law of harmonic oscillation (the Mass-Spring Model). The U-tube is filled with the sample by a peristaltic pump, and subjected to the electromagnetic force. Frequency measurement and vibration duration allows determination of the density value of the analyzed sample. The oscillation period τ , and density ρ , are expressed by equations 1 and 2, respectively:

$$\tau = 2\pi \sqrt{\frac{\rho v + m}{c}} \quad (1)$$

$$\rho = \frac{K}{4\pi^2 V_c} \tau^2 - \frac{m_c}{V_c} \quad (2)$$

Where ρ is density of the sample in the measuring cell [g/cm³], V_c is sample volume ergo capacity of the tube [cm³], m_c is the mass of the measuring cell [g], K is the measuring cell constant [g s²]. Before each measurement series the device calibration was controlled with a measurement of distilled water and dried air densities. The results were given with the accuracy to four decimal places.

$$V_\phi = \frac{M}{\rho} - \frac{10^3(\rho - \rho_0)}{\rho \rho_0 m} \quad (3)$$

Density coefficients were used to calculate the values of apparent molar volumes, V_ϕ , (equation 3), where M is the molar mass, ρ and ρ_0 are densities of the solution and the solvent, respectively, and m is the molality [97]. The values of V_ϕ plotted against surfactant concentration are also used for determination of CMC regions.



4.2.3. Dynamic viscosity determination

The dynamic viscosity values were measured using DV-III Ultra, Brookfield, Germany, with cone-plate method, equipped with CPE-40 spindle (sample volume 0.5 cm³). The measurements were performed at 15, 25, 35 and 45°C (±0.1 °C), adjusted with water bath. Dynamic viscosity indices were calculated with software provided by the producer, from the measured values of shear stress against shear rate, given by formula 4.

$$\eta = \frac{\tau}{\dot{\gamma}} = \frac{\text{shear stress}}{\text{shear rate}} \quad (4)$$

Dynamic viscosity values were determined for pure solvents and series of solutions with increasing surfactant concentrations in the range of temperatures.

4.2.4. Surface tension determination

Surface tension values were measured using OCA15 DataPhysics goniometer, Germany. The measurements were performed in pendant-drop mode in a thermostated chamber supported by water bath, at 15, 25, 35, 45°C (±0.1 °C). The apparatus was equipped with DataPhysics stainless steel or Teflon-coated needle, with 1.65 mm outer diameter. The Teflon-coated needle was used for liquids perfectly wetting the stainless steel needle, which took place in case of trifluoromethanesulfonate- bis(trifluoromethylsulfonyl)imide-based ILs, and in systems with elevated surfactant content. The surface tension values were calculated by SCA22 software, provided by the producer, basing on the Young-Laplace equation (formula 5) where γ = surface tension [mN/m], ΔP = pressure difference across the interface, and R_1 and R_2 = principal droplet radii (see figure 10). A number of five comparable values were collected within measurement series of each sample.

$$\Delta P = (P_{\text{int}} - P_{\text{ext}}) = \gamma \left(\frac{1}{R_1} + \frac{1}{R_2} \right) \quad (5)$$

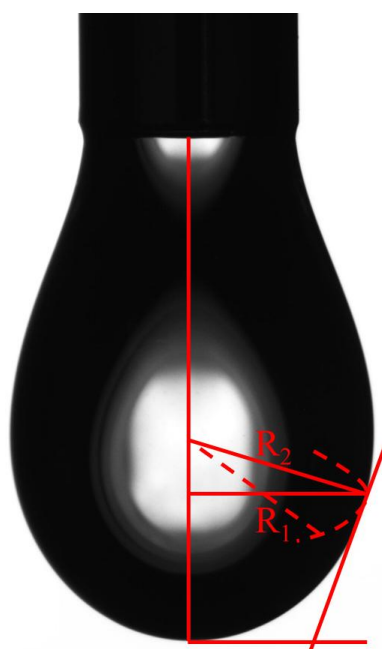


Figure 10. Derivation of the Young-Laplace fit on a pendant drop, where R_1 and R_2 are principal droplet radii

4.2.5. Conductivity - determination of associated cations number

Conductivity was measured with standard conductometric sensors, model EPEST-2ZAM (Eurosens, Poland; measurement range 1 $\mu\text{S}/\text{cm}$ – 100mS/cm, $k = 0.9 - 1 \text{ cm}^{-1}$, with epoxy resin body with 0.8 cm diameter), together with the Multifunction meter, model CX-710 (Elmetron, Poland). The measurements were performed in stable, controlled temperature conditions adjusted with water bath, coupled with a measurement glass vessel (10 cm^3). Before each measurement series the electrodes were calibrated with KCl buffer. The measurements were taken for each sample from the sample series, including pure solvents.

To calculate the number of ILs molecules which associate with the surfactant, an effective-medium approximation theories for suspensions of spherical particles were used, which assume that the properties of suspended particles are the same as the properties of the whole system [98], as it was showed by Lian *et al.*, with the use of theories, such as Looyenga, Bruggeman, or Maxwell-Wagner [99]. Basing on them, micellar solution of TX-100/IL may be treated as a system of scattered particles (dispersion of micelles), of a conductivity κ_p , dispersed in a conducting medium (ionic liquid), of conductivity κ_{IL} , at a volume fraction ϕ . According to Bruggeman's approximation, for systems consisting of spherical micelles, the conductivity meets the criteria of equation 6. When the system follows

conditions of $\kappa_s \gg \kappa_{IL} \gg \kappa_{surf}$, where κ_s is the conductivity of the solution, the formula may be simplified to formula 7.

$$\left(\frac{\kappa_s - \kappa_{surf}}{\kappa_{IL} - \kappa_{surf}} \right) \left(\frac{\kappa_{IL}}{\kappa_s} \right)^{\frac{1}{3}} = 1 - \phi \quad (6)$$

$$\left(\frac{\kappa_s}{\kappa_{IL}} \right)^{\frac{2}{3}} = 1 - \phi \quad (7)$$

As ILs possess hydrophilic character, the hydrophobic surfactant POE chains arrange themselves towards the micellar core. Consequently, $[\text{AMIM}]^+$ interact with surfactant OE groups on the micelle surface, and permeate into the aggregates, enlarging their effective volume from γ to $\gamma\phi$, where γ is an effective volume of pure surfactant micelle. Then the formula may be rewritten to formula 8, and consequently the volume ration $(1 - \gamma)$ is described by formula 9.

$$\left(\frac{\kappa_s}{\kappa_{IL}} \right)^{\frac{2}{3}} = 1 - \gamma\phi \quad (8)$$

$$\gamma - 1 = \frac{v_c}{v_{surf}} \frac{c_{ac} M_c}{c_{surf} M_{surf}} \quad (9)$$

Having partial specific volumes, \bar{v} , of the system components (equation 10) we may calculate n_{ac} , the number of $[\text{AMIM}]^+$ cations associated per surfactant molecule (equation 11), where c is the concentration, subscripts c and ac denote cations and associated cations.

$$\bar{v} = \frac{1}{\rho_s} \left(1 - \frac{d\rho}{dc} \right) \quad (10)$$

$$n_{ac} = \frac{c_{ac}}{c_{OE}} = (\gamma - 1) \frac{v_{surf} M_c}{c_{OE} v_c M_{surf}} \quad (11)$$



4.2.6. Hydrodynamic diameters - Dynamic Light Scattering

Micellar diameters were determined by means of Dynamic Light Scattering (DLS), using Zetasizer Nano, Malvern, UK. The device was equipped with He-Ne 4mW laser with 633nm wavelength, and an avalanche photodiode detector (Q.E 50% in 633nm). DLS method bases on Brownian motion, and is represented by Stokes-Einstein equation describing the relation of particle size and their velocity (formula 12), where D = diffusion constant, k_B = Boltzmann constant, T = absolute temperature, η = solvent viscosity, R = particle hydrodynamic diameter.

$$D = \frac{k_B T}{6\pi\eta R} \quad (12)$$

The measurements were performed in 15, 25, 35 and 45°C (± 0.1 °C), provided by Peltier temperature controller, in a standard quartz cuvette with square aperture. The results were calculated by the Malvern Zetasizer software, provided by the producer, using CONTIN analysis. The hydrodynamic diameters of the micelles are presented in plots as scattered light intensity (in %) vs. aggregates size (in nm).

4.2.7. Critical micelle concentration

Critical micelle concentration (CMC) is a concentration at which the association of surfactant molecules occurs, however the value may vary depending on the applied method of determination, therefore, CMC is rather a range of values, than a single concentration, as shown in figure 11. In aqueous solutions the CMCs of surfactants may be determined with a number of methods (e.g. surface tension, viscosity, density, and conductivity), however the micellization of nonionic surfactants in ionic liquids is best determined basing on surface tension vs. surfactant concentration plots, whereas the remaining methods give too blurred results or no proof for aggregation. Thus, besides surface tension measurements, the investigated systems may be analyzed for the presence of micelles by means of DLS and from density (or apparent molar volume) vs. surfactant concentration plots, as presented in the dissertation.

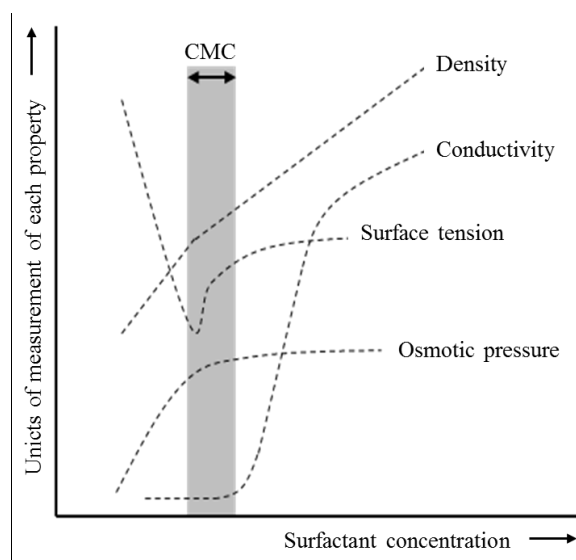


Figure 11. Inflection of solution parameters in the CMC region (from ref. [100])

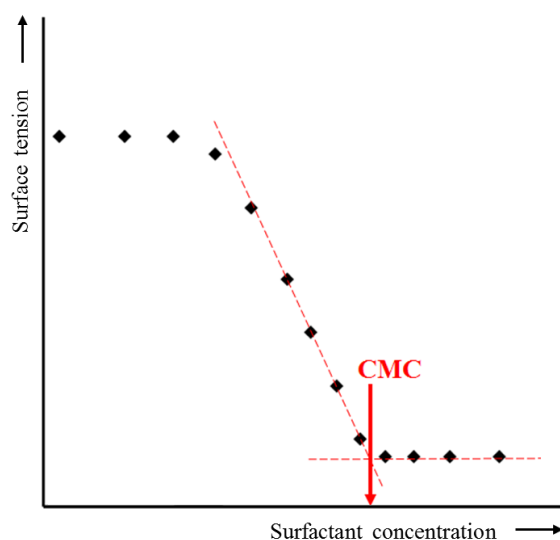


Figure 12. Determination of critical micelle concentration from a surface tension isotherm

In the investigation the critical micelle concentration values were determined from surface tension vs. surfactant concentration isotherms (figure 11). The critical micelle concentration values were calculated from the formulas describing the intersecting lines. Additional confirmation of the CMCs was performed by means of Dynamic Light Scattering (DLS) method as hydrodynamic diameters of the micelles, and with apparent molar volumes, which are derivatives of density values.

4.2.8. Physicochemical and thermodynamic parameters

Physicochemical and thermodynamic measurements give detailed information on the micellization process of binary solutions, its character, spontaneity, depending on the conditions. The parameters were calculated basing on the experimental results, using equations given in this section. Surface excess value, Γ_{\max} , and minimum surface area, A_{\min} , occupied by a single surfactant molecule on the air/solution interface were calculated using surface tension values by means of equations 13 and 14, where R = gas constant, T = absolute temperature, N_A = Avogadro's number, γ = surface tension. Surface pressure, Π_{cmc} , was calculated with equation 15.

$$\Gamma_{\max} = -\frac{1}{RT} \left[\frac{d\gamma}{d \ln c} \right]_{T,p} \quad (13)$$

$$A_{\min} = \frac{10^{16}}{N_A \cdot \Gamma_{\max}} \quad (14)$$

$$\Pi_{\text{CMC}} = \gamma_0 - \gamma_{\text{CMC}} \quad (15)$$

Free energy of micellization, ΔG_m , connected with the critical micelle concentration, was calculated using formula 16, where x_m denotes molar ratio at CMC. Enthalpy and entropy, ΔH_m , ΔS_m , were calculated using equations 17 and 18.

$$\Delta G_m = RT \ln x_m \quad (16)$$

$$\Delta H_m = \frac{\partial \left(\frac{\Delta G_m}{T} \right)}{\partial \left(\frac{1}{T} \right)} \quad (17)$$

$$\Delta S_m = \frac{(\Delta H_m - \Delta G_m)}{T} \quad (18)$$

Gordon parameter G , is a measure of cohesive energy density of a solvent, and is calculated from surface tension γ , divided by molar volume V_m to the power of 1/3. Molar volume is molar mass divided by density (equation 19).

$$G = \gamma / V_m^{1/3} \quad (19)$$

5. Results

The main goal of the investigation was to determine and describe micellar aggregation capability of selected Triton and Tween nonionic surfactants in 1-alkyl-3-methylimidazolium ionic liquids with tetrafluoroborate, hexafluorophosphate, trifluoromethanesulfonate and bis(trifluoromethanesulfonyl)imide anions. The investigation included analysis of 94 surfactant-in-IL systems composed of 7 types of nonionic surfactants and 18 imidazolium ionic liquids composed of a variation of four types of anions and a homologue series of 6 types of cations (see table 4).

5.1. Gordon parameter

The accuracy of calculated Gordon parameter strongly depends on the accuracy of determined density values. Due to the fact, that for the purpose of this investigation, the density values were measured using digital density meter providing an accuracy of four decimal places, therefore, further calculations based on this parameter (G values and apparent molar volumes) depend on this level of accuracy. Nevertheless, for the goal of evaluating micellization promoting abilities, such level of convenience is satisfactory.

Selected ionic liquids and model solvents, capable of supporting aggregation, together with density and Gordon values at 15.0, 25.0, 35.0 and 45.0°C, were listed in table 5 (for density and Gordon values of all investigated ILs at 25.0°C see table S. 1 in Supplementary Material). The temperature dependence of G parameter of investigated pure 1-alkyl-3-methylimidazolium ILs was also calculated (figure S. 1, Supplementary Material). The values of Gordon parameters at 25.0°C were plotted in figure 13, vs. the number of carbon atoms in ILs cation alkyl chains. The values strongly depend on ILs anion moiety, and decreases in the following order of anions present in ILs molecules $[\text{BF}_4] > [\text{PF}_6] > [\text{OTf}_2] > [\text{NTf}_2]$. The correlation results from increasing size of the anions, which limit micellization due to presence of more H-bonds and more intense solvent-solute interactions. What is more, increased length of alkyl chain in cations moiety provokes decrease of Gordon parameter. The presence of additional methyl groups in the chain provide more H-bond and van der Waals interactions, increasing solvation of amphiphile molecules, and thus, worse micellization supporting behavior.



Table 5. Gordon and density values of [AMIM][BF₄], water and ethylene glycol at 15, 25, 35 and 45°C

solvent	temperature [°C]	d ₀ [g/cm ³]	G [J/m ³]
[EMIM][BF₄]			
	15.0	1.2869 ±0.0002	1.0191
	25.0	1.2752 ±0.0001	0.9805
	35.0	1.2714 ±0.0003	0.9479
	45.0	1.2651 ±0.0001	0.9092
[PrMIM][BF₄]			
	15.0	1.2450 ±0.0001	0.9166
	25.0	1.2377 ±0.0002	0.8643
	35.0	1.2296 ±0.0002	0.8513
	45.0	1.2223 ±0.0001	0.8275
[BMIM][BF₄]			
	15.0	1.2073 ±0.0001	0.8041
	25.0	1.1994 ±0.0001	0.7831
	35.0	1.1925 ±0.0001	0.7619
	45.0	1.1853 ±0.0001	0.7522
[PMIM][BF₄]			
	15.0	1.1792 ±0.0003	0.7480
	25.0	1.1712 ±0.0001	0.6699
	35.0	1.1647 ±0.0001	0.6763
	45.0	1.2577 ±0.0002	0.6765
[HMIM][BF₄]			
	15.0	1.1530 ±0.0001	0.6787
	25.0	1.1454 ±0.0002	0.6442
	35.0	1.1387 ±0.0003	0.5956
	45.0	1.1316 ±0.0001	0.5692
water			
	15.0	0.9991 ±0.0001	2.8023
	25.0	0.9970 ±0.0001	2.7425
	35.0	0.9940 ±0.0001	2.6790
	45.0	0.9902 ±0.0002	2.6134
ethylene glycol			
	15.0	1.1170 ±0.0001	1.2350
	25.0	1.1097 ±0.0002	1.2185
	35.0	1.1028 ±0.0001	1.1857
	45.0	1.0955 ±0.0001	1.1586

The value of Gordon parameter for a solvent to support micellization, which is considered the lower limit for a solvent to support micellar aggregation, is 0.53 J m^{-3} [9], and is marked with a red line in figure 13. Therefore, it is assumed that all the ionic liquids above the red line should be capable of promoting micellization.

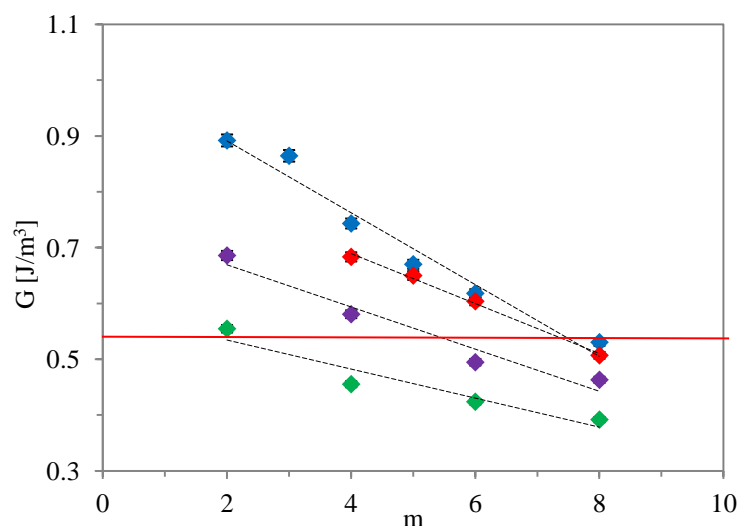


Figure 13. Gordon parameter (G) and the number of carbon atoms in ILs cation alkyl chain (m) regarding anion type: $[\text{BF}_4]$ (\blacklozenge), $[\text{PF}_6]$ (\blacklozenge), $[\text{OTf}]$ (\blacklozenge), and $[\text{NTf}_2]$ (\blacklozenge), at 25°C

5.2. Isotherms of nonionic surfactants in imidazolium ionic liquids

5.2.1. Cation type influence

In order to discuss the role of ILs structure, which includes both alkyl chain length in the imidazolium ring, and the anion moiety, on their capability to support micellar aggregation of the nonionic surfactants (Triton X-100, Triton X-114, Triton X-45, Triton X-15, Tween 20, Tween 60, Tween 80), the investigation included IL species having two to eight carbon atoms in the alkyl chains, $[\text{EMIM}]$, $[\text{PrMIM}]$, $[\text{BMIM}]$, $[\text{PMIM}]$, $[\text{HMIM}]$, $[\text{OMIM}]$, and four possible anions, $[\text{BF}_4]$, $[\text{PF}_6]$, $[\text{OTf}]$ and $[\text{NTf}_2]$. Obtained surface tension values (γ), plotted against surfactant concentrations in selected ILs were used to depict adsorption of the amphiphiles at the air/IL interface, and micellization, given by the critical micelle concentration values, and surface parameters (Γ_{max} , A_{min} , Π_{cmc} , ΔG_{m} , ΔG_{ad}).

Having the solutions of surfactants in ionic liquids with one type of anion moiety but different imidazolium cations, one may observe how the alkyl chain length affects the surface properties of obtained systems. Aggregation behaviour, visible as a discontinuity of the surface tension plot, may be divided into three stages. Firstly, at very low amphiphile



concentrations, the surfactant solubilizes in the IL, what is accompanied with adsorption of surfactant molecules at air/IL interface, replacing some of ILs molecules. At this stage the surface tension values are similar to the ones of pure solvent. In the second stage, surface tension values decrease, which is a result of continuing surfactant adsorption at air/liquid interface, until the saturation is reached. The molecules aggregate due to interactions between nonpolar fragments of the surfactant molecules. Finally, in the third stage, formation of micellar aggregates takes place, which is visible in the plot as horizontal line of the isotherm. The absence of a minimum in the area of the discontinuity in the plots confirms surfactants purity.

In figures 14-17 the isotherms of Triton X-100 in ionic liquids with different lengths of cations alkyl chains are presented (analogue isotherms of Triton X-114 and Tween 20 are presented in Supplementary Material). Surface tension decrease was observed in systems containing ionic liquids ranging from two to six carbon atoms in cations alkyl chains. None of ILs with 1-octyl-3-methylimidazolium cation, this is with eight carbon atoms in the chain, underwent significant reduction of surface tension with the characteristic plot bending, typical for micellization. The lack of micellization-supporting ability results from relatively high molar masses of 1-octyl-3-methylimidazolium ILs, and consequently stronger interactions amongst their ions, which provides solvation of surfactant molecules, instead of supporting aggregate formation.

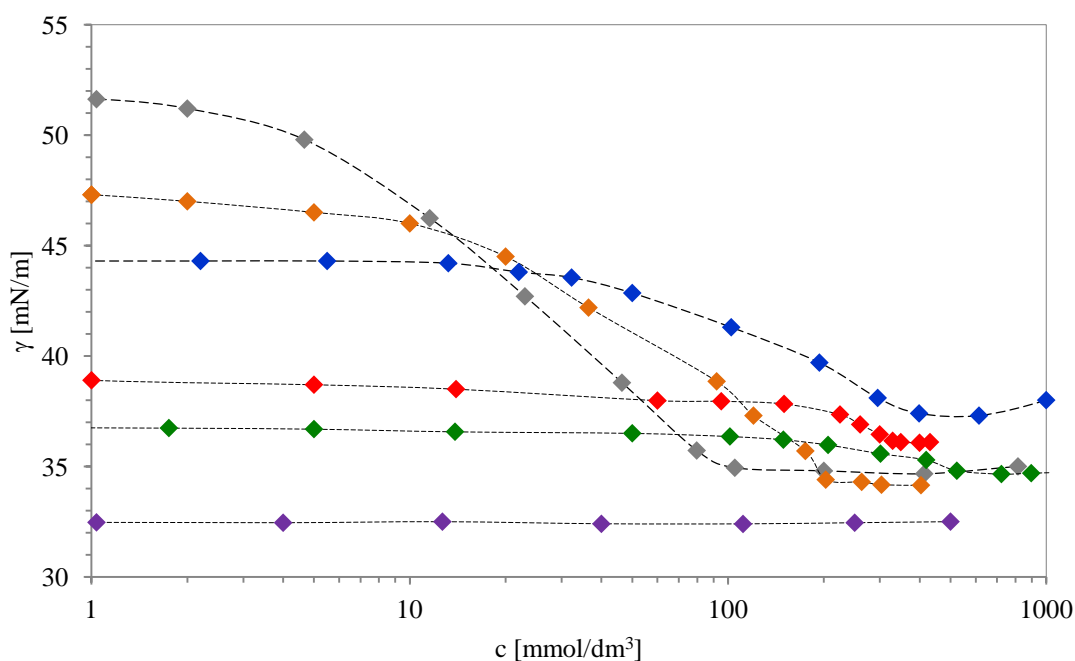


Figure 14. Surface tension of Triton X-100 in [EMIM][BF₄] (◆), [PrMIM][BF₄] (◆), [BMIM][BF₄] (◆), [PMIM][BF₄] (◆), [HMIM][BF₄] (◆), [OMIM][BF₄] (◆), at 25.0°C

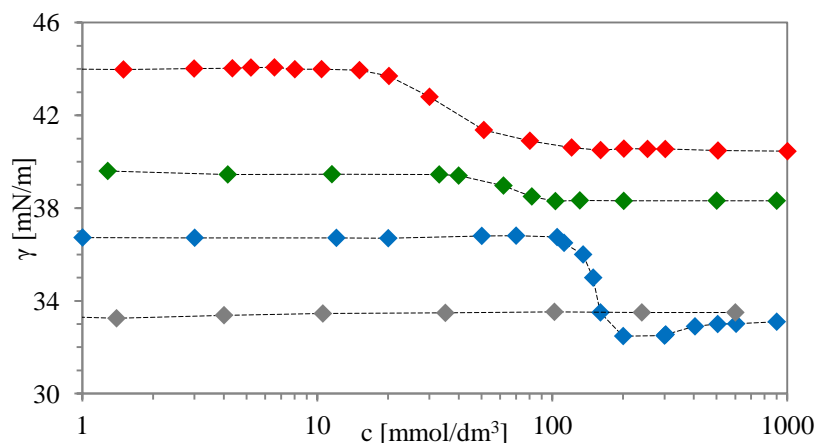


Figure 15. Surface tension of Triton X-100 in [BMIM][PF₆] (♦), [PMIM][PF₆] (♦), [HMIM][PF₆] (♦), [OMIM][PF₆] (♦) at 25.0°C

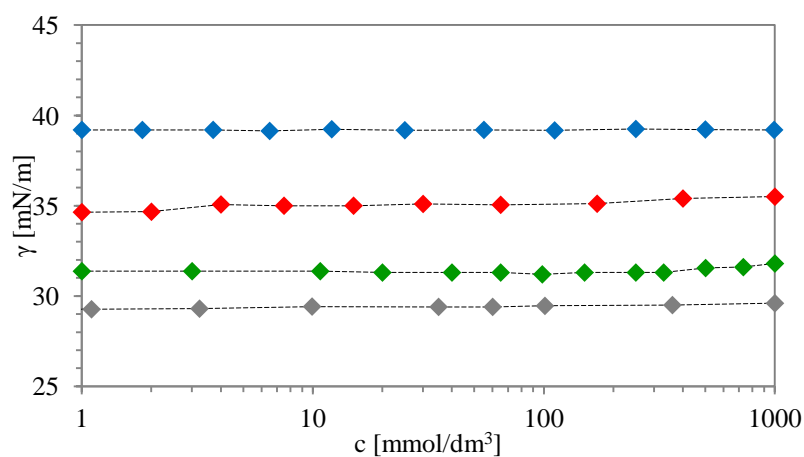


Figure 16. Surface tension of Triton X-100 in [EMIM][OTf] (♦), [BMIM][OTf] (♦), [HMIM][OTf] (♦), [OMIM][OTf] (♦), at 25.0°C

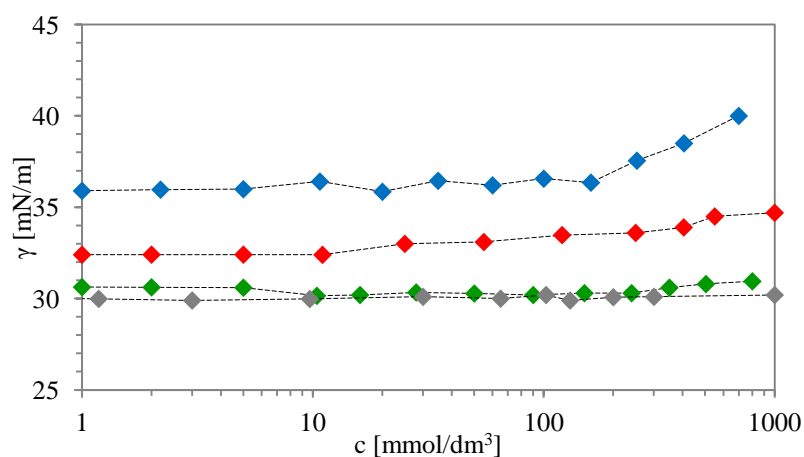


Figure 17. Surface tension of Triton X-100 in [EMIM][NTf₂] (♦), [BMIM][NTf₂] (♦), [HMIM][NTf₂] (♦), [OMIM][NTf₂] (♦), at 25.0°C

5.2.2. Anion type influence

To show the influence of ILs anions type on the surface behavior of obtained systems, each plot depicts systems containing ionic liquids with one type of cation each (one length of alkyl chain), and one of anion substituents – tetrafluoroborate [BF₄], hexafluoroborate [PF₆], trifluoromethanesulfonate [OTf] and bis(trifluoromethylsulfonyl)imide [NTf₂] (for Triton X-100 surfactants see figures 18-21, for the remaining surfactants see Supplementary Material). In 1-ethyl-3-methylimidazolium ionic liquids the discontinuity of surface tension isotherms was observed only in the presence of tetrafluoroborate anion, whereas in ILs with longer alkyl chains - [PrMIM], [BMIM], [PMIM] and [HMIM] cation, also the hexafluorophosphate anion was assisted with surface tension reduction, and therefore micellization.

The presence of the tetrafluoroborate anions provide in the evaluated systems provided more effective reduction of the surface tension values than corresponding systems with the hexafluorophosphate one. What is more, the discontinuities of the isotherms, characteristic for the CMC region, were observed for systems with [BF₄] anion at lower surfactant concentrations, than the analogue [PF₆] ones.

It was already written, that the size of anions strongly influence the character of given ionic liquid. Hexafluorophosphate anion, which is bigger than the tetrafluoroborate one, contains more fluorine atoms, and, therefore, is more prone to form stronger interactions with ILs cations and surfactant molecules. Consequently, more ordered structure of the ILs provides better conditions for surfactant molecules to dissolve, rather than to form aggregates.

Moreover, due to the fact, that the ability of ILs to support micellar aggregation depends on the strength of their hydrogen bonds, which are short-range interactions, their effectiveness in ILs with smaller anions is higher, because of better packing of the molecules, and at the same time – smaller distances between them. In systems containing trifluoromethanesulfonate [OTf] and bis(trifluoromethylsulfonyl)imide [NTf₂] anions no surface tension decrease (and no micellization) was observed. The only exception was reserved for Tween 20/[EMIM][OTf] system (figure 22) being the only example of micellization to be observed in a system containing trifluoromethanesulfonate anion.

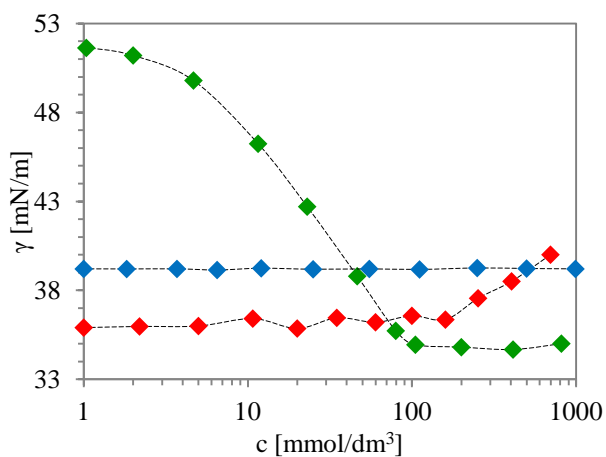


Figure 18. Surface tension of TX-100 in [EMIM][BF₄] (◆), [EMIM][NTf₂] (◆), [EMIM][OTf] (◆), at 25.0°C

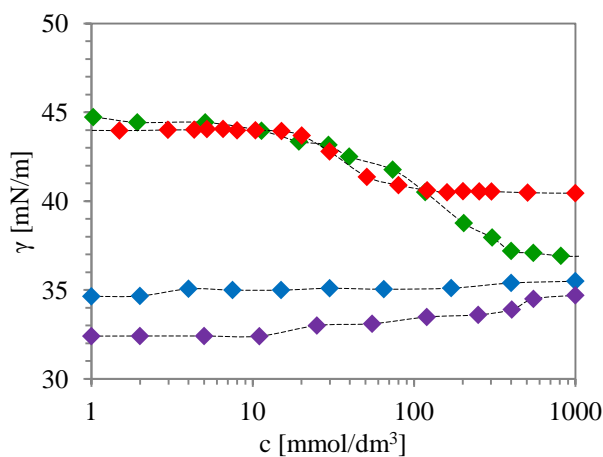


Figure 19. Surface tension of TX-100 in [BMIM][BF₄] (◆), [BMIM][PF₆] (◆), [BMIM][NTf₂] (◆), [BMIM][OTf] (◆), at 25.0°C.

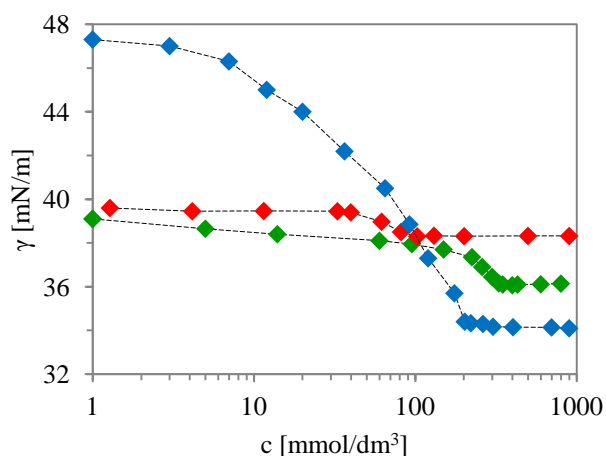


Figure 20. Surface tension of TX-100 in [PrMIM][BF₄] (◆), [PMIM][BF₄] (◆), [PMIM][PF₆] (◆), at 25.0°C

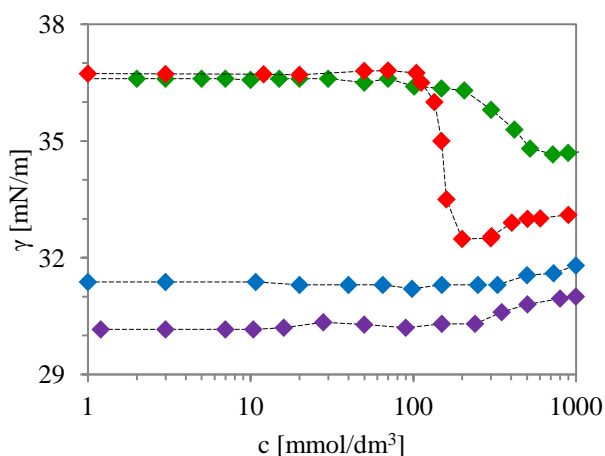


Figure 21. Surface tension of TX-100 in [HMIM][BF₄] (◆), [HMIM][PF₆] (◆), [HMIM][NTf₂] (◆), [HMIM][OTf] (◆), at 25.0°C

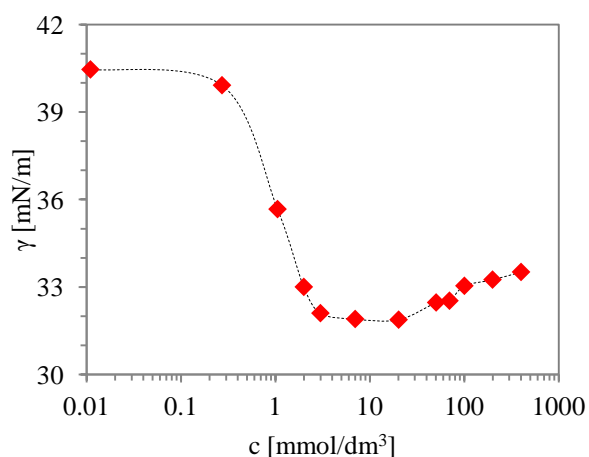


Figure 22. Surface tension of Tween 20 in [EMIM][OTf], at 25.0°C

5.2.3. Surfactant type influence

Nonionic surface active agents used in this investigation were Triton X-100, Triton X-114, Triton X-45 and Triton X-15, which differ by the number of OE units, and Tween 20, Tween 40 and Tween 80, which have the same number of OE groups, but differ by the length of side alkyl chains, as they are derivatives of different fatty acids. Surface tension isotherms of all the surfactants in [BMIM][BF₄] are shown in figure 23. Depending on the number of oxyethylene units, Triton surfactants decrease surface tension of the ionic liquids more efficiently, the shorter is the OE chain. Also the discontinuity of the isotherms, thereby the CMCs, are found in systems with Triton X-15 surfactant at lower concentrations than remaining ones. So the effectiveness of decreasing surface tension presents as follows: TX-100 > TX-114 > TX-45 > TX-15, which corresponds to following numbers of OE units: 9.5, 7.5, 4.5, and 1.5. Amongst the Tween surfactants the effectiveness of decreasing ILs surface tension was comparable, which results from the same number of OE groups. However the CMC values were different, thus it may be concluded that the presence of alkyl chains, as a source of van der Waals and hydrogen bonds, increase interactions and, therefore, solubilization in the IL. Nevertheless the CMC values do not depend on Tweens alkyl chains lengths in a consistent manner therefore no conclusion can be withdrawn basing on surface tension measurements performed in given experimental conditions.

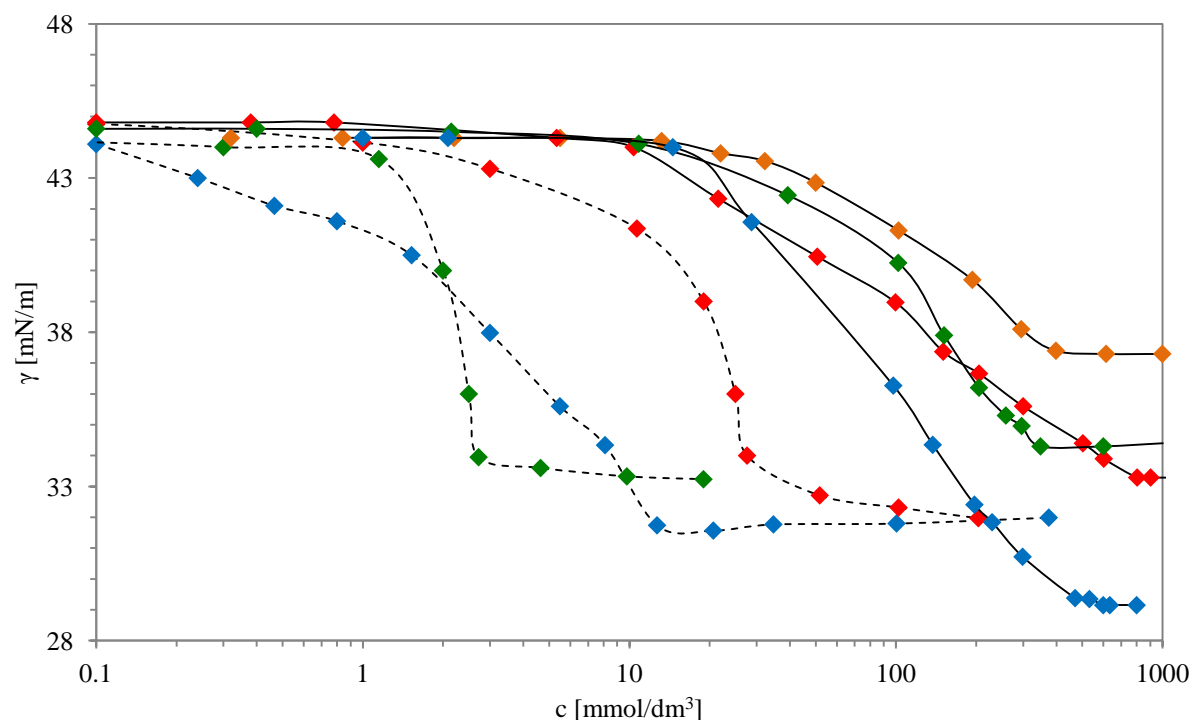


Figure 23. Surface tension of Tritons (solid lines): Triton X-100 (♦), Triton X-114 (♦), Triton X-45 (♦), Triton X-15 (♦), and Tweens (dashed lines): Tween 20 (♦), Tween 60 (♦), Tween 80 (♦), in [BMIM][BF₄], at 25.0°C

Tween surfactants were observed to possess better surface activity, what was expressed by more efficient decrease of surface tension of selected imidazolium ionic liquids than Triton surfactants (excepting Triton X-15). What is more, the concentration of Tween surfactants required to reach critical micelle concentrations is significantly lower than in case of Triton surfactants. Tween surfactants, due to possession of more oxyethylene units than Triton X ones, are observed to form micelles at lower concentrations, due to higher solvophobic character. In On the contrary, surfactants with fewer oxyethylene groups, such as Triton X-100, the solvophobic effect is weaker, due to formation of doubly ionic hydrogen bonds and van der Waals interactions between ILs ions and the surfactant [58, 70].

6. Comparison to model solvents

Surface tension isotherms of the nonionic surfactants in water and ethylene glycol are shown in plots 24, 25 and 26 (for the remaining plots see Supplementary Material). Because of better aggregation supporting properties than ILs, surface tension plots of systems based on the model solvents are more “detailed”, and the characteristic sections which depict micellization stages are clearly visible. The surface tension plots are the most detailed in the aqueous systems, due to the fact that surface tension of pure water is relatively high (72 mN/M), thus the addition of a surfactant provides a significant surface tension decrease.

Amongst the nonionic surfactants used in the investigation, the lowest CMC in water was obtained for Tween 20 (0.0002 mmol/dm³). Critical micelle concentrations for Triton X aqueous solutions in 25.0°C increased in the following order: TX-45<TX-114<TX-100 (0.1, 0.23, 0.25, respectively), whereas Triton X-15 was immiscible in water, therefore, no micellization took place.

Ethylene glycol was observed to undergo similar surface tension decrease by Tween 20 and Triton X-100, whereas other Triton X surfactants provided more effective reduction of the parameter. Such observation is valid for all the analyzed systems. What is more, CMC values of Tween 20-based systems were almost an order of magnitude smaller than the corresponding Triton X-based ones. The explanation of this behavior was already presented on the example of surface tension reduction by the surfactants (see section 5.2.3. Surfactant type influence).

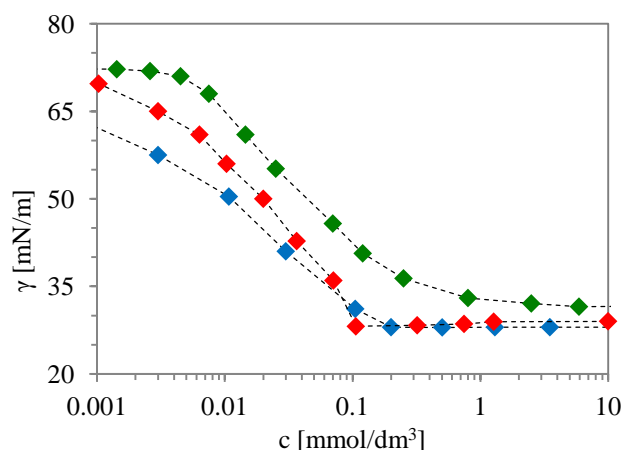


Figure 24. Surface tension of TX-100 (◆), TX-114 (◆) and TX-45 (◆) in water at 25.0°C

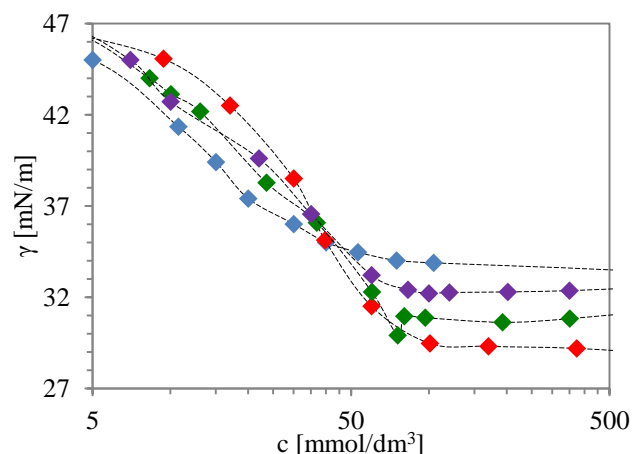


Figure 25. Surface tension of Triton X-100 (◆), Triton X-114 (◆), Triton X-45 (◆), Triton X-15 (◆) in ethylene glycol, at 25.0°C

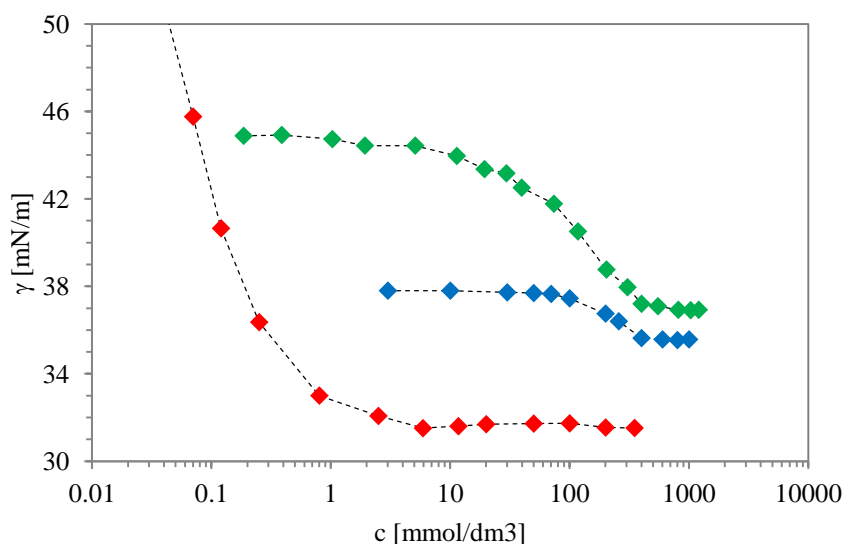


Figure 26. Surface tension of TX-100 in [BMIM][BF₄] (◆), water (◆) and ethylene glycol (◆) at 25.0°C

5.3. Temperature dependence and thermodynamics

Surface tension method was used to investigate the influence of temperature change on the micellar aggregation of selected surfactants in tetrafluoroborate-based ionic liquids and in the model solvent (water and ethylene glycol). Afterwards, thermodynamic parameters were calculated. The measurements were performed at 15.0, 25.0, 35.0 and 45.0°C. Obtained results were plotted against surfactant concentrations

Increased temperature resulted in the change of molecular interactions, i.e. weakening H-bonds, and, therefore, diminished surface tension [101]. This is why the change of surface tension isotherms is visible in the diagrams mostly as a vertical shift. However, after a closer look at the plots in the CMC region, a horizontal shift is also visible, as the critical micelle concentration values do not change linearly (figure 27).

To determine the most favorable temperatures for micellization, the CMC values were plotted against the temperature to detect the plot minima (figures 28-31), the way it is usually presented in the literature [39, 103]. Based on the critical micelle concentrations obtained from surface tension plots at 15.0-45.0°C, surface, micellar and thermodynamic parameters were determined and presented in tables 6-11.

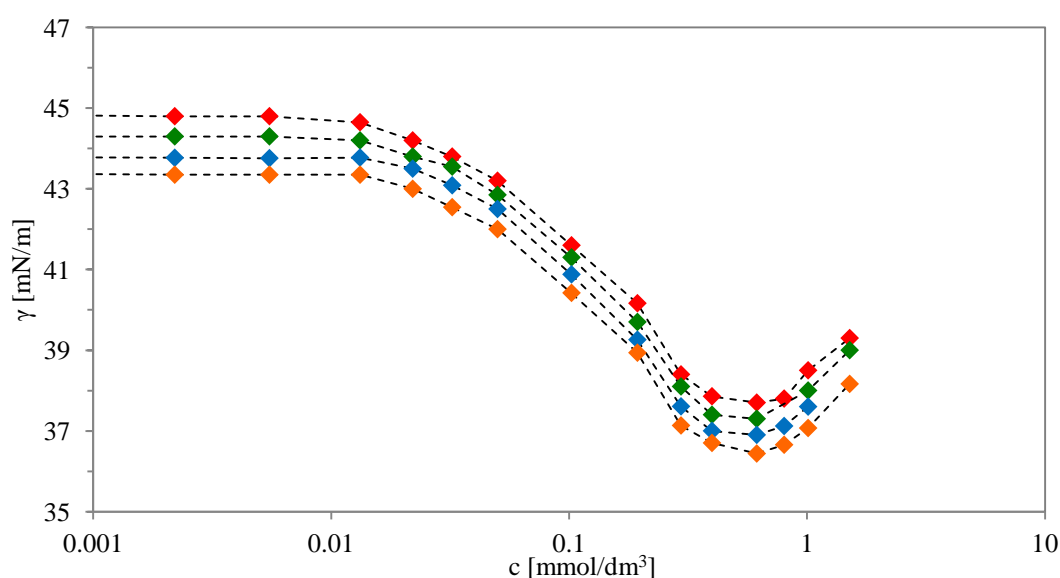


Figure 27. Surface tension isotherms of TX-100/[BMIM][BF₄] at 15.0°C (♦), 25.0°C (♦), 35.0°C (♦), 45.0°C (♦)

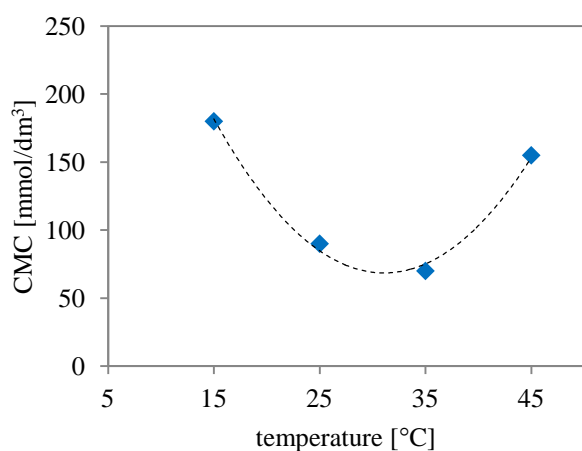


Figure 28. CMC vs. temperature of Triton X-100 in [EMIM][BF₄]

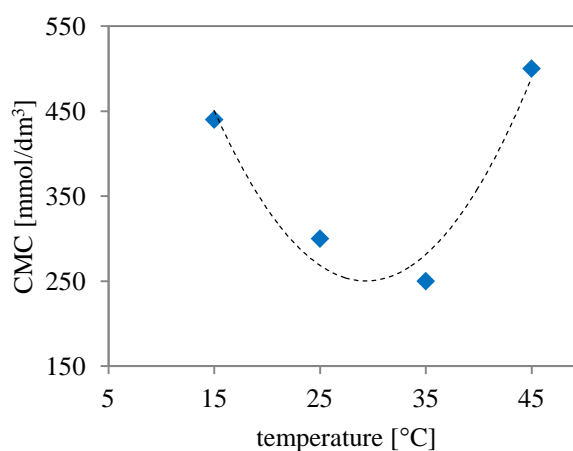


Figure 29. CMC vs. temperature of Triton X-100 in [BMIM][BF₄]

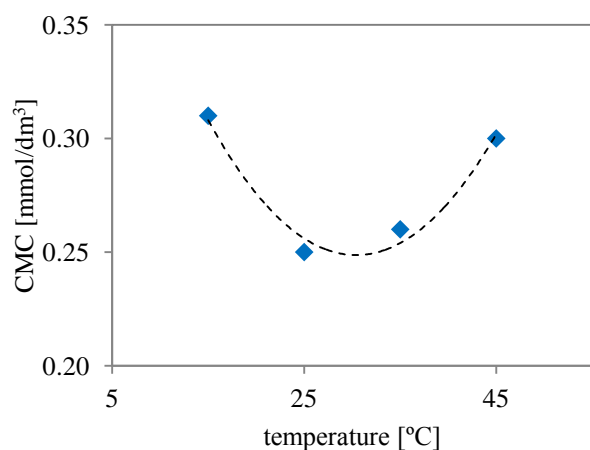


Figure 30. CMC vs. temperature of Triton X-100 in water

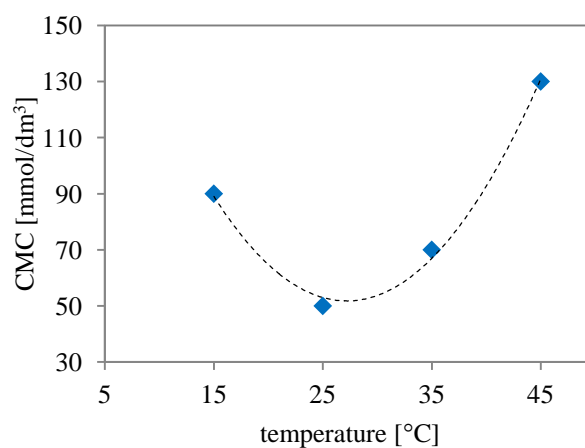


Figure 31. CMC vs. temperature of Triton X-100 in ethylene glycol

The plots show a U-shaped form, with the minimum CMC value located in the region of 25.0 to 35.0°C. In comparison to the analogue water- and ethylene glycol-based systems, the temperatures at which the minima are found are comparable in all investigated systems (also for Triton X-114, Triton X-45, Triton X-15 and Tween 20 – see Supplementary Material). Similar results were presented by Inoue et al. in a broad study on POE nonionic surfactants in ionic liquids, in which both shape of the plots and the temperature ranges of CMC minima were comparable with the investigated ones [39, 91, 102, 103].

It was observed, that systems containing Triton X-100 were the most sensitive to temperature changes amongst all Triton X-based systems (figure 32). The values of critical micelle concentration underwent the biggest change along the range of 15.0-45.0°C, independently from the solvents used.

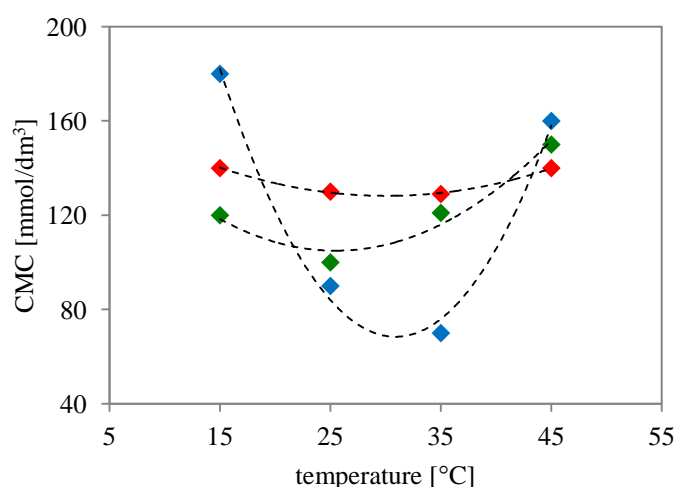


Figure 32. CMC vs. temperature of Triton X-100 (♦), Triton X-114 (♦) and Triton X-45 (♦) in [BMIM][BF₄]

Accordingly, the critical micelle concentration temperature dependence of Tween 20 in ILs systems show the U-shape relation (figures 33, S.22- S.26, Supplementary Material) similarly to Triton X-100, other surfactants, and to solutions of surfactant-type ionic liquids in other media [104], [105], [106]. According to the data on the aqueous systems, such behavior may indicate that below 20°C micellization is endothermic, and consequently, the temperature increase makes the process exothermic.

Given conclusion is supported with thermodynamic parameters, ΔG_m , ΔH_m , $-T\Delta S_m$ calculated from the CMC temperature dependence, using equations 16-18 [39, 107]. Thermodynamic parameters calculated for Triton X-100 in [EMIM][BF₄], [BMIM][BF₄] and [PMIM][BF₄] are shown in table 6, whereas for Tween 20 in 1-ethyl-3-methylimidazolium trifluoromethanesulfonate, are shown in figure 34. To indicate the contribution of entropy change to free energy of micellization, ΔG_m , it was given as $-T\Delta S_m$.

Table 6. Thermodynamic micellization parameters, ΔG_m , ΔH_m , $-T\Delta S_m$, of Triton X-100 in [EMIM][BF₄], [BMIM][BF₄] and [PMIM][BF₄]

	ΔG_m [kJ/mol]	ΔH [kJ/mol]	$T\Delta S$ [kJ/mol]
15.0°C			
[EMIM][BF ₄]	-8.96	-24.38	-15.80
[BMIM][BF ₄]	-6.19	-39.97	-33.81
[PMIM][BF ₄]	-6.55	4.99	-5.23
25.0°C			
[EMIM][BF ₄]	-10.60	-28.04	-17.46
[BMIM][BF ₄]	-7.07	-46.08	-39.52
[PMIM][BF ₄]	-6.50	5.77	-4.69
35.0°C			
[EMIM][BF ₄]	-11.20	-32.10	-20.33
[BMIM][BF ₄]	-7.56	-52.86	-46.38
[PMIM][BF ₄]	-6.18	6.64	-4.65
45.0°C			
[EMIM][BF ₄]	-17.74	-36.58	-26.99
[BMIM][BF ₄]	-5.82	-60.37	-58.64
[PMIM][BF ₄]	-5.82	7.61	-4.56

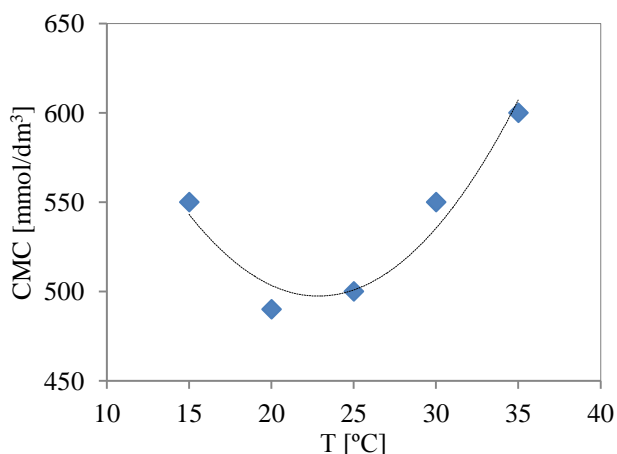


Figure 33. CMC of Tween 20 in [EMIM][TfO] vs. temperature

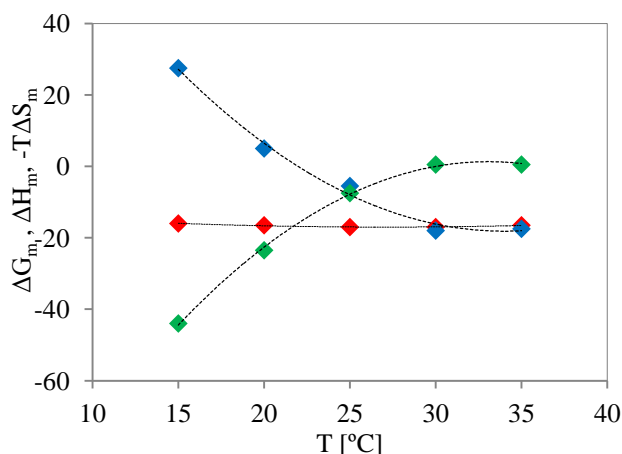


Figure 34. Thermodynamic parameters of micelle formation for Tween 20 in [EMIM][TfO]: ΔG_m (♦), ΔH_m (♦) and $-T\Delta S_m$ (♦)

Ionic liquid cation-anion interactions are responsible for the formation of highly organized, nanoscale structures [108, 109]. Therefore, as a network of ions, ILs are said to interact not only electrostatically, but also with extended hydrogen bond networks [110, 111]. Presence of surfactant molecule within ILs supramolecular structure results in solute-solvent interactions. The counterions of ILs and surfactants oxyethylene units compete with each other by means of H-bonds to interact with C(2)-H atoms in the imidazolium rings (see figure 1) [112].

An increase of temperature affects energy of interactions taking place in surfactant/IL systems, therefore, the strength of relatively weak hydrogen and van der Waals bonds decrease. As a result, solvophobicity of the surfactants in ILs increases and favors micellization at lower surfactant concentrations. Nevertheless, elevated temperature affects the three-dimensional structure of the ionic liquids by changing the energy of interactions between its counterions. It was already confirmed, that due to temperature increase, van der Waals interactions between imidazolium cation alkyl chains become reduced, and ILs become dominated with electrostatic forces of the polar groups [113]. What is more, the change of the interactions results in the size reduction of the supramolecular aggregates, reordering of ILs internal structure, and consequently – an increase of solvents entropy. Since low entropy is a driving force for micellization, an increase of ΔS_m is unfavorable for micelle formation. Moreover, weaker interactions amongst ionic liquid molecules are accompanied with their stronger interactions with surfactant molecules, and poorer self-aggregation. Concluding, at decreased temperatures the first effect described above is predominant, whereas when increased - the second one becomes more prevailing.

As already mentioned, at low temperatures (below 20°C) micellization of surfactants is endothermic ($\Delta H_m > 0$) and becomes exothermic at increased temperatures ($\Delta H_m < 0$). Positive contribution to ΔH_m comes from the energy required to release the structural ionic liquid from solvation layer around the amphiphilic molecule, which is necessary for hydrocarbons to self-assembly into micellar aggregates. A negative contribution to the micellization enthalpy, which is an opposite effect, is related with the transfer of surfactant molecule for ionic liquids solution to the micelle, and, therefore, rearrangement of the H-bonds between surfactant and solvent.

Due to the fact, that free energy of micellization is negative over the whole range of investigation temperatures, we can see that micellization is spontaneous. The shift of CMC values result from the change of free energy, which depends on the relative changes of enthalpy and entropy of the system. At low temperatures negative Gibbs free energy is controlled by highly negative $-T\Delta S_m$, which exceeds positive contribution of ΔH_m . At elevated temperatures a conversion of the two parameters takes place. At low temperatures the driving force of micellization is ΔS_m , whereas at elevated temperatures it is ΔH_m .

Similar dependence between micellization thermodynamic parameters of polyoxyethylene monoalkyl ether surfactants in ionic liquids was already observed - in a study of Inoue group on $C_{12}E_6$ solution in a mixture of 1-ethyl-3-methylimidazolium tetrafluoroborate and 1-hexyl-3-methylimidazolium tetrafluoroborate [94], as well as for C_nE_m in 1-butyl-3-methylimidazolium tetrafluoroborate [39, 103], and 1-butyl-3-methylimidazolium hexafluorophosphate [91]. The dependence was also showed by Wu and coworkers in a thermodynamic study on Tween 20 in 1-butyl-3-methylimidazolium tetrafluoroborate and 1-butyl-3-methylimidazolium hexafluorophosphate ionic liquids [6].

All the surface and micellar parameters, determined experimentally or calculated, are collected in tables 7 – 11, included below.

Table 7. Surface parameters of Triton X-100 ($n_{OE} = 9.5$) in [AMIM][BF₄] ILs, ethylene glycol and water, vs. temperature.

	CMC [mmol/dm ³]		γ_0 [mN/m]	γ_{CMC} [mN/m]	Π_{cmc} [mN/m]	$\Gamma_{max} \times 10^6$ [mol/m ²]	A_{min} [nm ²]	ΔG_m [kJ/mol]	ΔG_{ad} [kJ/mol]
	from γ	from ρ							
15.0°C									
[EMIM][BF ₄]	180.00	-	54.60 ± 0.02	33.32	20.07	1.98	0.82	-8.96	-19.11
[PrMIM][BF ₄]	290.00	-	48.80 ± 0.03	34.68	13.69	1.67	0.96	-7.82	-16.01
[BMIM][BF ₄]	440.00	-	45.10 ± 0.01	37.85	7.25	1.16	1.39	-6.19	-12.44
[PMIM][BF ₄]	350.00	-	40.08 ± 0.04	36.37	3.71	0.85	1.9	-6.55	-10.92
[HMIM][BF ₄]	1000.00	-	38.75 ± 0.02	34.40	3.60	0.76	2.11	-8.46	-3.34
ethylene glycol	90.00	-	47.14 ± 0.01	33.85	13.28	1.78	0.91	-13.13	-20.59
water	0.31	-	73.50 ± 0.02	31.95	41.55	3.59	0.45	-12.85	-24.44
25.0°C									
[EMIM][BF ₄]	90.00	90	53.96 ± 0.01	34.90	17.50	2.12	0.76	-10.60	-18.84
[PrMIM][BF ₄]	220.00	200	48.00 ± 0.02	34.40	12.90	2.14	0.75	-8.30	-14.42
[BMIM][BF ₄]	310.00	300	44.90 ± 0.02	37.09	7.85	0.97	1.67	-7.07	-15.20
[PMIM][BF ₄]	350.00	350	39.50 ± 0.04	36.10	2.60	0.77	2.08	-6.50	-9.89
[HMIM][BF ₄]	400.00	600	39.20 ± 0.01	35.60	1.80	0.69	2.33	-6.00	-8.65
[BMIM][PF ₆]	95.00	-	43.35 ± 0.04	41.03	2.32	3.98	0.41	-9.72	-10.31
[PMIM][PF ₆]	105.00	-	39.50 ± 0.04	38.30	1.20	10.06	0.16	-9.28	-9.40
[HMIM][PF ₆]	200.00	-	37.63 ± 0.02	32.48	5.16	7.90	0.20	-7.51	-8.16
ethylene glycol	50.00	-	46.30 ± 0.02	33.66	11.66	2.12	0.76	-13.25	-11.76
water	0.25	-	72.06 ± 0.02	32.00	40.06	4.16	0.39	-36.30	-45.92



Table 7(continuation). Surface parameters of Triton X-100 ($n_{OE} = 9.5$) in [AMIM][BF₄] ILs, ethylene glycol and water, vs. temperature

35.0°C									
[EMIM][BF ₄]	70.00	-	51.68 ± 0.03	34.80	19.16	2.13	0.76	-11.20	-20.19
[PrMIM][BF ₄]	200.00	-	46.90 ± 0.01	32.70	13.30	1.80	0.89	-8.34	-15.71
[BMIM][BF ₄]	250.00	-	43.77 ± 0.02	37.00	6.77	1.19	1.35	-7.56	-13.24
[PMIM][BF ₄]	400.00	-	38.97 ± 0.03	35.3	3.68	1.13	1.43	-6.18	-9.44
[HMIM][BF ₄]	-	-	37.70 ± 0.01						
ethylene glycol	75.00	-	45.45 ± 0.02	33.10	12.04	1.87	0.86	-13.55	-20.00
water	0.26	-	69.50 ± 0.02	31.06	38.44	2.60	0.62	-13.28	-28.09
45.0°C									
[EMIM][BF ₄]	155.00	-	50.30 ± 0.02	32.21	19.47	2.28	0.71	-17.74	-9.21
[PrMIM][BF ₄]	260.00	-	46.30 ± 0.02	32.70	13.60	1.53	1.05	-7.68	-16.55
[BMIM][BF ₄]	500.00	-	43.51 ± 0.01	36.70	6.80	0.89	1.82	-5.82	-13.49
[PMIM][BF ₄]	480.00	-	37.15 ± 0.03	34.6	2.57	0.86	1.87	-5.82	-8.81
[HMIM][BF ₄]	-	-	37.09 ± 0.02						
ethylene glycol	100.00	-	44.79 ± 0.01	32.48	12.31	1.66	0.97	-12.82	-20.23
water	0.30	-	68.75 ± 0.02	30.17	38.58	1.10	1.47	-12.91	-48.03



Table 8. Surface parameters of Triton X-114 ($n_{OE}=7,5$) in [AMIM][BF₄] ILs, ethylene glycol and water, vs. temperature

solvent	CMC [mmol/ dm ³]	γ_0 [mN/m]	γ_{CMC} [mN/m]	Π_{cmc} [mN/m]	$\Gamma_{max} \times 10^6$ [mol/m ²]	A_{min} [nm ²]	ΔG_m [kJ/mol]	ΔG_{ad} [kJ/mol]
15°C								
[EMIM][BF ₄]	140.00	54.61 ± 0,02	32.00	22.61	3.22	0.50	-7.09	-14.11
[BMIM][BF ₄]	500.00	45.10 ± 0,01	36.10	9.00	1.29	1.25	-5.87	-12.83
[HMIM][BF ₄]	<i>immiscible</i>	38.75 ± 0,02	-	-	-	-	-	-
ethylene glycol	600.00	49.50 ± 0,01	35.81	11.33	0.96	1.68	-8.43	-20.25
water	0.30	73.50 ± 0,02	29.10	44.40	9.82	0.24	-4.67	-11.18
25°C								
[EMIM][BF ₄]	130.00	52.70 ± 0,01	32.10	20.60	2.21	0.73	-7.19	-16.52
[BMIM][BF ₄]	800.00	44.90 ± 0,02	33.30	11.60	0.97	1.66	-4.69	-16.64
[HMIM][BF ₄]	<i>immiscible</i>	38.21 ± 0,01	-	-	-	-	-	-
ethylene glycol	100.00	48.00 ± 0,02	32.20	11.45	1.81	0.89	-12.85	-19.17
water	0.23	71.90 ± 0,02	28.20	43.76	4.97	0.32	-5.31	-14.11
35°C								
[EMIM][BF ₄]	129.00	51.00 ± 0,03	30.90	20.10	2.58	0.63	-7.21	-15.01
[BMIM][BF ₄]	430.00	43.77 ± 0,02	35.94	7.83	1.41	1.15	-6.21	-11.77
[HMIM][BF ₄]	<i>immiscible</i>	37.70 ± 0,01	-	-	-	-	-	-
ethylene glycol	450.00	46.66 ± 0,02	33.83	11.62	0.75	2.18	-14.81	-30.49
water	0.02	69.70 ± 0,02	28.50	41.80	3.31	0.49	-5.63	-18.27
45°C								
[EMIM][BF ₄]	140.00	49.00 ± 0,02	30.99	18.01	2.00	0.81	-7.28	-16.08
[BMIM][BF ₄]	230.00	43.51 ± 0,01	34.70	8.81	1.02	1.58	-7.75	-16.38
[HMIM][BF ₄]	<i>immiscible</i>	37.09 ± 0,02	-	-	-	-	-	-
ethylene glycol	600.00	44.79 ± 0,01	33.54	11.25	0.33	4.88	-14.08	-48.16
water	0.02	68.75 ± 0,02	27.37	41.38	3.94	0.41	-5.59	-16.09



Table 9. Surface parameters of Triton X-45 ($n_{OE} = 4,5$) in [AMIM][BF₄] ILs, ethylene glycol and water, vs. temperature

solvent	CMC [mmol/ dm ³]	γ_0 [mN/m]	γ_{CMC} [mN/m]	Π_{cmc} [mN/m]	$\Gamma_{max} \times 10^6$ [mol/m ²]	A _{min} [nm ²]	ΔG_m [kJ/mol]	ΔG_{ad} [kJ/mol]
15°C								
[EMIM][BF ₄]	120.00	54.60 ± 0.02	31.33	23.27	10.08	0.16	-11.58	-9.27
[BMIM][BF ₄]	350.00	45.10 ± 0.01	34.52	10.58	1.80	0.90	-6.75	-12.63
[HMIM][BF ₄]	<i>immiscible</i>	38.75 ± 0.02	-	-	-	-	-	-
ethylene glycol	80.00	49.50 ± 0.01	30.61	18.89	2.60	0.62	-13.42	-20.69
water	0.20	73.50 ± 0.02	27.59	45.91	1.37	1.18	-13.94	-47.46
25°C								
[EMIM][BF ₄]	100.00	52.14 ± 0.01	31.70	12.71	2.78	0.58	-12.02	-16.59
[BMIM][BF ₄]	320.00	44.90 ± 0.02	34.60	10.30	1.95	0.83	-6.96	-12.25
[HMIM][BF ₄]	<i>immiscible</i>	38.21 ± 0.01	-	-	-	-	-	-
ethylene glycol	77.00	46.60 ± 0.02	29.90	16.70	2.44	0.66	-13.50	-20.33
water	0.10	72.00 ± 0.02	28.00	44.00	3.08	0.52	-15.33	-29.59
35°C								
[EMIM][BF ₄]	121.00	51.00 ± 0.03	30.50	20.50	1.54	0.10	-11.53	-12.78
[BMIM][BF ₄]	300.00	43.82 ± 0.02	34.28	9.22	2.14	0.75	-7.10	-11.40
[HMIM][BF ₄]	<i>immiscible</i>	37.70 ± 0.01	-	-	-	-	-	-
ethylene glycol	80.00	46.66 ± 0.02	30.60	16.06	2.33	0.69	-13.39	-20.27
water	0.09	69.55 ± 0.02	27.00	43.30	2.46	0.66	-15.90	-33.54
45°C								
[EMIM][BF ₄]	150	49.00 ± 0.02	29.90	19.10	8.51	0.19	-10.99	-13.23
[BMIM][BF ₄]	350	43.51 ± 0.01	33.87	9.64	1.97	0.82	-6.71	-11.60
[HMIM][BF ₄]	<i>immiscible</i>	37.09 ± 0.02	-	-	-	-	-	-
ethylene glycol	85	44.79 ± 0.01	29.80	14.99	2.51	0.64	-13.22	-19.19
water	0.14	68.75 ± 0.02	26.40	42.35	2.77	0.58	-14.80	-30.08



Table 10. Surface parameters of Triton X-15 ($n_{OE} = 1.5$) in [AMIM][BF₄] and [AMIM][PF₆] ILs, ethylene glycol and water, at 25.0°C

solvent	CMC [mmol/ dm ³]		γ_0 [mN/m]	γ_{CMC} [mN/m]	Π_{cmc} [mN/m]	$\Gamma_{max} \times 10^6$ [mol/m ²]	A_{min} [nm ²]	ΔG_m [kJ/mol]	ΔG_{ad} [kJ/mol]
	from γ	from ρ							
[EMIM][BF ₄]	50.00	30.00	52.47 ± 0.01	34.64	22.07	1.29	1.25	-15.01	-32.14
[BMIM][BF ₄]	350.00	350.00	44.90 ± 0.02	29.50	15.40	1.53	1.05	-6.74	-16.77
[HMIM][BF ₄]	<i>immiscible</i>	-	38.21 ± 0.01	-	-	-	-	-	-
[BMIM][PF ₆]	1.02	-	43.00 ± 0.01	37.38	5.62	0.72	2.25	-20.99	-28.84
ethylene glycol	80.00	-	47.47 ± 0.02	30.00	17.47	2.41	0.67	3.71	-3.53
water	<i>immiscible</i>	-	71.90 ± 0.02	-	-	-	-	-	-

Table 11. Surface parameters of Tween 20 in selected ILs, ethylene glycol and water, vs. temperature

	CMC [mmol/ dm ³]	γ_0 [mN/m]	γ_{CMC} [mN/m]	Π_{cmc} [mN/m]	$\Gamma_{max} \times 10^6$ [mol/m ²]	A_{min} [nm ²]	ΔG_m [kJ/mol]	ΔG_{ad} [kJ/mol]
15°C								
[EMIM][BF ₄]	1.55	54.60 ± 0.02	39.00	15.60	3.76	0.43	-19.97	-24.13
[BMIM][BF ₄]	15.00	45.10 ± 0.01	32.55	12.55	1.18	1.36	-13.26	-23.88
[HMIM][BF ₄]	150.00	38.75 ± 0.02	34.78	4.13	0.50	3.26	-8.16	-16.50
ethylene glycol	2.80	47.14 ± 0,01	33.50	13.65	1.97	0.82	-21.00	-27.91
water	-	73.50 ± 0.02	-	-	-	-	-	-
25°C								
[EMIM][BF ₄]	2.00	52.14 ± 0.01	32.60	17.00	1.70	1.00	-20.60	-31.10
[BMIM][BF ₄]	9.00	44.90 ± 0.02	33.40	11.50	1.40	1.10	-12.80	-20.90
[HMIM][BF ₄]	125.00	39.20 ± 0.01	34.26	4.95	0.37	4.40	-8.88	-22.35
[EMIM][OTf]	3.00	40.51 ± 0.02	32.50	8.01	0.27	5.95	-18.53	-48.07
[PMIM][PF ₆]	30.00	39.50 ± 0.01	34.90	4.60	2.75	0.59	-12.39	-14.06
[HMIM][PF ₆]	40.00	37.63 ± 0.02	36.65	1.07	0.09	17.59	-11.50	-23.17
ethylene glycol	1.25	44.55 ± 0.02	33.40	11.15	1.95	0.83	-23.71	-29.46
water	0.0002	72.00 ± 0.01	38.18	33.82	1.81	0.89	-48.16	-66.87
35°C								
[EMIM][BF ₄]	1.00	51.00 ± 0.03	32.20	18.80	4.46	0.36	-22.45	-26.67
[BMIM][BF ₄]	14.00	43.82 ± 0.02	31.60	12.22	1.70	0.95	-15.19	-22.37
[HMIM][BF ₄]	150.00	37.70 ± 0.01	33.55	4.15	0.50	3.23	-8.70	-17.01
ethylene glycol	2.00	45.45 ± 0.02	32.70	12.75	1.59	1.02	-23.28	-31.32
water	0.0015	69.55 ± 0.02	-	-	-	-	-	-



Table 11 (continuation). Surface parameters of Tween 20 in selected ILs, ethylene glycol and water, vs. temperature

	CMC [mmol/ dm ³]	γ_0 [mN/m]	γ_{CMC} [mN/m]	Π_{cmc} [mN/m]	$\Gamma_{\text{max}} \times 10^6$ [mol/m ²]	A_{min} [nm ²]	ΔG_{m} [kJ/mol]	ΔG_{ad} [kJ/mol]
45°C								
[EMIM][BF ₄]	1.22	49.00 ± 0.02	34.00	15.00	1.83	0.88	-22.64	-30.86
[BMIM][BF ₄]	20.00	43.51 ± 0.01	31.00	12.50	1.10	1.47	-14.72	-26.10
[HMIM][BF ₄]	210.00	37.09 ± 0.02	32.63	4.46	0.87	1.86	-8.08	-13.21
ethylene glycol	2.50	44.79 ± 0.01	32.44	12.35	1.08	1.49	-23.43	-34.84
water	0.0016	68.75 ± 0.02	-	-	-	-	-	-

5.4. Isotherms, temperature dependence and thermodynamics of nonionic surfactants in mixed IL solutions

Ionic liquids used in this section were 1-methyl-3-butylimidazolium tetrafluoroborate and 1-methyl-3-butylimidazolium trifluoromethanesulfonate, together with Tween 20 nonionic surfactant. The decision on choosing [BMIM][BF₄] was its capability of supporting aggregation of nonionic surfactants, while [BMIM][OTf], which is unable to support micellization, presents more favorable handling properties, which are lower density and higher viscosity, but also better electrical conductivity, which may also be an advantage. Therefore in order to obtain a solvent with good handling properties but capable of supporting micellization, the two of them were mixed in different mass fractions.

The solutions were prepared in three different mass fractions of [BMIM][BF₄], 0.1, 0.3 and 0.5. The aggregation behavior of Tween 20 was analyzed in each of the binary solutions, and CMC values in 25.0°C were determined. The diagrams of surface tension values also include isotherms for Tween 20/[BMIM][OTf] and Tween20/[BMIM][BF₄] systems (figure 35). Viscosity values were the resultants of individual viscosities of the ILs according to their mass fractions in the binary solutions, whereas density coefficients did not show a linear dependence (see Supplementary Material). Surface parameter computed from surface tension isotherms are presented in table 14.

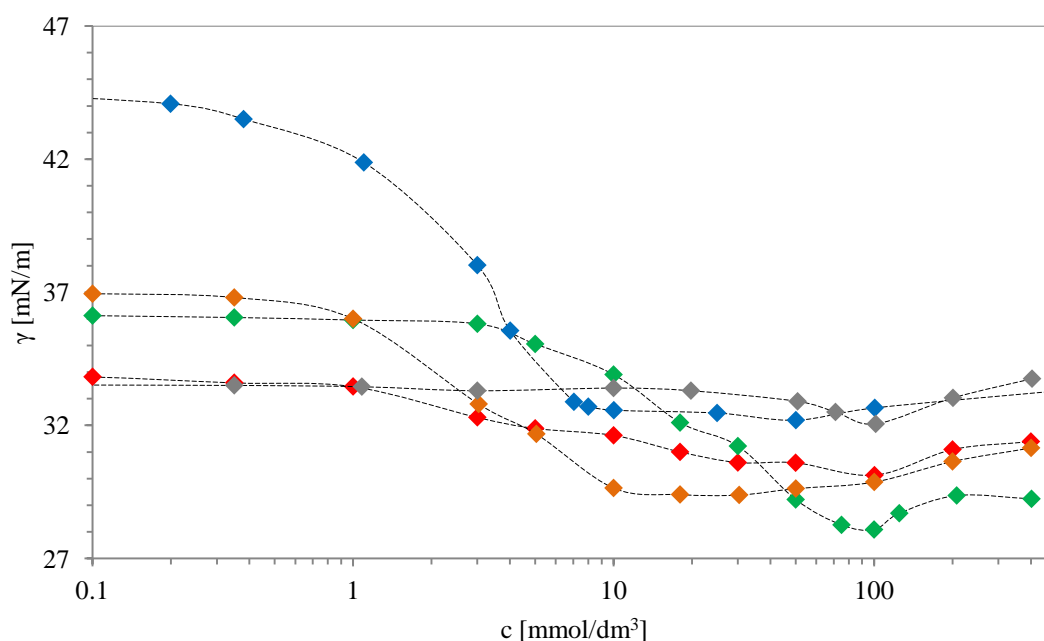


Figure 35. Surface tension isotherms of Tween 20 in pure and mixed 1-butyl-3-methylimidazolium ILs, [BMIM][OTf]/[BMIM][BF₄] with corresponding mass ratios: [BMIM][BF₄] (♦), [BMIM][OTf]/[BMIM][BF₄] 1:1 (♦), 7:3 (♦), 9:1 (♦), [BMIM][OTf] (♦)

As shown in the plot, addition of [BMIM][BF₄] to [BMIM][OTf] results in a change of the isotherms from the flat to the curved one. An addition of only 0.1 mass fraction of [BMIM][BF₄] facilitates micellization by changing mixtures surface properties, what is reflected by discontinuity of the plot. Increased tetrafluoroborate salt concentration enhances solvophobic properties, providing decrease of critical micelle concentration values. The initial surface tension values of IL mixtures rises with the addition of [BMIM][BF₄], due to its higher surface tension value.

The presence of only 0.1 mass fraction of 1-butyl-3-methylimidazolium tetrafluoroborate ionic liquid in the mixture facilitates formation of surfactant micelles in the ILs mixture. Further increase of [BMIM][BF₄] mass fraction enhances systems solvophobic properties providing lower CMC values of Tween 20. The dependence of critical micelle concentration of the surfactant on the mass fraction of [BMIM][BF₄] was observed to be linear (figure 36). Critical micelle concentration of Tween 20 in [BMIM][OTf]/[BMIM][BF₄] 1:1 mixture is similar to CMC value for pure [BMIM][BF₄] salt. However, due to the presence of [BMIM][OTf], the decrease of surface tension provided by the surfactant is less effective than in pure [BMIM][BF₄].

Increased mass fraction of 1-butyl-3-methylimidazolium tetrafluoroborate in the binary solution of the ionic liquids resulted in increased Γ_{\max} , and decreased A_{\min} (table 12), reflecting enhanced solvophobic interactions to take place and, therefore, an increase of surfactant concentration at the air-ILs interface.

At the same time, Π_{cmc} values increased too, reflecting more efficient reduction of surface tension, as well as a tendency of the ILs mixture to undergo a better surface tension lowering with an increased amount of the solvophobic compound. Free energy of micellization against mass fraction of the more solvophobic component in the mixture, [BMIM][BF₄], was plotted in figure 37. The value of ΔG_m was the most negative (micellization process was most spontaneous) at the highest content of [BMIM][BF₄].

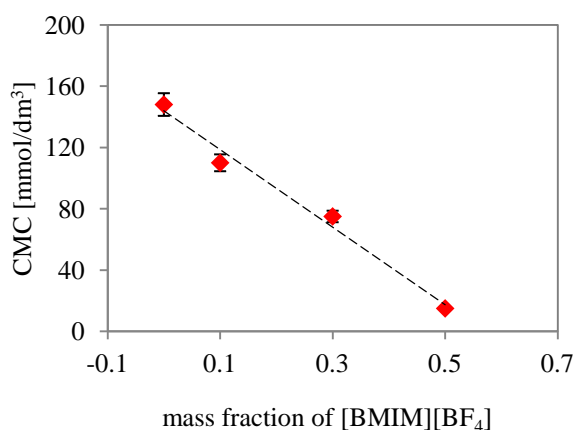


Figure 36. Dependence of the critical micelle concentration on [BMIM][BF₄] mass fraction in [BMIM][OTf]/[BMIM][BF₄] mixtures

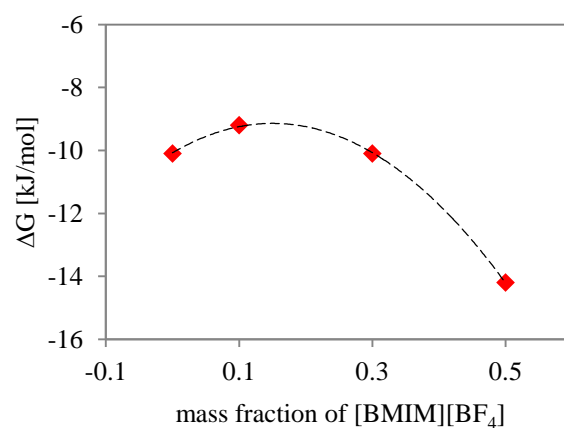


Figure 37. Dependence of Gibbs free energy of Tween 20 micelle formation on [BMIM][BF₄] mass fraction in [BMIM][OTf]/[BMIM][BF₄] mixtures

Table 12. Surface properties of Tween 20 in [BMIM][OTf]/[BMIM][BF₄] mixtures with different mass fractions

System	mass fraction	CMC [mmol/dm ³]	γ_{CMC} [mN/m]	$\Gamma_{\text{max}} \times 10^6$ [mol/m ²]	A_{min} [nm ²]	Π_{cmc} [mN/m]	ΔG_{m} [kJ/mol]
[BMIM][OTf]	0	148.0	31.8	0.8	2.2	2.6	-10.1
[BMIM][OTf]/[BMIM][BF ₄]	0.1	110.0	30.1	0.5	3.7	4.3	-9.2
[BMIM][OTf]/[BMIM][BF ₄]	0.3	70.0	28.1	1.0	1.5	8.0	-10.1
[BMIM][OTf]/[BMIM][BF ₄]	0.5	15.0	28.6	1.1	1.5	8.1	-14.2
[BMIM][BF ₄]	1	9.0	33.4	1.4	1.1	11.5	-12.8

5.5. Critical micelle concentration

The values of critical micelle concentration were determined from surface tension isotherms of the analyzed systems, and listed together with other surface parameters, in the range of temperatures, in tables 7-10. To verify obtained values, CMCs were also determined from apparent molar volumes, which, when plotted against surfactant concentration, allow determination of CMC values. The data for TX-100 in selected ionic liquids are listed in table 13. Obtained values were in agreement with the ones determined from surface tension measurements data.

Determined density data enabled calculation of corresponding apparent molar volumes of pure ionic liquids, as well as TX-100/IL binary solutions. For pure ionic liquids, elongation of the alkyl chain provokes a linear increase of V_{Φ} values, what is a consequence of occupying more space by ILs molecules. It was observed, that the values for tetrafluoroborate-based ILs are lower than corresponding [AMIM][PF₆] ones. An increase of the apparent molar volume by an addition of a methylene group to the alkyl chain was calculated to be close to 17, as shown previously by Tariq [114]. Moreover, apparent molar volumes of two ionic liquids belonging to each family and having the same cation and different anion differed by around 19.5 cm³/mol (figure 38).

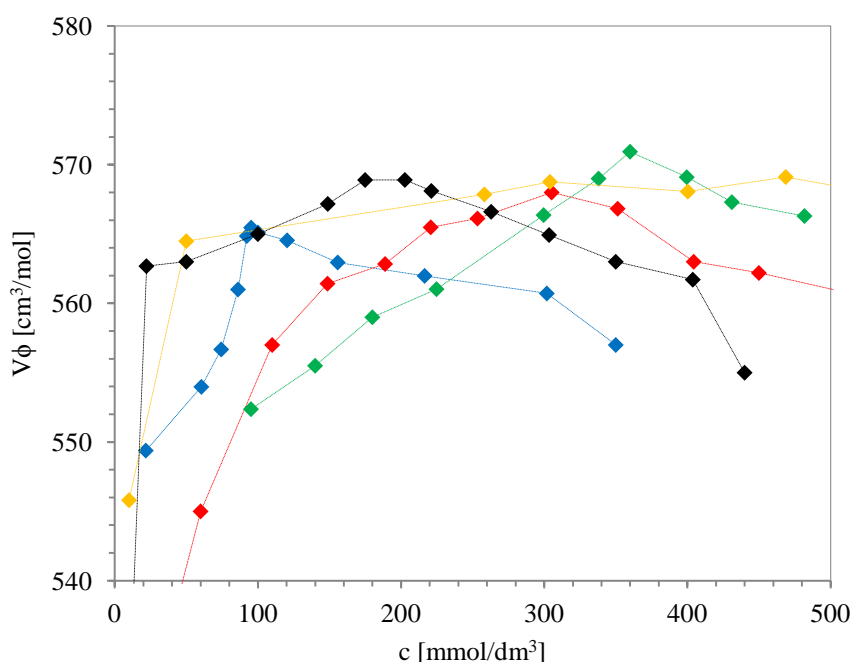


Figure 38. Apparent molar volume values, V_{Φ} , of TX-100 in 1-alkyl-3-methylimidazolium tetrafluoroborate ionic liquids, where [EMIM] (\blacklozenge), [PrMIM] (\blacklozenge), [BMIM] (\blacklozenge), [PMIM] (\blacklozenge), [HMIM] (\blacklozenge), at 25°C

Triton X-100, when added to ILs, provokes significant increase of the apparent molar volumes, due to relatively high V_{Φ} of the surfactant in comparison to ILs. Within the analyzed systems, the apparent molar volumes ranged 545 – 576 cm³/mol for 1-alkyl-3-methylimidazolium tetrafluoroborate and 480 – 570 cm³/mol for 1-alkyl-3-methylimidazolium hexafluorophosphate salts. It was observed, that in the pre-micellar region the increase of V_{Φ} is linear and after obtaining the maximum – in the CMC area – a linear decrease. Critical micelle concentration was determined from the intersection of the extensions of plot lines. Due to the fact, that solvation of micelles takes place differently than

solvation of the surfactant monomers, therefore, their contribution to the apparent molar volumes differs too. Here it was observed the linear decrease of V_{ϕ} in the micellar region, which is different than in case of aqueous micellar systems, where after the CMC the V_{ϕ} remains stable. Such a behavior was observed for aqueous sodium dodecylsulphate [115], dodecyltrimethylammonium bromide [116]. The profile of apparent molar volume strictly depends on the composition of the micellar system, which gathers a number of features – particularly surfactants hydrophilicity and hydrophobicity, V_{ϕ} of the surfactant in micellar and monomeric form, micellization equilibrium constant, aggregation number and solvents structure [106].

ILs-based systems undergo more intensive surfactant/solvent interactions than water-based systems, what may clarify observed trends. It was already described by Atkin and Warr, who revealed that effective interaction area for each oxyethylene unit in nonionic surfactant is much higher in ethylammonium nitrate ionic liquids than in water [117]. Also Behera et al. used conductivity studies supported with absorption and fluorescence spectra, to determine partitioning of 1-butyl-3-methylimidazolium hexafluorophosphate ionic liquid into TX-100 micelles [118]. Consequently, effective interaction area of ILs with Triton X-100 is stronger than in aqueous systems, and provides incorporation of ILs into micellar palisade layer. Also the range of the apparent molar volume for the hexafluorophosphate-based systems is smaller than for the tetrafluoroborate-based. The tendency may be the effect of weaker cation-anion interactions due to steric hindrance, this is the anion size. As a result, stronger electrostatic interactions between IL ions result in weaker association of imidazolium cation with TX-100 oxyethylene groups, thus the breakdown of ion pairs is more difficult [119, 120].

The general tendency observed is that CMC values increase with increased length of ILs cations alkyl chains of tetrafluoroborate and hexafluorophosphate ionic liquids (figure 39). What is more, this tendency is achieved independently from the anion present, and from the type of surfactant used. All the trend lines are linear, whereas for systems containing Tween 20 the increase rate is more rapid than for Triton X-100, due to more complex structure of Tween 20 surfactant - presence of a long alkyl chains and more oxyethylene chains, thus more hydrogen and van der Waals bond donors. However, due to the literature, in systems where imidazolium ionic liquids are used as surfactants, in IL-in-water systems, the dependence is just the opposite [102, 121, 122].

Table 13. CMCs of Triton X-100 in [AMIM][BF₄] and [AMIM][PF₆] determined from surface tension γ , and apparent molar volumes V_ϕ , at 25.0°C

ILs	CMC [mmol/dm ³]	
	from γ	from V_ϕ
[EMIM][BF ₄]	90.00	90
[PrMIM][BF ₄]	220.00	200
[BMIM][BF ₄]	310.00	300
[PMIM][BF ₄]	330.00	350
[HMIM][BF ₄]	1000.0	600
[BMIM][PF ₆]	90.00	90
[PMIM][PF ₆]	95.00	95
[HMIM][PF ₆]	150.00	110

It was observed that elongation of the oxyethylene chains of Triton X-100, Triton X-114, Triton X-45 and Triton X-15 (9.5, 7.5, 4.5 and 1.5 OE units, respectively), results firstly in the increase, and then in the decrease of critical micelle concentration values (figure 40). Such behavior was observed for selected ionic liquids, [EMIM][BF₄] and [BMIM][BF₄], and analogically for ethylene glycol.

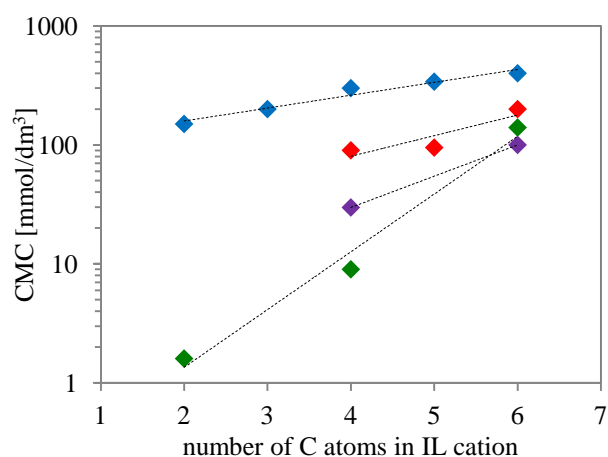


Figure 39. CMC values vs. IL structure: TX-100/[AMIM][BF₄] (♦), TX-100/[AMIM][PF₆] (♦), Tween 20/[AMIM][BF₄] (♦), Tween 20/[AMIM][PF₆] (♦), at 25.0°C

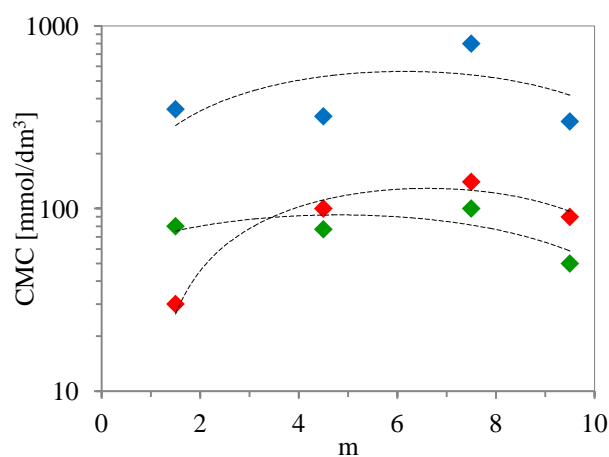


Figure 40. Number of OE units (m) of Triton X surfactants, vs. CMCs in [EMIM][BF₄] (♦), [BMIM][BF₄] (♦) and ethylene glycol (♦), at 25.0°C

5.6. Micellar diameter

The presence of micellar aggregates was confirmed by means of dynamic light scattering measurements of the solutions at 25.0°C in the wide range of surfactant concentrations, below and above the CMC values, which were determined by means of surface tension measurements. For each of the analyzed samples viscosity coefficients were determined and used for analyzes (see Supplementary Material). For pure solvents and below the CMCs, determined diameters were below 1 nm, indicating presence of surfactant monomers, however close to CMC an increase of scattered light intensity was observed. As shown in figures 41, 42 and 43, an increase of TX-100 concentration in the systems is accompanied with a preliminary growth of micelles, and size stabilization afterwards.

However, the type of ILs cation determines the size of micelles, therefore at CMCs larger diameters were detected for ionic liquids with shorter alkyl chains - 3.5, 1.6 and 0.9 nm for [EMIM][BF₄], [BMIM][BF₄] and [HMIM][BF₄], respectively. These results, together with data described above, confirm that [EMIM][BF₄] has the highest ability to support self-assembly due to higher solvophobicity, among given solvents. Also an increase of TX-100 concentration above the CMCs provides an enlargement of the micelles, even up to 8.5 nm for TX-100/[EMIM][BF₄] at 4xCMC, 2.5 nm for TX-100/[BMIM][BF₄] at 2xCMC, and 1.4 nm for TX-100/[HMIM][BF₄] at 1.35xCMC).

The average of hydrodynamic diameter of Tween 20 micelles in water was determined to be 8 nm in CMC, and fits with literature data [123]. Figures 44, 45 and 46 present DLS data for Tween 20 surfactant in selected ILs. For Tween20/[EMIM][BF₄] at CMC surfactant concentration (1.6 mmol/dm³) particles of 8 nm were detected, and with further increase to 6 x CMC (9.6 mmol/dm³) diameters of 25-27 nm were obtained. An average size of micelles detected in Tween20/[EMIM][OTf] at CMC (5 mmol/dm³) was smaller – 2 nm, and around 7 nm at 1.8 x CMC (9 mmol/dm³). Such difference in micellar sizes may result from relatively stronger interactions between Tween 20 and IL, and therefore higher solubility due to weaker interactions amongst ILs ions. Further increase of Tween 20 concentration to 2 x CMC provides significant increase of the average D_h to 100 nm, and to 200 nm at the concentration of 3 x CMC. The mean micellar diameters at CMCs in Tween20/[BMIM][BF₄] and Tween20/[BMIM][PF₆] were found to be 80 and 50 nm, respectively. In case of Tween20/[BMIM][OTf] system only structures of 1-1.3 nm at a concentration of 4 x CMC were determined. This may indicate formation of micelles, however so small diameters

require confirmation with other techniques. Micelles in Tween20/[HMIM][BF₄] detected at CMC had diameters of 10 nm in, and 100 nm above CMC.

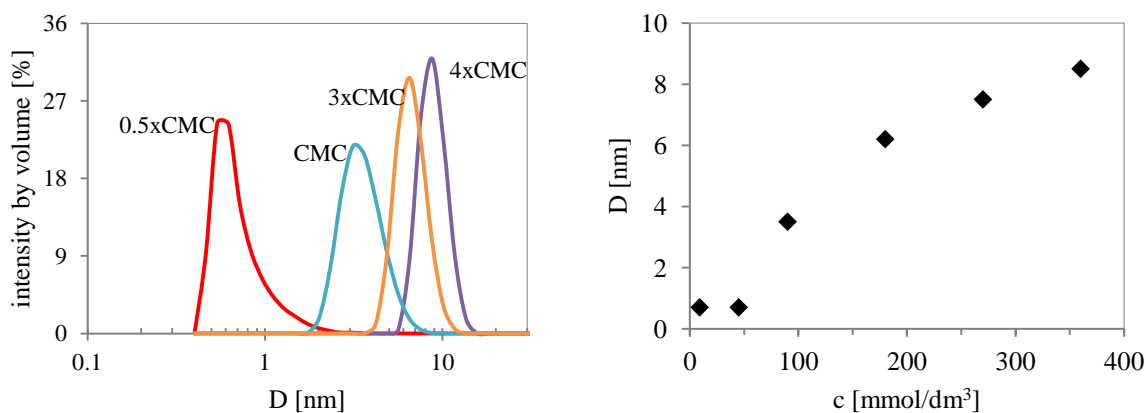


Figure 41. Size distribution curves determined for Triton X-100 in [EMIM][BF₄] (left), and mean hydrodynamic diameter as a function of surfactant concentration (right), at 25°C

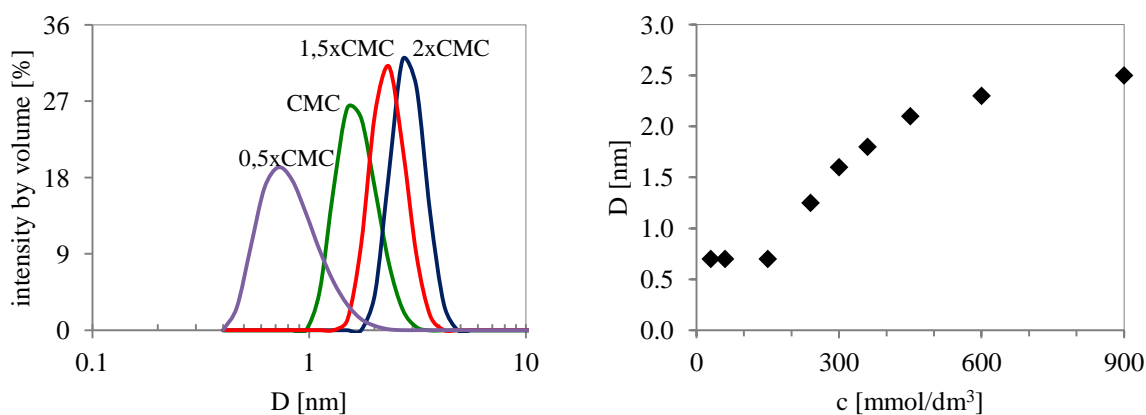


Figure 42. Size distribution curves determined for Triton X-100 in [BMIM][BF₄] (left), and mean hydrodynamic diameter as a function of surfactant concentration (right), at 25°C

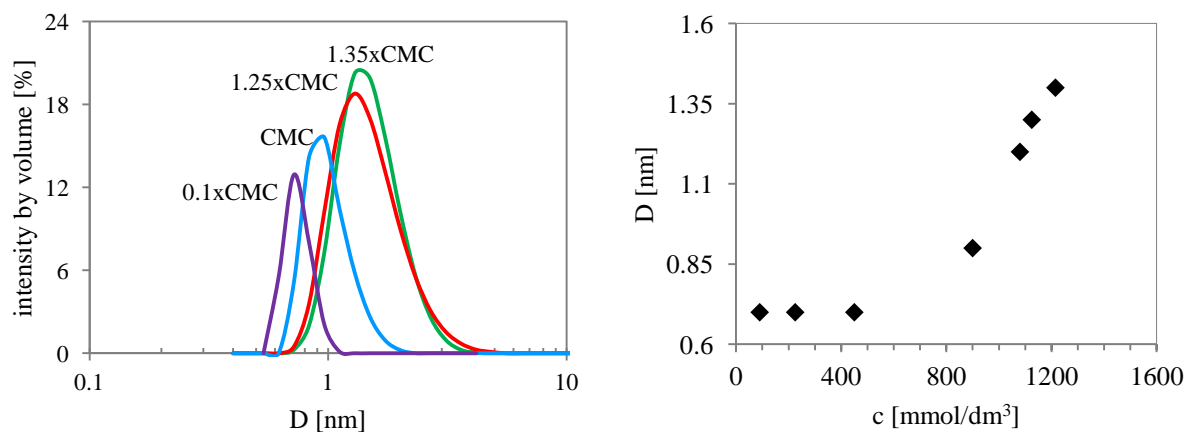


Figure 43. Size distribution curves determined for Triton X-100 in [HMIM][BF₄] (left), and mean hydrodynamic diameter as a function of surfactant concentration (right), at 25°C

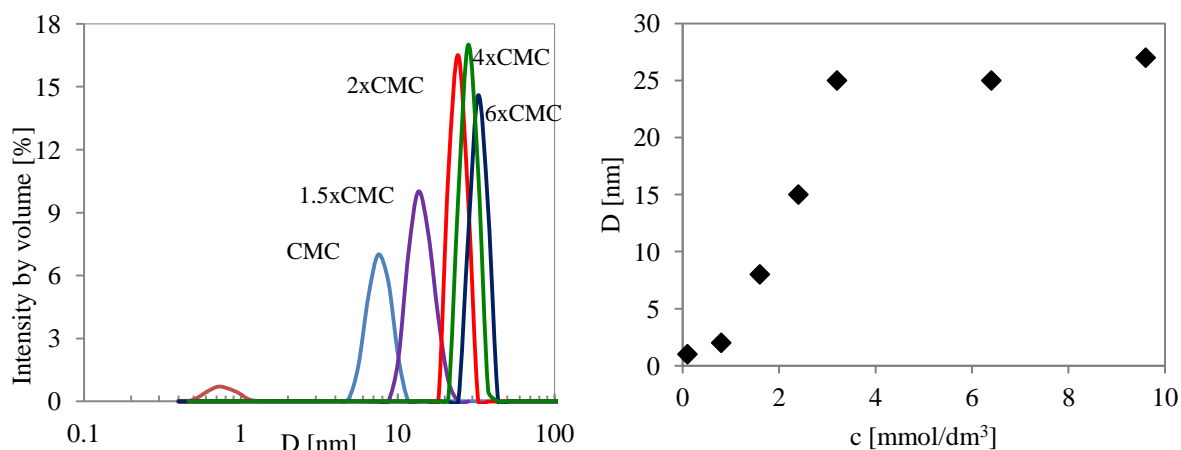


Figure 44. Tween 20/[EMIM][BF₄] size distribution (left), and mean hydrodynamic diameter vs. surfactant concentration (right), at 25°C

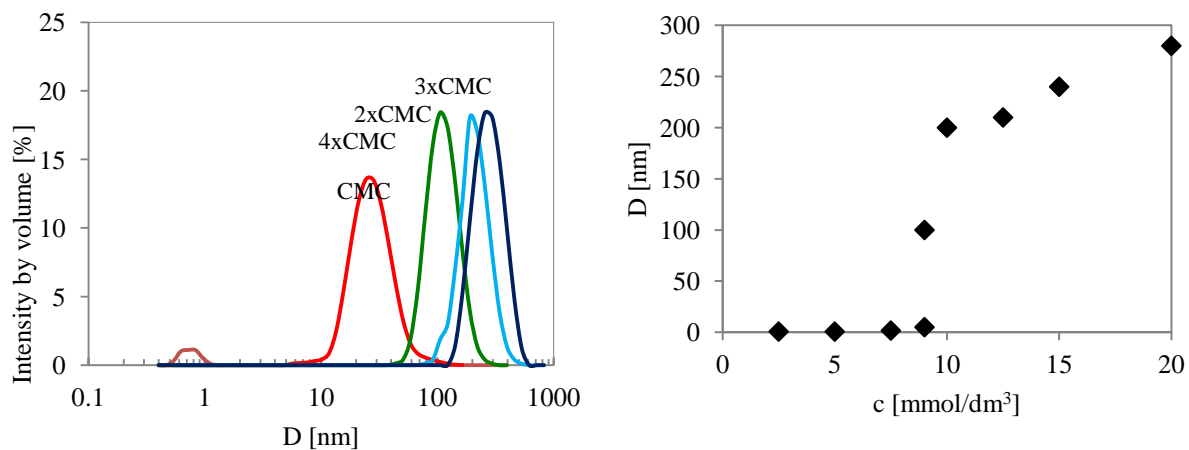


Figure 45. Size distribution curves determined for Tween 20 in [EMIM][OTf] (left), and mean hydrodynamic diameter as a function of surfactant concentration (right), at 25°C

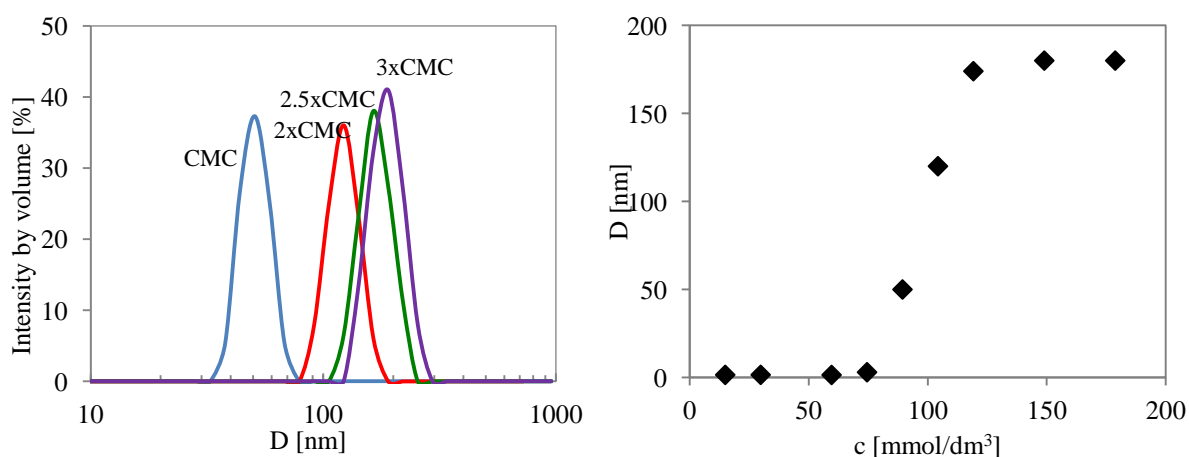


Figure 46. Size distribution curves determined for Tween 20 in [BMIM][PF₆] (left), and mean hydrodynamic diameter as a function of surfactant concentration (right), at 25°C

When comparing micellar diameters of Triton X-100 and Tween 20 in selected ionic liquids, we may see that Tween 20 micelles are significantly bigger what is a result of the differences between surfactants structures. Tween 20 molecule is bigger due to possession of three OE chains and long alkyl side chain, whereas Triton X-100 is much more complex and contains only one chain with fewer OE units and short alkyl side chain, therefore has smaller volume. Determined micellar diameters of Tween 20 in ethylene glycol were around 8 nm, whereas in water - 8.5 nm. On the contrary, Triton X-100 micelles in water were reported to be around 7 nm [124], which is more than the diameter detected in ILs, with exception of [EMIM][BF₄].

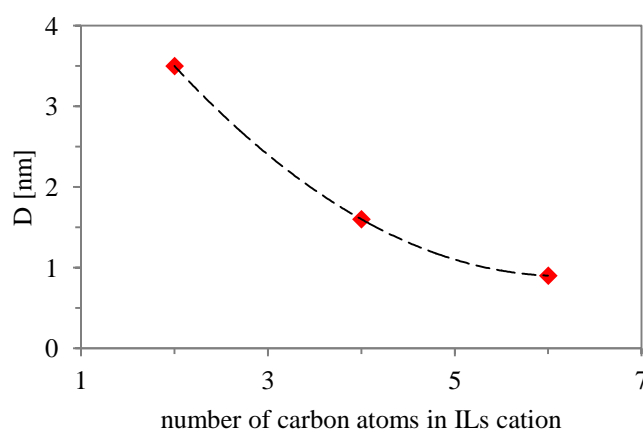


Figure 47. Micellar diameters of Triton X-100 vs. number of cation alkyl chain carbon atoms in [AMIM][BF₄], at 25°C

Basing on the DLS data the dependence of micellar sizes on the alkyl chain lengths of ILs cations was established (figure 47). Hydrodynamic diameters determined in TX-100 systems decrease with the increase of ILs sizes. In Tween 20 systems it was observed, that the size of D_h was the biggest in IL with tetrafluoroborate anions, and the smallest in the presence of trifluoromethanesulfonate anion (order of growth: BF₄>PF₆>OTf). Both relationships confirm the decrease of systems solvophobicity, resulting from the increase of intermolecular interactions amongst ILs and the amphiphiles. The sizes of determined micellar diameters of nonionic surfactants in ILs are much smaller than in aqueous systems. The observations presented here fit well with the conclusions presented by other authors, e.g. Patrascu *et al.*, who analyzed the series of POE surfactants (C_nE_m) in imidazolium ILs [86], and Inoue group, who performed a number of studies on the nonionic C_mE_n surfactants micellization in imidazolium ionic liquids [39, 91, 94], Also analogue observations were reported in the '80s by Evans, in the study on cationic cetyl trimethylammonium bromide in EAN [77].

5.7. Conductivity

Conductivity measurements were performed in order to determine the number of imidazolium cations associated with one OE unit of the surfactants. Conductivity values obtained in this investigation and the ones given in the literature present certain discrepancies, which result from varying qualities of the ILs (producers, lots), mainly depending on the contamination with water and other impurities (see section 4.1.1). Conductivity values determined in this study, together with the literature values are given in table 14. The conductivity dependence determined for different volume fractions of Triton X-100 and Tween 20 surfactants in 1-alkyl-3-methylimidazolium ionic liquid solutions are shown and compared in figures 48 and 49.

Table 14. Ionic liquids experimental and literature conductivity values

Compound	κ [mS]	
	experimental	literature
[EMIM][BF ₄]	14.00 ± 0.21	15.46 [125]
[EMIM][OTf]	8.25 ± 0.05	9.13 [126]
[EMIM][NTf ₂]	9.10 ± 0.09	9.47 [127]
[BMIM][BF ₄]	2.80 ± 0.03	3.52 [125]
[BMIM][PF ₆]	1.31 ± 0.05	1.37 [128]
[BMIM][OTf]	1.90 ± 0.06	2.9 [129]
[BMIM][NTf ₂]	1.91 ± 0.09	3.94 [128]
[HMIM][BF ₄]	1.29 ± 0.08	1.23 [125]
[OMIM][BF ₄]	0.55 ± 0.05	0.57 [130]
[OMIM][PF ₆]	0.25 ± 0.03	0.25 [131]
[OMIM][OTf]	0.56 ± 0.01	-
[OMIM][NTf ₂]	1.15 ± 0.02	1.31 [132]

Molecular parameters of the ionic liquids and surfactants, such as molar masses and molar volumes, required for calculation of n_{ac} , are collected tables S.3-S.7 (see Supplementary Material). Obtained conductivity κ , and normalized conductivity κ/κ_{IL} , were plotted against surfactant concentration shown in weight ratio, ϕ , and compared with Bruggeman fit. According to the literature, OE groups of POE-type surfactants interact with ILs by means of van der Waals, hydrogen bonds and electrostatic interactions [58]. With a use of techniques such as conductivity, dielectric relaxation spectroscopy, infrared spectroscopy and NMR,

it was demonstrated that 2-3 water molecules associate with one OE group of TX-100 surfactant [133], and such assumption was already employed for Tween 20 surfactant [102].

Electrical conductivity of the systems, normalized to pure ionic liquid conductivities, as a function of surfactant volume fraction, Φ , are given in figures 50, 51 and 52. Along the whole concentration range, Triton X-100 plots of normalized conductivity fit well with Looyenga approximation, whereas Tween 20 with Bruggeman approximation.

In case of mixed solvents, the higher was the solution content of Triton X-100, the normalized conductivity was shifted more towards Looyenga approximation line. It was observed that κ/κ_{IL} , depends on the structure of ILs and with changing e.g. viscosity coefficient, which is known to relate with the energy of hydrogen bonds or van der Waals interactions between surfactant and the solvent, the normalized conductivity changes too. Consequently, [EMIM][BF₄], having the shortest alkyl chain, is characterized by stronger interactions with surfactant molecules than [BMIM][BF₄] and [HMIM][BF₄], and therefore normalized conductivity of [EMIM][BF₄]-based solutions is lower than [BMIM][BF₄]- and [HMIM][BF₄]-based ones.

It was determined, that with elongation of ILs alkyl chains in cations substituents, the number of OE units associated with ILs molecule decreases, independently from the surfactant used, however in case of Tween 20 the decrease is more rapid (figure 53). Such behavior is related with the size of both components of the systems, e.g. in the same IL more bulky Tween 20 surfactant needs more space than TX-100, therefore limitation of the space with elongated ILs chains results with more rapid decrease of n_{ac} .

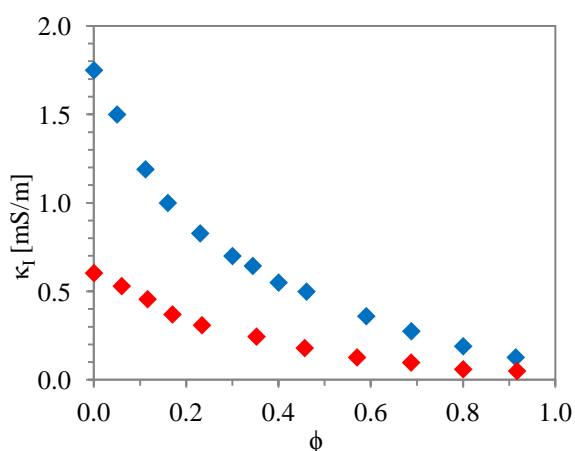


Figure 48. Conductivity vs. weight ratio of TX-100 in [BMIM][BF₄] (♦) and [BMIM][PF₆] (♦)

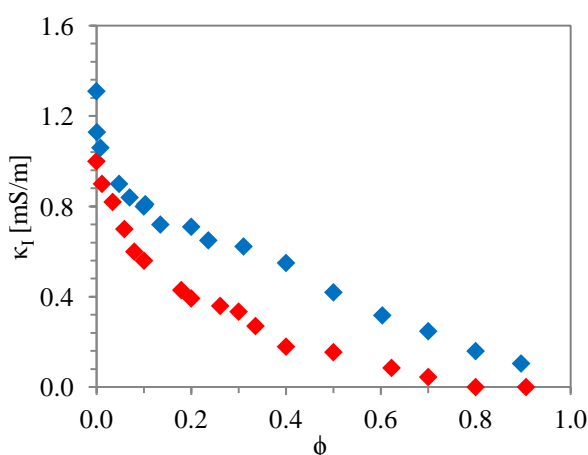


Figure 49. Conductivity vs. weight ratio of Tween 20 in [BMIM][BF₄] (♦) and [BMIM][PF₆] (♦)

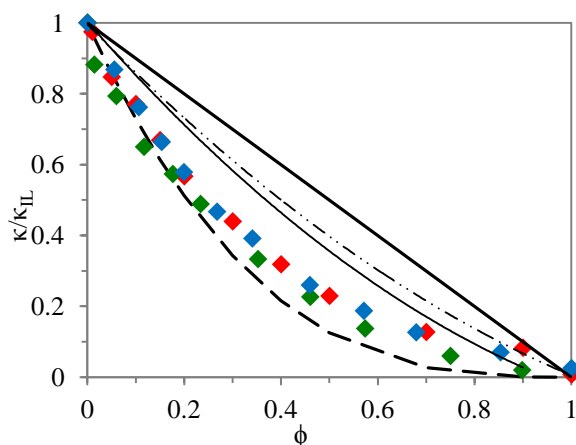


Figure 50. Dependence of normalized conductivity values of (κ/κ_{IL}) on the volume fractions (ϕ) of the surfactant in TX-100/IL solutions: [EMIM][BF₄] (◆), [BMIM][BF₄] (◆), [HMIM][BF₄] (◆).

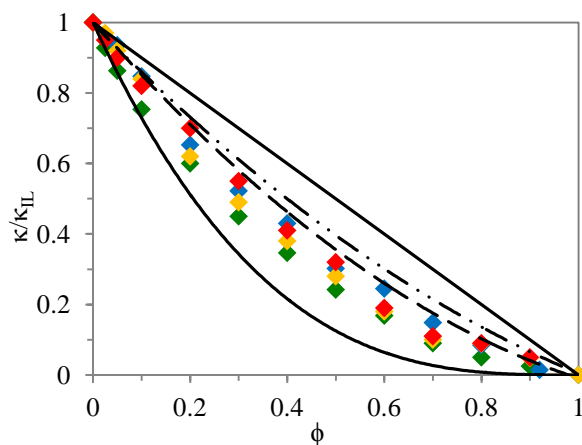


Figure 51. Dependence of normalized conductivity values (κ/κ_{IL}) on the volume fractions (ϕ) of the surfactant in Tween 20/IL binary solutions: [BMIM][BF₄] (◆), [BMIM][PF₆] (◆), [BMIM][NTf₂] (◆), [BMIM][OTf] (◆).

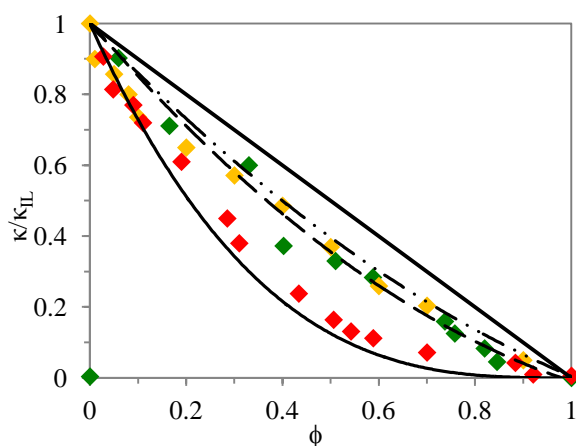


Figure 52. Dependence of normalized conductivity values of (κ/κ_{IL}) on the volume fractions (ϕ) of Tween 20 in [BMIM][OTf]/[BMIM][BF₄] of 0.1 (◆), 0.3 (◆), and 0.5 (◆) mass fractions of [BMIM][BF₄]

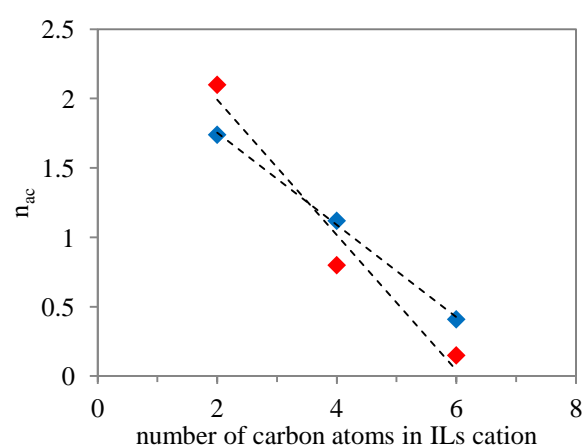


Figure 53. Dependence of the number of [AMIM][BF₄] cations carbon atoms on surfactant aggregation numbers, n_{ac} , of TX-100 (◆) and Tween 20 (◆), at 25.0°C

Aggregation numbers of Triton X-100 and Tween 20 determined in the homologue series of 1-alkyl-3-methylimidazolium tetrafluoroborate ionic liquids show a decreasing trend when elongating ILs alkyl chains, as depicted in plot 53. Systems based on Tween 20 surfactant undergo more rapid decrease than Triton X-100 based ones, what is presented by the angle of the trend lines toward x-axis. The explanation of the behavior is increased solubility of surfactant molecules in the ionic liquids (stronger solvent-solute interaction due to elongation of ILs alkyl chains), which is more intense in case of Tween 20 due to higher number of oxyethylene groups, which interact with the alkyl chains by means of hydrogen bonds.



5.8. Statistical evaluation of results

Dixon's Q-Test

Dixon Q-Test is a statistical test used to detect and reject the outliers (gross values). Obtained values are arranged in an increasing sequence, and then Q_A and Q_B parameters are determined using formula 20:

$$Q_A = \frac{x_2 - x_1}{x_n - x_1}, \quad Q_B = \frac{x_n - x_{n-1}}{x_n - x_1} \quad (20)$$

Calculated Q_A and Q_B values were compared with proper critical value Q_{cr} , taken from table 15. If Q_A/Q_B ratio was higher than Q_{cr} , then the value was rejected.

Table 15. Critical values for Dixon's Q-Test for 95% confidence level.

n	3	4	5	6	7	8	9	10
Q_{cr}	0.970	0.829	0.710	0.628	0.569	0.608	0.504	0.530

Arithmetic mean

After rejecting the gross values from Dixon Q-Test, from the remaining (at least 3) values mean value was calculated, according to formula (equation 21), where n = number of measurements, X_i = following value:

$$\bar{X} = \sum_{i=1}^n \frac{X_i}{n} = \frac{(X_1 + X_2 + X_3 + \dots + X_n)}{n} \quad (21)$$

Standard deviation of single measurement

Standard deviation of single measurement, which is a measure of dispersion of obtained values around the mean values, and is measured from equation 22.

$$s = \sqrt{\frac{\sum_{i=1}^n (X_i - \bar{X})^2}{n-1}} = \sqrt{\frac{(X_1 - \bar{X})^2 + (X_2 - \bar{X})^2 + \dots + (X_n - \bar{X})^2}{n-1}} \quad (22)$$

Standard deviation of the mean

$$S = \frac{s}{\sqrt{n}} \quad (23)$$

Confidence interval

A confidence interval gives an estimated range of values being likely to include an unknown value of an estimated parameter. The confidence level chosen here is 95%.

$$\mu = \bar{X} \pm t \cdot S \quad (24)$$

Parameter t, according to the number of measurements, was taken from the table below.

Table 16. Parameter t related with the number of measurements n

n	2	3	4	5	6	7	8	9	10
t	12.4	4.3	3.18	2.78	2.57	2.45	2.36	2.31	2.26

Example

Dixon's Q-Test of exemplary surface tension values measured for TX-114/[BMIM][BF₄], c = 21.55 mmol/dm³, at 25.0°C are shown below.

Table 17. Statistical evaluation of surface tension values

γ [mN/m]	Q _A	Q _B	Q _{cr}	\bar{X}	s	S	$\bar{X} \pm t \cdot S$
42.24							
42.30							
42.33	0.375	0.125	0.710	42.33	0.064	0,028	42.33 ± 0,08
42.38							
42.40							

6. Discussion of the results

The most significant surface tension decrease, which is surface pressure and surface tension at CMC, was observed in 1-ethyl-3-methylimidazolium tetrafluoroborate, which is the ionic liquid of the shortest cations alkyl chain and the smallest, least diffusive anion, and Triton X-100 surfactant, so the amphiphile with the highest number of oxyethylene units and the simplest structure amongst surface active agents used in the investigation. Remaining Triton X surfactants, along with the decrease of the number of OE groups, presented worse ability to decrease ILs surface tension. Nevertheless, Triton X-100 underwent micellization in the broadest number of ILs. On the contrary, Tween 20, Tween 60 and Tween 80 have the same number of OE units, but they differ by the length of alkyl chains, therefore their ability to decrease surface tension of ILs was comparable, whereas their amount required to obtain maximum decrease of surface tension was different. No surface tension decrease was detected in 1-octyl-3-methylimidazolium ILs, what was elucidated with too weak solvophobic interactions between the species. Proposed interactions of selected ionic liquids and Triton X surfactants are shown in figures 54-56.

Despite similarities between structures and interactions amongst ionic liquids, only the ones containing tetrafluoroborate $[\text{BF}_4]$ and hexafluorophosphate $[\text{PF}_6]$ anions were able to support micellar aggregation. An exception was $[\text{EMIM}][\text{OTf}]$ ionic liquid, which supported aggregation of only one surface active agent - Tween 20. None of the systems containing $[\text{NTf}_2]$ anion underwent characteristic decrease of surface tension values with increasing concentration of the surfactants in the samples.

In the case of Triton X surfactants, also none of the systems containing $[\text{OTf}]$ anion was observed to form micelles. There is clear evidence that a proper balance between ILs cationic and anionic groups is crucial for the amphiphilic compounds to decrease surface tension of a system, leading to self-ordering of its molecules. Certain groups of the surfactants are responsible for their limited solubility which provide spontaneous adsorption on the surface of the solvent phase, enable interactions amongst surfactant, solvent and gas molecules, and support aggregation. Since ionic liquids with bigger anions (OTf , NTf_2) and longer cation hydrocarbon substituents generally do not undergo surface tension reduction in the presence of a surfactant, it may be assumed that some of surfactants functions are insufficient. On the other hand, a distortion of ILs supramolecular structure may be predicted due to the presence of amphiphilic molecules.

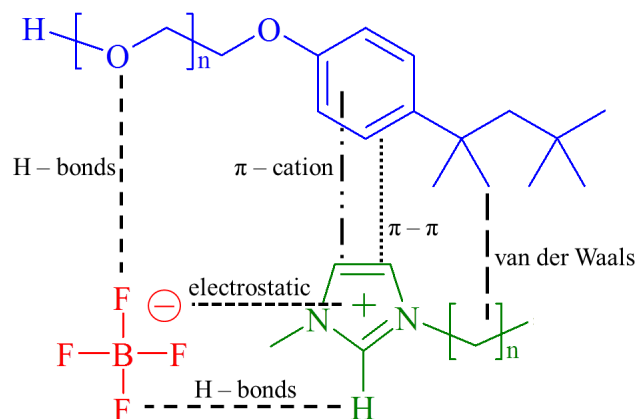
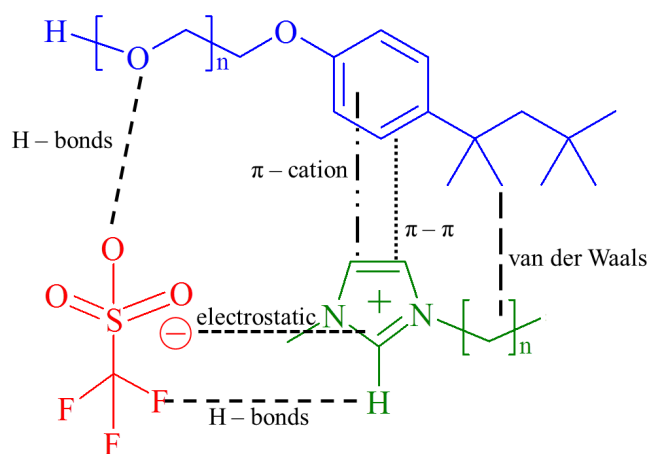
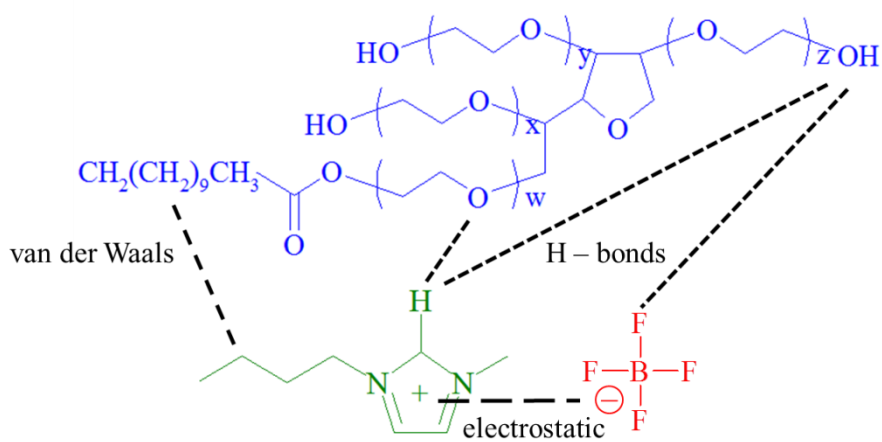
Figure 54. Proposed interactions between Triton X surfactants and [BMIM][BF₄] ionic liquids' ions

Figure 55. Proposed interactions between Triton X surfactants [BMIM][OTf] ionic liquids' ions

Figure 56. Proposed interactions between Tween 20 surfactant and [BMIM][BF₄] ionic liquids' ions

Micellization behavior was most effective in the system composed of Triton X-100 surfactant, which has the longest oxyethylene chain from surfactants used in the investigation, and 1-ethyl-3-methylimidazolium tetrafluoroborate ionic liquid, [EMIM][BF₄], which has the shortest cation alkyl chain from ILs used here, and the smallest and simplest anion. The surface pressure, Π_{cmc} , which is the ability of the surfactant to decrease ILs surface tension, is the highest from the systems investigated, which results also from the fact, that initial surface tension of [EMIM][BF₄] is the highest from ILs investigated here. Critical micelle concentration of TX-100/[EMIM][BF₄] system (90 mmol/dm³) was the lowest from TX-100/[AMIM][BF₄] system, but still higher than in the remaining [EMIM][BF₄]-based system.

The ability of 1-methyl-3-alkylimidazolium ionic liquids to support micellization of nonionic surfactants was compared with model solvents – ethylene glycol and formamide, and depicted as a dependence of Gibbs free energy of micellization of Triton X-100 surfactant in mentioned solvents, towards Gordon values (figure 57). Water was not included in the graph, because due to perfect properties for supporting micellization, the value was too far from the data given here, to present the relationship. The lower is the value of ΔG_m , the more spontaneous is aggregation, and at the same time, the higher is the Gordon value, the more spontaneously micellization takes place. Thus solvents possessing the best ability to support TX-100 micellization are located at the bottom right corner of the graph.

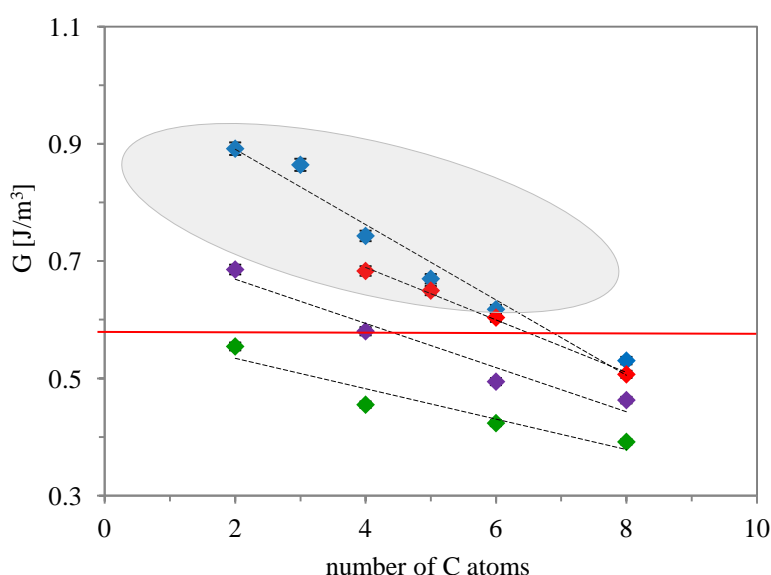


Figure 57. Gordon parameter (G) and the number of carbon atoms in ILs cation alkyl chain (m) regarding anion type: ([BF₄] (♦), [PF₆] (♦), [OTf] (♦), and [NTf₂] (♦), at 25°C. Salts promoting micellar aggregates formation are in the shaded area

The bulk phase energy density, described through its Gordon parameter, shows clear linear relation (correlation coefficient, $r \approx 0.94$) regarding ΔG_m of Triton X-100 in 1-alkyl-3-methylimidazolium tetrafluoroborate ILs. Thermodynamic parameters indicate that elongation of ILs alkyl chain makes micellization less favorable in each of the three surfactants. The decreasing ability of ILs to promote self-assembly of the surfactant is with agreement with values obtained from surface tension measurements and CMCs.

Similar analysis is presented in figure 59, where systems of Triton X-100, Triton X-114 and Triton X-45 in 1-alkyl-3-methylimidazolium tetrafluoroborate are shown. Again, the micellization supporting behavior of the ionic liquids decreases with their alkyl chain elongation, independently from the surfactant used. What is more, the shorter is the oxyethylene chain in a surfactant – the higher are Gordon and Gibbs free energy values. Fewer oxyethylene units in a surfactant result in fewer bonds with the solvent.

Consequently, surfactants with short OE chains form aggregates instead of incorporating into IL mesh. The values for systems with [PrMIM][BF₄] and [PMIM][BF₄] are shifted towards lower G and ΔG_m values due to worse quality of those ionic liquids, therefore, impurities present there affect aggregation supporting behavior.

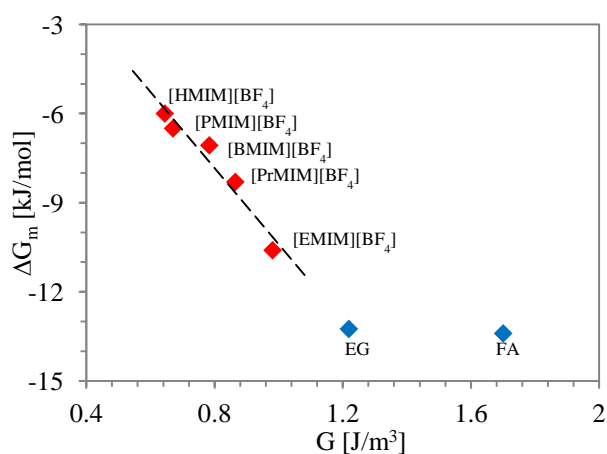


Figure 58. Triton X-100 in [AMIM][BF₄] ILs, ethylene glycol (EG) and formamide (FA) ΔG_m vs. Gordon parameter (G), at 25.0°C

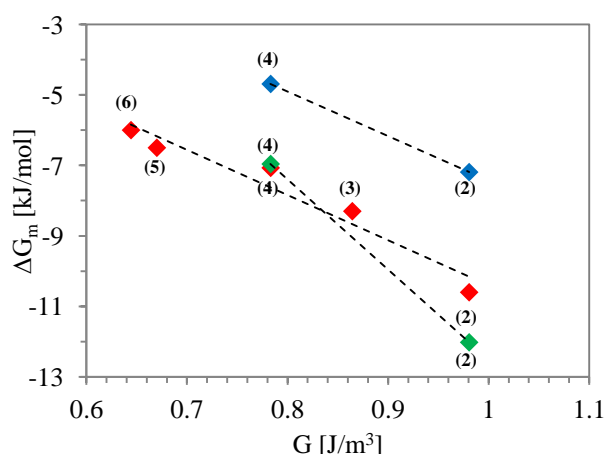


Figure 59. Variation of ΔG_m of Triton X-100 (♦), Triton X-114 (◆), Triton X-45 (◆) surfactants as a function of Gordon parameter (G) in [EMIM][BF₄] (2), [PrMIM][BF₄] (3), [BMIM][BF₄] (4), [PMIM][BF₄] (5), [HMIM][BF₄] (6), at 25°C

Table 18. List of ILs systems analyzed within the dissertation

		TX-100	TX-114	TX-45	TX-15	Tween 20	Tween 60	Tween 80
[EMIM]	[BF ₄]	micellization	micellization	micellization	micellization	micellization	immiscible	immiscible
	[OTf]	no micellization	no micellization	no micellization	immiscible	micellization	immiscible	immiscible
	[NTf ₂]	no micellization	no micellization	no micellization	immiscible	no micellization	no micellization	no micellization
[PrMIM]	[BF ₄]	micellization				micellization	immiscible	immiscible
[BMIM]	[BF ₄]	micellization	micellization	micellization	micellization	micellization	micellization	micellization
	[PF ₆]	micellization	micellization	micellization	micellization	micellization	micellization	micellization
	[OTf]	no micellization	micellization		no micellization	no micellization		
	[NTf ₂]	no micellization	micellization	micellization	no micellization	no micellization	no micellization	no micellization
[PMIM]	[BF ₄]	micellization			immiscible	micellization		
	[PF ₆]	micellization			immiscible	micellization		
[HMIM]	[BF ₄]	micellization	micellization	immiscible	immiscible	micellization		
	[PF ₆]	micellization		immiscible	immiscible	micellization		
	[OTf]	no micellization						
	[NTf ₂]	no micellization	no micellization	no micellization	no micellization	no micellization	no micellization	no micellization
[OMIM]	[BF ₄]	no micellization	no micellization	no micellization	no micellization	no micellization	no micellization	no micellization
	[PF ₆]	no micellization	no micellization		no micellization	no micellization		
	[OTf]	no micellization	no micellization	no micellization	no micellization	no micellization		
	[NTf ₂]	no micellization	no micellization		no micellization	no micellization	no micellization	no micellization

micellization
 no micellization
 immiscible
 unexamined

7. Conclusions

The dissertation includes investigation of 94 systems based on four Triton X and three Tween surfactants, in eighteen 1-alkyl-3-methylimidazolium ionic liquids, composed of two-to-eight carbon atoms in cations alkyl chain, and one of four anions – [BF₄], [PF₆], [OTf] and [NTf₂], (for graphical summary of analysed systems see table 18). The systems were analysed for their surface tension, density, viscosity, conductivity, particle size distribution and aggregation numbers. Critical micelle concentration values were determined from surface tension isotherms, whereas presence of micelles was confirmed in selected systems by means of Dynamic Light Scattering technique. Surface and thermodynamic parameters were calculated based on CMC and surface tension data. Performed investigation allowed to confirm dissertation theses.

Analysis of surface tension and density parameters provided information on the ability of the surfactants to undergo micellization in selected ionic liquids. Out of 93 analyzed systems, 36 were determined to form micellar aggregates. In selected systems the presence of micelles was confirmed by means of dynamic light scattering method and density-derived parameter – apparent molar volume diagrams.

The investigation included determination of broadening solvents phase properties by mixing two ionic liquids of different properties, [BMIM][BF₄] and [BMIM][OTf], where only the tetrafluoroborate-based one provided self-assembly of amphiphiles. The trifluoromethanesulfonate-based IL was selected based on lower density, higher viscosity, higher conductivity. The presence of only 0.1 mass fraction of [BMIM][BF₄] in the solvent mixture enabled aggregation thus the most favorable properties of [BMIM][OTf] were maintained. A linear relationship between CMC values as well as the Gibbs enthalpy versus [BMIM][BF₄] mass fraction was observed, however, the total decrease of surface tension due to Tween 20 addition was less effective in all the mixtures, than in pure [BMIM][BF₄].

Surface tension isotherms of the analyzed surfactant-in-IL systems were compared with aqueous and ethylene glycol systems containing corresponding surfactants. All the IL-based systems were characterized by worse surface activity of the surfactants expressed by poorer surface tension reduction due to weaker solvophobic effect than ethylene glycol, and significantly poorer than water.

It was observed that formation of micelles strongly depends on the structures of both system components. Surface tension decrease, resulting from micellization, was determined only in systems based on ionic liquids having 2-6 carbon atoms in cations alkyl substituent, but no micellization was observed in 1-octyl-3-methylimidazolium ILs, what was elucidated by the presence of too weak solvophobic effect. Micellization was determined only in ILs containing tetrafluoroborate [BF₄], and hexafluorophosphate [PF₆] ions, but not with trifluoromethanesulfonate [OTf] and bis(trifluoromethylsulfonyl)imide [NTf₂] anions. The [EMIM][OTf] ionic liquid was an exception, which was observed to support micellization of Tween 20 surfactant. The influence of the nonionic surfactants on micellization is also significant. It was determined, that due to decrease of the number of oxyethylene groups in a surfactant, the micellization takes place more easily, what is expressed by lower CMCs and more negative Gibbs free energy values.

Critical micelle concentration values also depend on the structures of ionic liquids and surfactants. CMC values were observed to decrease linearly with increased length of ILs cations alkyl chains, while, the higher CMCs were observed for ILs with tetrafluoroborate anions. Presence of amphiphiles possessing long oxyethylene chains resulted in high CMC values (Triton X surfactants), whereas, their exchange with the bulkier and more branched surfactants (Tweens) resulted in CMC decrease, therefore better solvophobic interactions.

Solvents properties of the ILs were described by means of Gordon value, calculated from density coefficients. Obtained data fit with the assumption that the value of Gordon parameter of a solvent should exceed 0.54 J/m³ to support micelle formation. Determined plots of ΔG_m vs. Gordon values showed decreasing linear relationship with the elongation of ILs cations alkyl chains, independently from anions present and surfactants used, what only confirms former conclusions based on surface tension measurements.

The presence of micellar aggregates was confirmed by means of dynamic light scattering method. The investigation revealed the influence of ILs structure on the size of micellar hydrodynamic diameters. The decrease of ILs cations alkyl chains was followed with the increase of micelles, whereas the anionic moiety provided the increase of the aggregates as follows: [BF₄], [TFO], [PF₆]. Micelles formed by Triton X-100 were smaller than Tween 20. Increasing surfactant content in the solutions, also above CMC, provides growth of micelles.

Thermodynamic evaluation revealed that formation of micelles is most favorable at 25-35°C, what was depicted with the U-shaped plots of CMC on temperature dependences. Free energy of micellization is negative over the whole concentration range of the analyzed systems, indicating the process to be spontaneous.

Conductometric measurements of micellar solutions revealed, that depending on the surfactant used, the systems fitted with Looyenga (Triton X-100) or Bruggeman approximations (Tween 20), following the assumptions of the model. The number of IL cations associating with each OE unit of the surfactant was reported to depend on both anion and cation ILs moieties. Also the smaller is the cation and the weaker are cation-anion interactions, the better is ILs ability to interact with surfactants OE groups.

8. Final comments

The scientific novelty of performed investigation is description of solvent-solute synergy, and system conditions, which enable and affect micellar aggregation and its parameters. Gathered data may serve as a powerful tool in designing new micellar systems based on nonionic surfactants with oxyethylene groups and ionic liquids of similar structured to the imidazolium ones, such as pyridinium, pyrrolidinium, and piperidinium. Presented issues were published in “*Micellar aggregation of Triton X-100 surfactant in imidazolium ionic liquids*” in *Journal of Molecular Liquids*, and in “*Micelle formation of Tween 20 nonionic surfactant in imidazolium ionic liquids*” in *Colloids and Surfaces A: Physicochemical and Engineering Aspects*. Performed investigation is a chemical concept, being a part of a chemical technology project.

The capability of selected imidazolium ionic liquids to support micellar aggregation of selected nonionic surfactants, the mechanism and conditions supporting the aggregation are provided in the dissertation. Surface active agents represent two types of structures amongst the vast family of nonionic surfactants, therefore, for better characterization of imidazolium ILs in terms of micellization, further research is needed regarding amphiphiles of different structures, such as simple-chained polyoxyethylene alkyl ethers (C_mE_n) or a variety of branched sorbitan esters, to determine broader characteristics of interactions of ionic liquid ions and surfactants structures. For better understanding of micellization thermodynamics, the

temperature range for conducted measurements requires broadening. The overall characteristics should be also supported with some type of Fourier transform analyzes, to obtain better outlook on the molecular interactions, especially hydrogen bonds, which play dominant role in the interactions of ILs with other species. Another important feature is replacement of ILs imidazolium cation with other, already well characterized ones, such as pyridinium, pyrrolidinium, and piperidinium, which are often described in the literature concerning their character, behavior and a broad range of applications.

Surfactants-in-ILs micelles were already reported to be a tool for synthesis of nanostructured materials, such as “highly organized hybrid nanostructures with unparalleled quality” [134]. Systems similar to the ones described in dissertation may be used for pharmaceutical purposes like drug delivery and medical synthesis [9]. Aggregation of surface active pharmaceutical ingredients in ionic liquids may be controlled by tuning ILs structure, like type of anions and cations, and cations chains lengths [135]. Another example of drug delivery, including ionic liquids as media for encapsulation and controlled release, was presented by Greaves [136]. Other possible applications which utilize amphiphiles self-assembly are dispersions, wetting, detergency/dry cleaning, and lubrication. Binary micellar systems of amphiphiles in ionic liquids are used as basis for formulation of microemulsions, which help to extend the solvating properties of neat ionic liquids, by e.g. improving solubility of apolar substances, initially insoluble in pure ILs, e.g. micro-reactors for organic and inorganic synthesis [136-138].

9. Bibliography

1. Fletcher, K.A. and S. Pandey, *Surfactant Aggregation within Room-Temperature Ionic Liquid 1-Ethyl-3-methylimidazolium Bis(trifluoromethylsulfonyl)imide*. Langmuir, 2003. **20**(1): p. 33-36.
2. Seddon, K.S., A.; Torres, M.-J., *Viscosity and density of 1-alkyl-3-methylimidazolium ionic liquids*. ACS Symp. Ser., 2002. **819**: p. 34-49.
3. Gao, J., Z.G. Luo, and F.X. Luo, *Ionic liquids as solvents for dissolution of corn starch and homogeneous synthesis of fatty-acid starch esters without catalysts*. Carbohydrate Polymers, 2012. **89**(4): p. 1215-1221.
4. Bogel-Lukasik, R., *Ionic liquids in the biorefinery concept : challenges and perspectives*. RSC green chemistry, xviii, 297 pages.
5. Plechkova, N.V. and K.R. Seddon, *Applications of ionic liquids in the chemical industry*. Chemical Society Reviews, 2008. **37**(1): p. 123-150.
6. Wu, J., et al., *Aggregation Behavior of Polyoxyethylene (20) Sorbitan Monolaurate (Tween 20) in Imidazolium Based Ionic Liquids*. Langmuir, 2008. **24**(17): p. 9314-9322.
7. Gao, Y., et al., *Microstructures of Micellar Aggregations Formed within 1-Butyl-3-methylimidazolium Type Ionic Liquids*. The Journal of Physical Chemistry B, 2008. **113**(1): p. 123-130.
8. Fletcher, K.A. and S. Pandey, *Surfactant aggregation within room-temperature ionic liquid 1-ethyl-3-methylimidazolium bis(trifluoromethylsulfonyl)imide*. Langmuir : the ACS journal of surfaces and colloids, 2004. **20**(1): p. 33-6.
9. Greaves, T.L. and C.J. Drummond, *Solvent nanostructure, the solvophobic effect and amphiphile self-assembly in ionic liquids*. Chemical Society Reviews, 2013. **42**(3): p. 1096-1120.
10. Greaves, T.L. and C.J. Drummond, *Protic ionic liquids: Properties and applications*. Chemical Reviews, 2008. **108**(1): p. 206-237.
11. Greaves, T.L. and C.J. Drummond, *Ionic liquids as amphiphile self-assembly media*. Chemical Society Reviews, 2008. **37**(8): p. 1709-1726.
12. Hallett, J.P. and T. Welton, *Room-Temperature Ionic Liquids: Solvents for Synthesis and Catalysis*. 2. Chemical Reviews, 2011. **111**(5): p. 3508-3576.
13. Jaworska, M.M., T. Kozlecki, and A. Gorak, *Review of the application of ionic liquids as solvents for chitin*. Journal of Polymer Engineering, 2012. **32**(2): p. 67-69.
14. Nagarajan, S. and E. Kandasamy, *Reusable 1,2,4-Triazolium Based Brønsted Acidic Room Temperature Ionic Liquids as Catalyst for Mannich Base Reaction*. Catalysis Letters, 2014. **144**(9): p. 1507-1514.
15. Feroci, M., et al., *The Double Role of Ionic Liquids in Electroorganic Synthesis: Green Solvents and Precursors of N-Heterocyclic Carbenes*. Current Organic Synthesis, 2012. **9**(1): p. 40-52.

16. Zhao, H. and G.A. Baker, *Ionic liquids and deep eutectic solvents for biodiesel synthesis: a review*. Journal of Chemical Technology and Biotechnology, 2013. **88**(1): p. 3-12.
17. Janusz Nowicki, M.M., *Ionic Liquids as Catalysts and Reaction Media in Oleochemical Raw Materials Processing: A Review*. Current Organic Chemistry, 2014. **18**: p. 2797-2807.
18. Corderi, S., et al., *Ionic liquids as solvents to separate the azeotropic mixture hexane/ethanol*. Fluid Phase Equilibria, 2013. **337**: p. 11-17.
19. Lei, Z.G., et al., *Solubility of CO₂ in Binary Mixtures of Room-Temperature Ionic Liquids at High Pressures*. Journal of Chemical and Engineering Data, 2012. **57**(8): p. 2153-2159.
20. Sun, X., et al., *A novel ammonium ionic liquid based extraction strategy for separating scandium from yttrium and lanthanides*. Separation and Purification Technology, 2011. **81**(1): p. 25-30.
21. Tomasz Koźlecki, W.S., Adam Sokołowski, Wojciech Ludwig, Izabela Polowczyk, *Extraction of organic impurities using 1-butyl-3-methylimidazolium hexafluorophosphate [BMIM][PF₆]*. Polish Journal of Chemical Technology, 2008. **10**(1): p. 79-83.
22. Mercy, M., N.H. de Leeuw, and R.G. Bell, *Mechanisms of CO₂ capture in ionic liquids: a computational perspective*. Faraday Discussions, 2016. **192**(0): p. 479-492.
23. Cichowska-Kopczyńska, I., et al., *Influence of Ionic Liquid Structure on Supported Ionic Liquid Membranes Effectiveness in Carbon Dioxide/Methane Separation*. Journal of Chemistry, 2013. **2013**: p. 10.
24. Qureshi, Z., K. Deshmukh, and B. Bhanage, *Applications of ionic liquids in organic synthesis and catalysis*. Clean Technologies and Environmental Policy, 2014. **16**(8): p. 1487-1513.
25. Łuczak, J., et al., *Ionic liquids for nano- and microstructures preparation. Part 1: Properties and multifunctional role*. Advances in Colloid and Interface Science, 2016. **230**: p. 13-28.
26. Hallett, J.P. and T. Welton, *Room-temperature ionic liquids: solvents for synthesis and catalysis*. 2. Chemical Reviews, 2011. **111**(5): p. 3508-76.
27. Mohammad Fauzi, A.H. and N.A.S. Amin, *An overview of ionic liquids as solvents in biodiesel synthesis*. Renewable and Sustainable Energy Reviews, 2012. **16**(8): p. 5770-5786.
28. Fauzi, A.H.M. and N.A.S. Amin, *An overview of ionic liquids as solvents in biodiesel synthesis*. Renewable & Sustainable Energy Reviews, 2012. **16**(8): p. 5770-5786.
29. Azevedo, A.M.O., et al., *Imidazolium ionic liquids as solvents of pharmaceuticals: Influence on HSA binding and partition coefficient of nimesulide*. International Journal of Pharmaceutics, 2013. **443**(1-2): p. 273-278.
30. Fanun, M., *Microemulsions as delivery systems*. Current Opinion in Colloid & Interface Science, 2012. **17**(5): p. 306-313.

31. Moniruzzaman, M., N. Kamiya, and M. Goto, *Ionic liquid based microemulsion with pharmaceutically accepted components: Formulation and potential applications*. Journal of Colloid and Interface Science, 2010. **352**(1): p. 136-142.
32. D'Anna, F., et al., *Ionic liquid binary mixtures: Promising reaction media for carbohydrate conversion into 5-hydroxymethylfurfural*. Applied Catalysis a-General, 2014. **482**: p. 287-293.
33. Ingildeev, D., et al., *Comparison of direct solvents for regenerated cellulosic fibers via the lyocell process and by means of ionic liquids*. Journal of Applied Polymer Science, 2013. **128**(6): p. 4141-4150.
34. Grasvik, J., B. Eliasson, and J.P. Mikkola, *Halogen-free ionic liquids and their utilization as cellulose solvents*. Journal of Molecular Structure, 2012. **1028**: p. 156-163.
35. Tian, G.-c., J. Li, and Y.-x. Hua, *Application of ionic liquids in hydrometallurgy of nonferrous metals*. Transactions of Nonferrous Metals Society of China, 2010. **20**(3): p. 513-520.
36. Abbott, A.P., et al., *Processing of metals and metal oxides using ionic liquids*. Green Chemistry, 2011. **13**(3): p. 471-481.
37. Lopes, J.N.A.C. and A.A.H. Padua, *Nanostructural organization in ionic liquids*. Journal of Physical Chemistry B, 2006. **110**(7): p. 3330-3335.
38. Greaves, T.L., S.T. Mudie, and C.J. Drummond, *Effect of protic ionic liquids (PILs) on the formation of non-ionic dodecyl poly(ethylene oxide) surfactant self-assembly structures and the effect of these surfactants on the nanostructure of PILs*. Physical Chemistry Chemical Physics, 2011. **13**(45): p. 20441-20452.
39. Inoue, T. and H. Yamakawa, *Micelle formation of nonionic surfactants in a room temperature ionic liquid, 1-butyl-3-methylimidazolium tetrafluoroborate: Surfactant chain length dependence of the critical micelle concentration*. Journal of Colloid and Interface Science, 2011. **356**(2): p. 798-802.
40. Sedov, I.A. and B.N. Solomonov, *Thermodynamic description of the solvophobic effect in ionic liquids*. Fluid Phase Equilibria, 2016. **425**: p. 9-14.
41. Song, X.D., et al., *Structural Heterogeneity and Unique Distorted Hydrogen Bonding in Primary Ammonium Nitrate Ionic Liquids Studied by High-Energy X-ray Diffraction Experiments and MD Simulations*. Journal of Physical Chemistry B, 2012. **116**(9): p. 2801-2813.
42. Mele, A., et al., *The local structure of ionic liquids: Cation-cation NOE interactions and internuclear distances in neat [BMIM][BF₄] and [BDMIM]-[BF₄]*. Angewandte Chemie-International Edition, 2006. **45**(7): p. 1123-1126.
43. Dong, K., et al., *Hydrogen bonds in imidazolium ionic liquids*. Journal of Physical Chemistry A, 2006. **110**(31): p. 9775-9782.
44. Ranke, J., et al., *Design of sustainable chemical products--the example of ionic liquids*. Chemical Reviews, 2007. **107**(6): p. 2183-206.
45. Berg, R.W., et al., *Raman and ab Initio Studies of Simple and Binary 1-Alkyl-3-methylimidazolium Ionic Liquids*. The Journal of Physical Chemistry B, 2005. **109**(40): p. 19018-19025.

46. Burba, C.M., et al., *Using FT-IR Spectroscopy to Measure Charge Organization in Ionic Liquids*. The Journal of Physical Chemistry B, 2013. **117**(29): p. 8814-8820.
47. Weingartner, H., *NMR studies of ionic liquids: Structure and dynamics*. Current Opinion in Colloid & Interface Science, 2013. **18**(3): p. 183-189.
48. Lynden-Bell, R.M., et al., *Simulations of Ionic Liquids, Solutions, and Surfaces*. Accounts of Chemical Research, 2007. **40**(11): p. 1138-1145.
49. Peñalber, C.Y., G.A. Baker, and S. Baldelli, *Sum Frequency Generation Spectroscopy of Imidazolium-Based Ionic Liquids with Cyano-Functionalized Anions at the Solid Salt-Liquid Interface*. The Journal of Physical Chemistry B, 2013. **117**(19): p. 5939-5949.
50. Xiao, D., et al., *Nanostructural Organization and Anion Effects on the Temperature Dependence of the Optical Kerr Effect Spectra of Ionic Liquids*. The Journal of Physical Chemistry B, 2007. **111**(18): p. 4669-4677.
51. Yamamoto, K., M. Tani, and M. Hangyo, *Terahertz Time-Domain Spectroscopy of Imidazolium Ionic Liquids*. The Journal of Physical Chemistry B, 2007. **111**(18): p. 4854-4859.
52. Heimer, N.E., R.E. Del Sesto, and W.R. Carper, *Evidence for spin diffusion in a H,H-NOESY study of imidazolium tetrafluoroborate ionic liquids*. Magnetic Resonance in Chemistry, 2004. **42**(1): p. 71-75.
53. Fumino, K. and R. Ludwig, *Analyzing the interaction energies between cation and anion in ionic liquids: The subtle balance between Coulomb forces and hydrogen bonding*. Journal of Molecular Liquids, 2014. **192**: p. 94-102.
54. Bhargava, B.L. and S. Balasubramanian, *Intermolecular structure and dynamics in an ionic liquid: A Car-Parrinello molecular dynamics simulation study of 1,3-dimethylimidazolium chloride*. Chemical Physics Letters, 2006. **417**(4-6): p. 486-491.
55. Bhuiyan, L.B., et al., *Monte Carlo Simulation for the Double Layer Structure of an Ionic Liquid Using a Dimer Model: A Comparison with the Density Functional Theory*. The Journal of Physical Chemistry B, 2012. **116**(34): p. 10364-10370.
56. Vyas, S., et al., *Electronic Structure and Spectroscopic Analysis of 1-Ethyl-3-methylimidazolium Bis(trifluoromethylsulfonyl)imide Ion Pair*. Journal of Physical Chemistry A, 2014. **118**(34): p. 6873-6882.
57. Izgorodina, E.I., U.L. Bernard, and D.R. MacFarlane, *Ion-Pair Binding Energies of Ionic Liquids: Can DFT Compete with Ab Initio-Based Methods?* The Journal of Physical Chemistry A, 2009. **113**(25): p. 7064-7072.
58. Hunt, P.A., C.R. Ashworth, and R.P. Matthews, *Hydrogen bonding in ionic liquids*. Chemical Society Reviews, 2015.
59. Skarmoutsos, I., T. Welton, and P.A. Hunt, *The importance of timescale for hydrogen bonding in imidazolium chloride ionic liquids*. Physical Chemistry Chemical Physics, 2014. **16**(8): p. 3675-3685.
60. Roth, C., et al., *Hydrogen bonding in ionic liquids probed by linear and nonlinear vibrational spectroscopy*. New Journal of Physics, 2012. **14**.

61. Hunt, P.A., *Why does a reduction in hydrogen bonding lead to an increase in viscosity for the 1-butyl-2,3-dimethyl-imidazolium-based ionic liquids?* Journal of Physical Chemistry B, 2007. **111**(18): p. 4844-4853.
62. Kun Dong, Y.S., Xiaomin Liu, Weiguo Cheng, Xiaoqian Yao, Suojiang Zhang, *Understanding Structures and Hydrogen Bonds of Ionic Liquids at the Electronic Level.* J. Phys. Chem. B, 2012(116): p. 1007-1017.
63. Zhao, W., et al., *Are There Stable Ion-Pairs in Room-Temperature Ionic Liquids? Molecular Dynamics Simulations of 1-n-Butyl-3-methylimidazolium Hexafluorophosphate.* Journal of the American Chemical Society, 2009. **131**(43): p. 15825-15833.
64. Freire, M.G., et al., *Surface tensions of imidazolium based ionic liquids: Anion, cation, temperature and water effect.* Journal of Colloid and Interface Science, 2007. **314**(2): p. 621-630.
65. Schrekker, H.S., et al., *Preparation, cation-anion interactions and physicochemical properties of ether-functionalized imidazolium ionic liquids.* Journal of the Brazilian Chemical Society, 2008. **19**: p. 426-433.
66. Shimizu, K., C.E.S. Bernardes, and J.N.C. Lopes, *Structure and Aggregation in the 1-Alkyl-3-Methylimidazolium Bis(trifluoromethylsulfonyl)imide Ionic Liquid Homologous Series.* Journal of Physical Chemistry B, 2014. **118**(2): p. 567-576.
67. Xiao, D., et al., *Effect of Cation Symmetry and Alkyl Chain Length on the Structure and Intermolecular Dynamics of 1,3-Dialkylimidazolium Bis(trifluoromethanesulfonyl)amide Ionic Liquids.* The Journal of Physical Chemistry B, 2009. **113**(18): p. 6426-6433.
68. Russina, O., et al., *Morphology and intermolecular dynamics of 1-alkyl-3-methylimidazolium bis{(trifluoromethane)sulfonyl}amide ionic liquids: structural and dynamic evidence of nanoscale segregation.* Journal of Physics-Condensed Matter, 2009. **21**(42).
69. Martinelli, A., et al., *Insights into the interplay between molecular structure and diffusional motion in 1-alkyl-3-methylimidazolium ionic liquids: a combined PFG NMR and X-ray scattering study.* Physical Chemistry Chemical Physics, 2013. **15**(15): p. 5510-5517.
70. Matthews, R.P., T. Welton, and P.A. Hunt, *Competitive pi interactions and hydrogen bonding within imidazolium ionic liquids.* Physical Chemistry Chemical Physics, 2014. **16**(7): p. 3238-3253.
71. Gordon, J.E., *The Organic Chemistry of Electrolyte Solutions* 1975: Wiley.
72. Wijaya, E.C., et al., *Micelle formation of a non-ionic surfactant in non-aqueous molecular solvents and protic ionic liquids (PILs).* Physical Chemistry Chemical Physics, 2016. **18**(35): p. 24377-24386.
73. Wijaya, E.C., T.L. Greaves, and C.J. Drummond, *Linking molecular/ion structure, solvent mesostructure, the solvophobic effect and the ability of amphiphiles to self-assemble in non-aqueous liquids.* Faraday Discussions, 2013. **167**(0): p. 191-215.

74. del Mar Graciani, M., et al., *Water–N,N-Dimethylformamide Alkyltrimethylammonium Bromide Micellar Solutions: Thermodynamic, Structural, and Kinetic Studies*. *Langmuir*, 2005. **21**(8): p. 3303-3310.
75. Franks, F., *Water Science Reviews 4: Volume 4: Hydration Phenomena in Colloidal Systems* 1989: Cambridge University Press.
76. Kunz, W., T. Zemb, and A. Harrar, *Using ionic liquids to formulate microemulsions: Current state of affairs*. *Current Opinion in Colloid & Interface Science*, 2012. **17**(4): p. 205-211.
77. Evans, D.F., et al., *Micelle size in ethylammonium nitrate as determined by classical and quasi-elastic light scattering*. *The Journal of Physical Chemistry*, 1983. **87**(18): p. 3537-3541.
78. Esumi, K. and M. Ueno, *Structure-performance relationships in surfactants*. 2nd ed. Surfactant science series 2003, New York: Marcel Dekker. viii, 802 p.
79. Moya, M.L., et al., *Role of the solvophobic effect on micellization*. *Journal of Colloid and Interface Science*, 2007. **316**(2): p. 787-795.
80. Sedov, I.A. and B.N. Solomonov, *Solvophobic effects: Qualitative determination and quantitative description*. *Journal of Structural Chemistry*, 2013. **54**(2): p. 262-270.
81. Sedov, I.A., M.A. Stolov, and B.N. Solomonov, *Solvophobic effects and relationships between the Gibbs energy and enthalpy for the solvation process*. *Journal of Physical Organic Chemistry*, 2011. **24**(11): p. 1088-1094.
82. Anderson, J.L., et al., *Surfactant solvation effects and micelle formation in ionic liquids*. *Chemical Communications*, 2003(19): p. 2444-2445.
83. Tang, J., et al., *Temperature dependant self-assembly of surfactant Brij 76 in room temperature ionic liquid*. *Colloids and Surfaces A: Physicochemical and Engineering Aspects*, 2006. **273**(1–3): p. 24-28.
84. Tran, C.D. and S. Yu, *Near-infrared spectroscopic method for the sensitive and direct determination of aggregations of surfactants in various media*. *Journal of Colloid and Interface Science*, 2005. **283**(2): p. 613-618.
85. Chakraborty, A., et al., *Dynamics of solvent and rotational relaxation of coumarin 153 in room-temperature ionic liquid 1-butyl-3-methylimidazolium hexafluorophosphate confined in Brij-35 micelles: A picosecond time-resolved fluorescence spectroscopic study*. *Journal of Physical Chemistry A*, 2005. **109**(49): p. 11110-11116.
86. Patrascu, C., et al., *Micelles in Ionic Liquids: Aggregation Behavior of Alkyl Poly(ethyleneglycol)-ethers in 1-Butyl-3-methyl-imidazolium Type Ionic Liquids*. *ChemPhysChem*, 2006. **7**(1): p. 99-101.
87. Seth, D., et al., *Dynamics of solvent and rotational relaxation of coumarin-153 in room-temperature ionic liquid 1-butyl-3-methyl imidazolium tetrafluoroborate confined in poly(oxyethylene glycol) ethers containing micelles*. *Journal of Physical Chemistry B*, 2007. **111**(18): p. 4781-4787.
88. Gao, Y.N., et al., *Microstructures of Micellar Aggregations Formed within 1-Butyl-3-methylimidazolium Type Ionic Liquids*. *Journal of Physical Chemistry B*, 2009. **113**(1): p. 123-130.

89. Inoue, T. and T. Misono, *Cloud point phenomena for POE-type nonionic surfactants in a model room temperature ionic liquid*. Journal of Colloid and Interface Science, 2008. **326**(2): p. 483-489.
90. Inoue, T. and T. Misono, *Cloud point phenomena for POE-type nonionic surfactants in imidazolium-based ionic liquids: Effect of anion species of ionic liquids on the cloud point*. Journal of Colloid and Interface Science, 2009. **337**(1): p. 247-253.
91. Misono, T., et al., *Surface adsorption and aggregate formation of nonionic surfactants in a room temperature ionic liquid, 1-butyl-3-methylimidazolium hexafluorophosphate (bmimPF₆)*. Journal of Colloid and Interface Science, 2011. **358**(2): p. 527-533.
92. Li, H., et al., *Thermodynamic study on the interaction of imidazolium salts and POE-type nonionic surfactant in the adsorbed film*. Colloid and Polymer Science, 2014. **292**(5): p. 1209-1215.
93. Inoue, T. and Y. Iwasaki, *Cloud point phenomena of polyoxyethylene-type surfactants in ionic liquid mixtures of emimBF₄ and hmimBF₄*. Journal of Colloid and Interface Science, 2010. **348**(2): p. 522-528.
94. Inoue, T., K. Kawashima, and Y. Miyagawa, *Aggregation behavior of nonionic surfactants in ionic liquid mixtures*. Journal of Colloid and Interface Science, 2011. **363**(1): p. 295-300.
95. Rao, V.G., et al., *Aggregation Behavior of Triton X-100 with a Mixture of Two Room-Temperature Ionic Liquids: Can We Identify the Mutual Penetration of Ionic Liquids in Ionic Liquid Containing Micellar Aggregates?* The Journal of Physical Chemistry B, 2012. **116**(47): p. 13868-13877.
96. Thomaier, S. and W. Kunz, *Aggregates in mixtures of ionic liquids*. Journal of Molecular Liquids, 2007. **130**(1-3): p. 104-107.
97. Ali, A., et al., *Study of Micellization of Sodium Dodecyl Sulfate in Non-Aqueous Media Containing Lauric Acid and Dimethylsulfoxide*. Journal of Surfactants and Detergents, 2014. **17**(1): p. 151-160.
98. Bruggeman, D.A.G., *Berechnung verschiedener physikalischer Konstanten von heterogenen Substanzen*. Annals of Physics 1935. **24**: p. 636-679.
99. Lian, Y.W. and K.S. Zhao, *Study of micelles and microemulsions formed in a hydrophobic ionic liquid by a dielectric spectroscopy method. I. Interaction and percolation*. Soft Matter, 2011. **7**(19): p. 8828-8837.
100. Preston, W.C., *Some Correlating Principles of Detergent Action*. Journal of Physical and Colloid Chemistry, 1948. **52**(1): p. 84-97.
101. Tariq, M., et al., *Surface tension of ionic liquids and ionic liquid solutions*. Chemical Society Reviews, 2012. **41**(2): p. 829-868.
102. Inoue, T., et al., *Electrical conductivity study on micelle formation of long-chain imidazolium ionic liquids in aqueous solution*. Journal of Colloid and Interface Science, 2007. **314**(1): p. 236-241.
103. Inoue, T., *Micelle formation of polyoxyethylene-type nonionic surfactants in bmimBF₄ studied by ¹H NMR and dynamic light-scattering*. Journal of Colloid and Interface Science, 2009. **337**(1): p. 240-246.

104. Łuczak, J., et al., *Thermodynamics of micellization of imidazolium ionic liquids in aqueous solutions*. Journal of Colloid and Interface Science, 2009. **336**(1): p. 111-116.
105. Muller, N., *Temperature dependence of critical micelle concentrations and heat capacities of micellization for ionic surfactants*. Langmuir, 1993. **9**(1): p. 96-100.
106. Mehta, S.K., et al., *Effect of temperature on critical micelle concentration and thermodynamic behavior of dodecyltrimethylammonium bromide and dodecyltrimethylammonium chloride in aqueous media*. Colloids and Surfaces A: Physicochemical and Engineering Aspects, 2005. **255**(1-3): p. 153-157.
107. Inoue, T., *Micelle formation of polyoxyethylene-type nonionic surfactants in bmimBF₄ studied by ¹H NMR and dynamic light-scattering*. Journal of Colloid and Interface Science, 2009. **337**: p. 240-246.
108. Aslanov, L.A., *Ionic liquids: Liquid structure*. Journal of Molecular Liquids, 2011. **162**(3): p. 101-104.
109. Ji, Y., et al., *Effect of the Chain Length on the Structure of Ionic Liquids: from Spatial Heterogeneity to Ionic Liquid Crystals*. The Journal of Physical Chemistry B, 2013. **117**(4): p. 1104-1109.
110. Consorti, C.S., et al., *Identification of 1,3-Dialkylimidazolium Salt Supramolecular Aggregates in Solution*. The Journal of Physical Chemistry B, 2005. **109**(10): p. 4341-4349.
111. Dong, K., et al., *Hydrogen Bonds in Imidazolium Ionic Liquids*. The Journal of Physical Chemistry A, 2006. **110**(31): p. 9775-9782.
112. Sharma, R. and R.K. Mahajan, *Influence of various additives on the physicochemical properties of imidazolium based ionic liquids: a comprehensive review*. RSC Advances, 2014. **4**(2): p. 748-774.
113. Triolo, A., et al., *Morphology of 1-alkyl-3-methylimidazolium hexafluorophosphate room temperature ionic liquids*. Chemical Physics Letters, 2008. **457**(4-6): p. 362-365.
114. Tariq, M., et al., *Densities and refractive indices of imidazolium- and phosphonium-based ionic liquids: Effect of temperature, alkyl chain length, and anion*. The Journal of Chemical Thermodynamics, 2009. **41**(6): p. 790-798.
115. Török, S.V., G. Jákli, and E. Berecz, *Comparison of sodium dodecylsulfate apparent molar volumes and micellar aggregation numbers*, in *Trends in Colloid and Interface Science II*, V. Degiorgio, Editor 1988, Steinkopff. p. 221-223.
116. De Lisi, R., et al., *Mass action model for solute distribution between water and micelles. Partial molar volumes of butanol and pentanol in dodecyl surfactant solutions*. Journal of Solution Chemistry, 1985. **15**: p. 23-54.
117. Atkin, R. and G.G. Warr, *Phase Behavior and Microstructure of Microemulsions with a Room-Temperature Ionic Liquid as the Polar Phase*. The Journal of Physical Chemistry B, 2007. **111**(31): p. 9309-9316.
118. Behera, K., V. Kumar, and S. Pandey, *Role of the Surfactant Structure in the Behavior of Hydrophobic Ionic Liquids within Aqueous Micellar Solutions*. ChemPhysChem, 2010. **11**: p. 1044-1052.

119. Łuczak, J., A. Latowska, and J. Hupka, *Micelle formation of Tween 20 nonionic surfactant in imidazolium ionic liquids*. *Colloids and Surfaces A: Physicochemical and Engineering Aspects*, 2015. **471**: p. 26-37.
120. Piekart, J. and J. Luczak, *Transport properties of aqueous ionic liquid microemulsions: influence of the anion type and presence of the cosurfactant*. *Soft Matter*, 2015.
121. Blesic, M., et al., *Self-aggregation of ionic liquids: micelle formation in aqueous solution*. *Green Chemistry*, 2007. **9**(5): p. 481-490.
122. Jungnickel, C., et al., *Micelle formation of imidazolium ionic liquids in aqueous solution*. *Colloids and Surfaces A: Physicochemical and Engineering Aspects*, 2008. **316**(1-3): p. 278-284.
123. Weiszhar, Z., et al., *Complement activation by polyethoxylated pharmaceutical surfactants: Cremophor-EL, Tween-80 and Tween-20*. *European Journal of Pharmaceutical Sciences*, 2012. **45**(4): p. 492-498.
124. Paradies, H.H., *Shape and size of a nonionic surfactant micelle. Triton X-100 in aqueous solution*. *The Journal of Physical Chemistry*, 1980. **84**(6): p. 599-607.
125. Stoppa, A., et al., *The Conductivity of Imidazolium-Based Ionic Liquids from (-35 to 195) °C. A. Variation of Cation's Alkyl Chain*. *Journal of Chemical & Engineering Data*, 2010. **55**(5): p. 1768-1773.
126. Mbondo Tsamba, B.E., et al., *Transport Properties and Ionic Association in Pure Imidazolium-Based Ionic Liquids as a Function of Temperature*. *Journal of Chemical & Engineering Data*, 2014. **59**(6): p. 1747-1754.
127. Bansal, S., et al., *Physicochemical Properties of New Formulations of 1-Ethyl-3-methylimidazolium Bis(trifluoromethylsulfonyl)imide with Tritons*. *Journal of Chemical & Engineering Data*, 2014. **59**(12): p. 3988-3999.
128. Kanakubo, M., et al., *Effect of Pressure on Transport Properties of the Ionic Liquid 1-Butyl-3-methylimidazolium Hexafluorophosphate*. *The Journal of Physical Chemistry B*, 2007. **111**(8): p. 2062-2069.
129. Tokuda, H., et al., *How Ionic Are Room-Temperature Ionic Liquids? An Indicator of the Physicochemical Properties*. *The Journal of Physical Chemistry B*, 2006. **110**(39): p. 19593-19600.
130. Harris, K.R., M. Kanakubo, and L.A. Woolf, *Temperature and pressure dependence of the viscosity of the ionic liquids 1-hexyl-3-methylimidazolium hexafluorophosphate and 1-butyl-3-methylimidazolium bis(trifluoromethylsulfonyl)imide*. *Journal of Chemical and Engineering Data*, 2007. **52**(3): p. 1080-1085.
131. Harris, K.R., M. Kanakubo, and L.A. Woolf, *Temperature and pressure dependence of the viscosity of the ionic liquids 1-methyl-3-octylimidazolium hexafluorophosphate and 1-methyl-3-octylimidazolium tetrafluoroborate*. *Journal of Chemical and Engineering Data*, 2006. **51**(3): p. 1161-1167.
132. Nazet, A., et al., *Densities, Viscosities, and Conductivities of the Imidazolium Ionic Liquids [Emim][Ac], [Emim][FAP], [Bmim][BETI], [Bmim][FSI], [Hmim][TFSI], and [Omim][TFSI]*. *Journal of Chemical & Engineering Data*, 2015. **60**(8): p. 2400-2411.

133. Bordi, F., C. Cametti, and A. Di Biasio, *Electrical conductivity behavior of poly(ethylene oxide) in aqueous electrolyte solutions*. The Journal of Physical Chemistry, 1988. **92**(16): p. 4772-4777.
134. Antonietti, M., et al., *Ionic Liquids for the Convenient Synthesis of Functional Nanoparticles and Other Inorganic Nanostructures*. Angewandte Chemie International Edition, 2004. **43**(38): p. 4988-4992.
135. Tourne-Peteilh, C., et al., *Surfactant behavior of ionic liquids involving a drug: from molecular interactions to self-assembly*. Langmuir : the ACS journal of surfaces and colloids, 2014. **30**(5): p. 1229-38.
136. Greaves, T.L., et al., *Many protic ionic liquids mediate hydrocarbon-solvent interactions and promote amphiphile self-assembly*. Langmuir, 2007. **23**(2): p. 402-404.
137. Piekart, J. and J. Luczak, *Transport properties of microemulsions with ionic liquid apolar domains as a function of ionic liquid content*. RSC Advances, 2016. **6**(95): p. 92605-92620.
138. Długokęcka, M., et al., *The effect of microemulsion composition on the morphology of Pd nanoparticles deposited at the surface of TiO₂ and photoactivity of Pd-TiO₂*. Applied Surface Science, 2017. **405**: p. 220-230.

List of figures

Figure 1. Structure of 1-methyl-3-alkylimidazolium cation.....	8
Figure 2. Types of interactions within ILs structures.....	10
Figure 3. Interactions of n-alkyl-3-methylimidazolium ionic liquids	11
Figure 4. Spatial organization of ILs cations, a) sandwich (parallel), b) sandwich (anti-parallel) c) shifted sandwich (rotated), d) T-shape, d) sandwich.....	12
Figure 5. Schematic depiction of channels between imidazolium cations, where X denotes anions	13
Figure 6. Mesh-like organization of [EMIM][BF ₄] ions [43], [58].....	13
Figure 7. Formation of a) normal and c) reverse micelles from b) surfactant monomers	15
Figure 8. Structure of Triton X surfactants, where n = 9.5, 7.5, 4.5 and 1.5 for TX-100, TX-114, TX-45 and TX-15, respectively	25
Figure 9. Structures of Tween surfactants: a) Tween 20, b) Tween 40, c) Tween 60, c) Tween 80.....	26
Figure 10. Derivation of the Young-Laplace fit on a pendant drop, where R ₁ and R ₂ are principal droplet radii	29
Figure 11. Inflection of solution parameters in the CMC region (from ref. [100]).....	32
Figure 12. Determination of critical micelle concentration from a surface tension isotherm	32
Figure 13. Gordon parameter (G) and the number of carbon atoms in ILs cation alkyl chain (m) regarding anion type: ([BF ₄] (◆), [PF ₆] (◆), [OTf] (◆), and [NTf ₂] (◆), at 25°C	36
Figure 14. Surface tension of Triton X-100 in [EMIM][BF ₄] (◆), [PrMIM][BF ₄] (◆), [BMIM][BF ₄] (◆), [PMIM][BF ₄] (◆), [HMIM][BF ₄] (◆), [OMIM][BF ₄] (◆), at 25.0°C.....	37
Figure 15. Surface tension of Triton X-100 in [BMIM][PF ₆] (◆), [PMIM][PF ₆] (◆), [HMIM][PF ₆] (◆), [OMIM][PF ₆] (◆) at 25.0°C	38
Figure 16. Surface tension of Triton X-100 in [EMIM][OTf] (◆), [BMIM][OTf] (◆), [HMIM][OTf] (◆), [OMIM][OTf] (◆), at 25.0°C	38
Figure 17. Surface tension of Triton X-100 in [EMIM][NTf ₂] (◆), [BMIM][NTf ₂] (◆), [HMIM][NTf ₂] (◆), [OMIM][NTf ₂] (◆), at 25.0°C	38
Figure 18. Surface tension of TX-100 in [EMIM][BF ₄] (◆), [EMIM][NTf ₂] (◆), [EMIM][OTf] (◆), at 25.0°C	40
Figure 19. Surface tension of TX-100 in [BMIM][BF ₄] (◆), [BMIM][PF ₆] (◆), [BMIM][NTf ₂] (◆), [BMIM][OTf] (◆), at 25.0°C.	40
Figure 20. Surface tension of TX-100 in [PrMIM][BF ₄] (◆), [PMIM][BF ₄] (◆), [PMIM][PF ₆] (◆), at 25.0°C	40
Figure 21. Surface tension of TX-100 in [HMIM][BF ₄] (◆), [HMIM][PF ₆] (◆), [HMIM][NTf ₂] (◆), [HMIM][OTf] (◆), at 25.0°C	40
Figure 22. Surface tension of Tween 20 in [EMIM][OTf], at 25.0°C.....	40

Figure 23. Surface tension of Tritons (solid lines): Triton X-100 (◆), Triton X-114 (◆), Triton X-45 (◆), Triton X-15 (◆), and Tweens (dashed lines): Tween 20 (◆), Tween 60 (◆), Tween 80 (◆), in [BMIM][BF ₄], at 25.0°C.....	41
Figure 24. Surface tension of TX-100 (◆), TX-114 (◆) and TX-45 (◆) in water at 25.0°C	43
Figure 25. Surface tension of Triton X-100 (◆), Triton X-114 (◆), Triton X-45 (◆), Triton X-15 (◆) in ethylene glycol, at 25.0°C.....	43
Figure 26. Surface tension of TX-100 in [BMIM][BF ₄] (◆), water (◆) and ethylene glycol (◆) at 25.0°C	43
Figure 27. Surface tension isotherms of TX-100/[BMIM][BF ₄] at 15.0°C (◆), 25.0°C (◆), 35.0°C (◆), 45.0°C (◆).....	44
Figure 28. CMC vs. temperature of Triton X-100 in [EMIM][BF ₄]	44
Figure 29. CMC vs. temperature of Triton X-100 in [BMIM][BF ₄].....	44
Figure 30. CMC vs. temperature of Triton X-100 in water.....	45
Figure 31. CMC vs. temperature of Triton X-100 in ethylene glycol.....	45
Figure 32. CMC vs. temperature of Triton X-100 (◆), Triton X-114 (◆) and Triton X-45 (◆) in [BMIM][BF ₄]	45
Figure 33. CMC of Tween 20 in [EMIM][TfO] vs. temperature	47
Figure 34. Thermodynamic parameters of micelle formation for Tween 20 in [EMIM][TfO]: ΔG_m (◆), ΔH_m (◆) and $-T\Delta S_m$ (◆).....	47
Figure 35. Surface tension isotherms of Tween 20 in pure and mixed 1-butyl-3-methylimidazolium ILs, [BMIM][OTf]/[BMIM][BF ₄] with corresponding mass ratios: [BMIM][BF ₄] (◆), [BMIM][OTf]/[BMIM][BF ₄] 1:1 (◆), 7:3 (◆), 9:1 (◆), [BMIM][OTf] (◆)	56
Figure 36. Dependence of the critical micelle concentration on [BMIM][BF ₄] mass fraction in [BMIM][OTf]/[BMIM][BF ₄] mixtures	58
Figure 37. Dependence of Gibbs free energy of Tween 20 micelle formation on [BMIM][BF ₄] mass fraction in [BMIM][OTf]/[BMIM][BF ₄] mixtures.....	58
Figure 38. Apparent molar volume values, V_ϕ , of TX-100 in 1-alkyl-3-methylimidazolium tetrafluoroborate ionic liquids, where [EMIM] (◆), [PrMIM] (◆), [BMIM] (◆), [PMIM] (◆), [HMIM] (◆), at 25°C	59
Figure 39. CMC values vs. IL structure: TX-100/[AMIM][BF ₄] (◆), TX-100/[AMIM][PF ₆] (◆), Tween 20/[AMIM][BF ₄] (◆), Tween 20/[AMIM][PF ₆] (◆), at 25.0°C	61
Figure 40. Number of OE units (m) of Triton X surfactants, vs. CMCs in [EMIM][BF ₄] (◆), [BMIM][BF ₄] (◆) and ethylene glycol (◆), at 25.0°C.....	61
Figure 41. Size distribution curves determined for Triton X-100 in [EMIM][BF ₄] (left), and mean hydrodynamic diameter as a function of surfactant concentration (right), at 25°C.....	63
Figure 42. Size distribution curves determined for Triton X-100 in [BMIM][BF ₄] (left), and mean hydrodynamic diameter as a function of surfactant concentration (right), at 25°C.....	63
Figure 43. Size distribution curves determined for Triton X-100 in [HMIM][BF ₄] (left), and mean hydrodynamic diameter as a function of surfactant concentration (right), at 25°C.....	63

Figure 44. Tween 20/[EMIM][BF ₄] size distribution (left), and mean hydrodynamic diameter vs. surfactant concentration (right), at 25°C	64
Figure 45. Size distribution curves determined for Tween 20 in [EMIM][OTf] (left), and mean hydrodynamic diameter as a function of surfactant concentration (right), at 25°C.....	64
Figure 46. Size distribution curves determined for Tween 20 in [BMIM][PF ₆] (left), and mean hydrodynamic diameter as a function of surfactant concentration (right), at 25°C.....	64
Figure 47. Micellar diameters of Triton X-100 vs. number of cation alkyl chain carbon atoms in [AMIM][BF ₄], at 25°C	65
Figure 48. Conductivity vs. weight ratio of TX-100 in [BMIM][BF ₄] (◆) and [BMIM][PF ₆] (◆).....	67
Figure 49. Conductivity vs. weight ratio of Tween 20 in [BMIM][BF ₄] (◆) and [BMIM][PF ₆] (◆) ...	67
Figure 50. Dependence of normalized conductivity values of (κ/κ_{IL}) on the volume fractions (ϕ) of the surfactant in TX-100/IL solutions: [EMIM][BF ₄] (◆), [BMIM][BF ₄] (◆), [HMIM][BF ₄] (◆).	68
Figure 51. Dependence of normalized conductivity values (κ/κ_{IL}) on the volume fractions (ϕ) of the surfactant in Tween 20/IL binary solutions: [BMIM][BF ₄] (◆), [BMIM][PF ₆] (◆), [BMIM][NTf ₂] (◆), [BMIM][OTf] (◆)	68
Figure 52. Dependence of normalized conductivity values of (κ/κ_{IL}) on the volume fractions (ϕ) of Tween 20 in [BMIM][OTf]/[BMIM][BF ₄] of 0.1 (◆), 0.3 (◆), and 0.5 (◆) mass fractions of [BMIM][BF ₄]	68
Figure 53. Dependence of the number of [AMIM][BF ₄] cations carbon atoms on surfactant aggregation numbers, n_{ac} , of TX-100 (◆) and Tween 20 (◆), at 25.0°C	68
Figure 54. Proposed interactions between Triton X surfactants and [BMIM][BF ₄] ionic liquids' ions	72
Figure 55. Proposed interactions between Triton X surfactants [BMIM][OTf] ionic liquids' ions.....	72
Figure 56. Proposed interactions between Tween 20 surfactant and [BMIM][BF ₄] ionic liquids' ions	72
Figure 57. Gordon parameter (G) and the number of carbon atoms in ILs cation alkyl chain (m) regarding anion type: ([BF ₄] (◆), [PF ₆] (◆), [OTf] (◆), and [NTf ₂] (◆), at 25°C. Salts promoting micellar aggregates formation are in the shaded area.....	73
Figure 58. Triton X-100 in [AMIM][BF ₄] ILs, ethylene glycol (EG) and formamide (FA) ΔG_m vs. Gordon parameter (G), at 25.0°C	74
Figure 59. Variation of ΔG_m of Triton X-100 (◆), Triton X-114 (◆), Triton X-45 (◆) surfactants as a function of Gordon parameter (G) in [EMIM][BF ₄] (2), [PrMIM][BF ₄] (3), [BMIM][BF ₄] (4), [PMIM][BF ₄] (5), [HMIM][BF ₄] (6), at 25°C.....	74

List of tables

Table 1. Instrumental and theoretical methods for studying ILs bonds and interactions	9
Table 2. Structures of ILs cations.....	23
Table 3. Structures of ILs anions.....	24
Table 4. Water content in ionic liquids used in the study	24
Table 5. Gordon and density values of [AMIM][BF ₄], water and ethylene glycol at 15, 25, 35 and 45°C.....	35
Table 6. Thermodynamic micellization parameters, ΔG_m , ΔH_m , $-T\Delta S_m$, of Triton X-100 in [EMIM][BF ₄], [BMIM][BF ₄] and [PMIM][BF ₄]	46
Table 7. Surface parameters of Triton X-100 ($n_{OE} = 9.5$) in [AMIM][BF ₄] ILs, ethylene glycol and water, vs. temperature.	49
Table 8. Surface parameters of Triton X-114 ($n_{OE} = 7.5$) in [AMIM][BF ₄] ILs, ethylene glycol and water, vs. temperature	51
Table 9. Surface parameters of Triton X-45 ($n_{OE} = 4.5$) in [AMIM][BF ₄] ILs, ethylene glycol and water, vs. temperature	52
Table 10. Surface parameters of Triton X-15 ($n_{OE} = 1.5$) in [AMIM][BF ₄] and [AMIM][PF ₆] ILs, ethylene glycol and water, at 25.0°C.....	53
Table 11. Surface parameters of Tween 20 in selected ILs, ethylene glycol and water, vs. temperature	54
Table 12. Surface properties of Tween 20 in [BMIM][OTf]/[BMIM][BF ₄] mixtures with different mass fractions.....	58
Table 13. CMCs of Triton X-100 in [AMIM][BF ₄] and [AMIM][PF ₆] determined from surface tension γ , and apparent molar volumes $V\phi$, at 25.0°C.....	61
Table 14. Ionic liquids experimental and literature conductivity values.....	66
Table 15. Critical values for Dixon's Q-Test for 95% confidence level.....	69
Table 16. Parameter t related with the number of measurements n	70
Table 17. Statistical evaluation of surface tension values	70
Table 18. List of ILs systems analyzed within the dissertation.....	75

Summary

A number of imidazolium ionic liquids, with 2 - 8 carbon atoms in cation alkyl chains, and tetrafluoroborate, hexafluorophosphate, bis(trifluoromethylsulfonyl)imide and trifluoromethanesulfonate anions, were characterized for their ability to support micellar aggregation of nonionic surfactants in binary solutions. Performed measurements included determination of surface tension, viscosity, density, conductivity and surfactant micellar diameters. Goniometric measurements carried out in the range of 15.0 – 45.0°C allowed thermodynamic characterization of the investigated systems. Calculated Gordon parameter was confirmed to provide information on the ability of ionic liquids to support micellization. It was observed, that structures of both, surfactant (number of oxyethylene groups) and ionic liquid (anion and cation type and alkyl chain length), strongly influence micellization process, critical micelle concentration values, size of micellar hydrodynamic diameters and aggregation numbers. Formulated binary solutions were compared to well described aqueous and ethylene glycol surfactant micellar systems. Modification of micellar parameters was performed by mixing different mass ratios of two ionic liquids of unlike characters. The research gives broader outlook on the possible applications, potentials and limitations of imidazolium ionic liquids in the field of surface chemistry, as solvents supporting micellization.

Streszczenie

Scharakteryzowano grupę imidazoliowych cieczy jonowych, zawierających 2-8 atomów węgla w podstawniku alkilowym kationu, oraz aniony: tetrafluoroboranowy, heksafluorofosforanowy, bis(trifluorometylosulfonylo)imidkowy oraz trifluorosulfonylowy, pod kątem zdolności do wspierania micelizacji surfaktantów niejonowych w układach dwuskładnikowych. W ramach przeprowadzonych badań wyznaczono napięcie powierzchniowe, lepkość, gęstość, przewodnictwo oraz średnice hydrodynamiczne micel. Charakterystykę termodynamiczną układów wykonano na podstawie wyników pomiarów napięcia powierzchniowego, przeprowadzonych w przedziale 15,0 – 45,0°C. Wykazano przydatność parametru Gordona w predykcji zdolności rozpuszczalnika, do wspierania agregacji micelarnej. Zaobserwowano, że zarówno struktura surfaktantu (ilość grup oksyetylenowych) jak i cieczy jonowej (długość łańcucha alkilowego w kationie oraz rodzaj anionu) ma znaczący wpływ na zdolność cieczy jonowej do wspierania micelizacji, wartości krytycznego stężenia micelizacji, wielkość micel oraz liczby agregacji. Analizowane układy zostały porównane z układami micelarnymi opartymi na wodzie i glikolu etylenowym, które zostały szczegółowo opisane w literaturze. Możliwość modyfikowania właściwości fazy rozpuszczalnikowej zbadano poprzez zmieszanie serii ułamków masowych dwóch cieczy jonowych o odmiennych właściwościach. Przedstawione w dysertacji wyniki badań mogą być istotnym narzędziem do projektowania nowych układów micelarnych zawierających imidazoliowe ciecze jonowe, jako fazę rozpuszczalnikową.